



8-2017

# The Study of Sulfenate and Sterically Hindered Chalcogenide Anions as Organocatalysts for the Construction of C-C Bonds

Christopher M. Annunziato

University of Pennsylvania, [cannunz@sas.upenn.edu](mailto:cannunz@sas.upenn.edu)

Follow this and additional works at: [https://repository.upenn.edu/mcs\\_capstones](https://repository.upenn.edu/mcs_capstones)

 Part of the [Chemistry Commons](#)

Annunziato, Christopher M., "The Study of Sulfenate and Sterically Hindered Chalcogenide Anions as Organocatalysts for the Construction of C-C Bonds" (2017). *Master of Chemical Sciences Capstone Projects*. 6.  
[https://repository.upenn.edu/mcs\\_capstones/6](https://repository.upenn.edu/mcs_capstones/6)

This paper is posted at Scholarly Commons. [https://repository.upenn.edu/mcs\\_capstones/6](https://repository.upenn.edu/mcs_capstones/6)  
For more information, please contact [repository@pobox.upenn.edu](mailto:repository@pobox.upenn.edu).

---

# The Study of Sulfenate and Sterically Hindered Chalcogenide Anions as Organocatalysts for the Construction of C-C Bonds

## Abstract

Chalcogenides are highly redox active and biologically potent nucleophiles with significant unexplored catalytic potential. In particular, sulfenate anions potential as organocatalyst has largely been overlooked in the literature due to their esoteric status. A unique sulfenate anion catalyzed Baylis Hillman (BH) reaction forming sp<sup>2</sup>-sp<sup>3</sup> C-C bonds is in development. In this two-part study, part one focuses on screening conditions suitable for both cleavage of a precatalyst and subsequent BH reaction. Whereas part two focuses on the proclivity of chalcogenide oxyanions to disproportionate. Sterically hindered analogs were investigated, to prevent catalyst decomposition. The sulfenate anion catalyzed (20 mol %) BH reaction was conducted in the presence of  $\alpha,\beta$ -unsaturated nitriles, ketones and esters to generate allylic alcohols in yields up to 37%. Precatalyst cleavage studies were an integral part to the realization of smooth sulfenate anion generation. Efforts to optimize the BH reaction conditions are ongoing.

## Keywords

Organic methodology, organocatalysis, sulfenate anion, sulfur, chalcogenide, catalysis

## Disciplines

Chemistry

## Creative Commons License



This work is licensed under a [Creative Commons Attribution-NonCommercial-Share Alike 4.0 License](https://creativecommons.org/licenses/by-nc-sa/4.0/).

# AN ABSTRACT OF THE CAPSTONE REPORT OF

Christopher M. Annunziato for the degree of Master of Chemical Sciences

Title: The Study of Sulfenate and Sterically Hindered Chalcogenide Anions as  
Organocatalysts for the Construction of C-C Bonds

Project conducted at: *University of Pennsylvania 231 South 34<sup>th</sup> Street,  
Philadelphia, PA 19104*

Supervisor: *Patrick J. Walsh, Professor of Chemistry*

Dates of Project: *May 2017 - August 2017*

Abstract approved:

*Patrick J. Walsh, Academic Advisor*

Chalcogenides are highly redox active and biologically potent nucleophiles with significant unexplored catalytic potential. In particular, sulfenate anions potential as organocatalyst has largely been overlooked in the literature due to their esoteric status. A unique sulfenate anion catalyzed Baylis Hillman (BH) reaction forming  $sp^2$ - $sp^3$  C-C bonds is in development. In this two-part study, part one focuses on screening conditions suitable for both cleavage of a precatalyst and subsequent BH reaction. Whereas part two focuses on the proclivity of chalcogenide oxyanions to disproportionate. Sterically hindered analogs were investigated, to prevent catalyst decomposition.

The sulfenate anion catalyzed (20 mol %) BH reaction was conducted in the presence of  $\alpha,\beta$ -unsaturated nitriles, ketones and esters to generate allylic alcohols in yields up to 37%. Precatalyst cleavage studies were an integral part to the realization of smooth sulfenate anion generation. Efforts to optimize the BH reaction conditions are ongoing.

*The Study of Sulfenate and Sterically Hindered  
Chalcogenide Anions as  
Organocatalysts for the Construction of C-C Bonds*

by

*Christopher M. Annunziato*

A CAPSTONE REPORT

submitted to the

University of Pennsylvania

In partial fulfillment of

the requirements for

the degree of

Master of Chemical Sciences

Presented *August 11<sup>th</sup>, 2017*  
Commencement *August 2017*

Master of Chemical Sciences Capstone Report of

Christopher M. Annunziato presented on *August 11<sup>th</sup>, 2017.*

APPROVED:

---

*Patrick J. Walsh, representing Organic Chemistry*

I understand that my Capstone Report will become part of the permanent collection of the University of Pennsylvania Master of Chemical Sciences Program. My signature below authorizes release of my final report to any reader upon request.

---

*Christopher M. Annunziato, Author*

## Acknowledgements

I would first like to thank Professor Patrick J. Walsh for his guidance and support through a difficult project and year. I am grateful that I could be a part of his lab and grow and chemist and person during this time. Continuing into my Ph.D. here at Penn, I hope to utilize the knowledge I have gained to showcase my skills as an expert researcher and conduct quality chemistry in his laboratory.

I would like to thank Dr. Ana-Rita Mayol for her endless support, during my first year and writing of this capstone thesis. Most importantly, for guiding me through this difficult process that is graduate school. I would like to thank Dr. Marisa Kozlowski for being my secondary reader and helping me to develop as a thinker in her Physical Organic class.

Next, I would like to thank the members of the Walsh lab for helpful suggestions and teaching me Schleck technique. I would particularly like to thank Grace Panetti, Russel Shelp, Elena Varela and Zhipeng Zheng for helping with various aspects of this thesis.

I would like to thank my parents John and Barbara Annunziato for their continued support and endless lunches that kept me satisfied and efficient in my work.

## Table of Contents

Abstract .....	i
Title Page .....	ii
Approval Page .....	iii
Acknowledgements .....	iv
Table of Contents .....	v
List of Figures, Tables, and Schemes .....	vi
List of Appendices .....	vii
Introduction.....	1
Materials and Methods .....	8
Results and Discussion .....	17
Conclusion and Future Work .....	28
References .....	29
Appendices.....	33

## List of Figures

<b>Figure 1.</b> 2,6-Hindered variants of selenolate, selenenate and sulfenate anions	2
<b>Figure 2.</b> Sulfenate anion disproportionation in the presence of a proton source	4
<b>Figure 3.</b> Proposed disproportionation mechanism between two chalcogenide oxyanions .....	4
<b>Figure 4.</b> General properties of a sulfenate anion.....	5
<b>Figure 5.</b> Proposed sulfenate anion catalyzed Baylis-Hillman mechanism .....	6
<b>Figure 6.</b> Two types of sulfenate anion precatalysts tested in BH reaction .....	7
<b>Figure 7.</b> Oxidation product of sulfenate anion upon workup.....	21
<b>Figure 8.</b> Generic Pictet Spengler reaction with iminium cation activation .....	22
<b>Figure 9.</b> High throughput screening results for stilbene formation catalyzed by 2,6-dimethylbenzene sulfenate .....	25

## List of Tables

<b>Table 1.</b> BH reaction of acrylonitrile and benzaldehyde with <b>7.1</b> , <b>7.2</b> at RT .....	17
<b>Table 2.</b> BH reaction of acrylonitrile, benzaldehyde and <b>7.1</b> at RT / 50 °C.....	18
<b>Table 3.</b> Cleavage of 2-(trimethylsilyl)ethyl sulfoxide <b>8</b> with fluoride .....	20
<b>Table 4.</b> Cleavage of 2-(trimethylsilyl)ethyl sulfoxide with TBAT at RT .....	23

## List of Schemes

<b>Scheme 1.</b> Previous work using sulfenate anions as organocatalysts by Walsh and co-workers .....	3
<b>Scheme 2.</b> Singleton and Plata show significant deuterium incorporation in intermediate <b>5</b> before product <b>6</b> is formed .....	7
<b>Scheme 3.</b> General sulfide preparation.....	10
<b>Scheme 4.</b> General sulfide oxidation preparation .....	11
<b>Scheme 5.</b> Possible Stetter/Benzoin product in BH at 50 °C .....	18
<b>Scheme 6.</b> Strong base testing cleavage of sulfoxide precatalyst .....	19
<b>Scheme 7.</b> Palladium catalyzed arylation of sulfenate anions.....	19
<b>Scheme 8.</b> BH reaction with <b>8</b> to produce nitrile <b>13</b> .....	21
<b>Scheme 9.</b> BH using sulfoxide <b>8</b> to produce ester <b>14</b> .....	22
<b>Scheme 10.</b> BH reaction with L-proline to product ketone <b>15</b> .....	23
<b>Scheme 11.</b> Synthesis progress of ortho-ortho hindered chalcogenides .....	24
<b>Scheme 12.</b> Hindered selenide stilbene experiment using <b>17</b> .....	25
<b>Scheme 13.</b> Stilbene catalysis using <b>21</b> at 10 mol % loading .....	26



## List of Appendices

<b>Appendix 1.</b>	<sup>1</sup> H NMR spectrum absence of <b>9</b> with <b>7.1</b> , no additive .....	32
<b>Appendix 2.</b>	<sup>1</sup> H NMR spectrum absence of <b>9</b> with <b>7.2</b> , no additive .....	33
<b>Appendix 3.</b>	<sup>1</sup> H NMR spectrum absence of <b>9</b> with <b>7.1</b> and 2,4-dinitrophenol as additive .....	33
<b>Appendix 4.</b>	<sup>1</sup> H NMR spectrum absence of <b>9</b> with <b>7.2</b> and 2,4-dinitrophenol as additive .....	34
<b>Appendix 5.</b>	<sup>1</sup> H NMR spectrum absence of <b>9</b> with <b>7.1</b> and deionized water as additive .....	34
<b>Appendix 6.</b>	<sup>1</sup> H NMR spectrum absence of <b>9</b> with <b>7.1</b> and KO <sup>t</sup> Bu as base at 25 °C.....	35
<b>Appendix 7.</b>	<sup>1</sup> H NMR spectrum absence of <b>9</b> with <b>7.1</b> and KO <sup>t</sup> Bu as base at 50 °C.....	35
<b>Appendix 8.</b>	<sup>1</sup> H NMR spectrum absence of <b>9</b> with <b>7.1</b> and KHMDS as base at 50 °C.....	36
<b>Appendix 9.</b>	<sup>1</sup> H NMR spectrum absence of <b>9</b> with <b>7.1</b> and KHMDS as base at 50 °C.....	36
<b>Appendix 10.</b>	<sup>1</sup> H NMR spectrum of possible Stetter <b>4</b> and Benzoin <b>5</b> product ..	37
<b>Appendix 11.</b>	<sup>1</sup> H NMR spectrum absence of <b>4</b> with <b>1.2</b> and presence of <b>5</b> with NaHMDS as base.....	38
<b>Appendix 12.</b>	<sup>1</sup> H NMR spectrum absence of <b>4</b> with <b>1.2</b> and presence of <b>5</b> with LiHMDS as base .....	39
<b>Appendix 13.</b>	<sup>1</sup> H NMR spectrum absence of <b>4</b> with <b>1.2</b> and KO <sup>t</sup> Bu as base .....	39
<b>Appendix 14.</b>	<sup>1</sup> H NMR spectrum of <b>8</b> , Entry <b>1</b> of fluoride cleavage study .....	40
<b>Appendix 15.</b>	<sup>1</sup> H NMR spectrum of <b>8</b> , Entry <b>2</b> of fluoride cleavage study .....	40
<b>Appendix 16.</b>	<sup>1</sup> H NMR spectrum of <b>8</b> , Entry <b>3</b> of fluoride cleavage study .....	41
<b>Appendix 17.</b>	<sup>1</sup> H NMR spectrum of <b>8</b> , Entry <b>4</b> of fluoride cleavage study .....	41
<b>Appendix 18.</b>	<sup>1</sup> H NMR spectrum of <b>8</b> , Entry <b>5</b> of fluoride cleavage study .....	42
<b>Appendix 19.</b>	<sup>1</sup> H NMR spectrum of <b>8</b> , Entry <b>6</b> of fluoride cleavage study .....	42
<b>Appendix 20.</b>	<sup>1</sup> H NMR spectrum of <b>8</b> , Entry <b>7</b> of fluoride cleavage study .....	43
<b>Appendix 21.</b>	<sup>1</sup> H NMR spectrum of <b>8</b> , Entry <b>8</b> of fluoride cleavage study .....	43
<b>Appendix 22.</b>	<sup>1</sup> H NMR spectrum of <b>8</b> , Entry <b>9</b> of fluoride cleavage study .....	44
<b>Appendix 23.</b>	<sup>1</sup> H NMR spectrum of <b>8</b> , Entry <b>10</b> of fluoride cleavage study .....	44
<b>Appendix 24.</b>	<sup>1</sup> H NMR spectrum of <b>8</b> , Entry <b>11</b> of fluoride cleavage study .....	45
<b>Appendix 25.</b>	<sup>1</sup> H NMR spectrum of <b>8</b> , Entry <b>12</b> of fluoride cleavage study .....	45
<b>Appendix 26.</b>	<sup>1</sup> H NMR spectrum of product <b>13</b> with impurity <b>7.3</b> .....	46
<b>Appendix 27.</b>	<sup>13</sup> C NMR spectrum of product <b>13</b> with impurity <b>7.3</b> .....	46
<b>Appendix 28.</b>	<sup>1</sup> H NMR spectrum of product <b>14</b> .....	47
<b>Appendix 29.</b>	<sup>13</sup> C NMR spectrum of product <b>14</b> .....	47
<b>Appendix 30.</b>	<sup>1</sup> H NMR spectrum of <b>13</b> using <b>8</b> and 4-bromophenol as additive	48
<b>Appendix 31.</b>	<sup>1</sup> H NMR spectrum of <b>13</b> using <b>8</b> as precatalyst and no additive ..	49
<b>Appendix 32.</b>	<sup>1</sup> H NMR spectrum of <b>14.1</b> using <b>8</b> as precatalyst .....	50
<b>Appendix 33.</b>	<sup>1</sup> H NMR spectrum of <b>14.2</b> using <b>8</b> as precatalyst .....	51

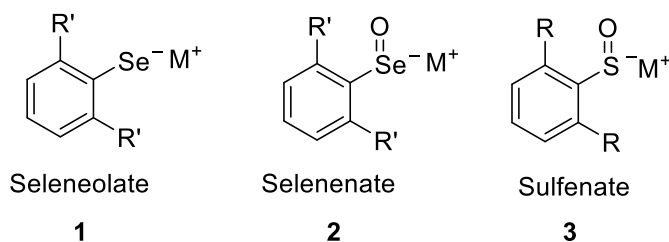
<b>Appendix 34.</b>	<sup>1</sup> H NMR spectrum of <b>14.3</b> using <b>8</b> as precatalyst .....	51
<b>Appendix 35.</b>	<sup>1</sup> H NMR spectrum of <b>15</b> using <b>8</b> as precatalyst and L-proline .....	52
<b>Appendix 36.</b>	<sup>1</sup> H NMR spectrum of <b>15.1</b> using <b>8</b> as precatalyst .....	52
<b>Appendix 37.</b>	<sup>1</sup> H NMR spectrum of <b>15.2</b> using <b>8</b> as precatalyst .....	53
<b>Appendix 38.</b>	<sup>1</sup> H NMR spectrum of <b>15.3</b> using <b>8</b> as precatalyst .....	53
<b>Appendix 39.</b>	<sup>1</sup> H NMR spectrum of <b>8.1</b> using <b>2</b> as precatalyst with DMF .....	54
<b>Appendix 40.</b>	<sup>1</sup> H NMR spectrum of <b>8.1</b> using <b>2</b> as precatalyst with MeOH .....	54
<b>Appendix 41.</b>	<sup>1</sup> H NMR spectrum of <b>8</b> Entry <b>1</b> of Table 2 .....	55
<b>Appendix 42.</b>	<sup>1</sup> H NMR spectrum of <b>8</b> Entry <b>2</b> of Table 2 .....	55
<b>Appendix 43.</b>	<sup>1</sup> H NMR spectrum of <b>8</b> Entry <b>3</b> of Table 2 .....	56
<b>Appendix 44.</b>	<sup>1</sup> H NMR spectrum of <b>8</b> Entry <b>4</b> of Table 2 .....	56
<b>Appendix 45.</b>	<sup>1</sup> H NMR spectrum of <b>8</b> Entry <b>5</b> of Table 2 .....	57
<b>Appendix 46.</b>	<sup>1</sup> H NMR spectrum of <b>8</b> Entry <b>6</b> of Table 2 .....	57
<b>Appendix 47.</b>	<sup>1</sup> H NMR spectrum of <b>7.1</b> before oxidation .....	58
<b>Appendix 48.</b>	<sup>13</sup> C NMR spectrum of <b>7.1</b> before oxidation .....	58
<b>Appendix 49.</b>	<sup>1</sup> H NMR spectrum of <b>7.2</b> before oxidation .....	59
<b>Appendix 50.</b>	<sup>13</sup> C NMR spectrum of <b>7.2</b> before oxidation .....	59
<b>Appendix 51.</b>	<sup>1</sup> H NMR spectrum of <b>7.2</b> .....	60
<b>Appendix 52.</b>	<sup>13</sup> C NMR spectrum of <b>7.2</b> .....	60
<b>Appendix 53.</b>	<sup>1</sup> H NMR spectrum of <b>8</b> .....	61
<b>Appendix 54.</b>	<sup>13</sup> C NMR spectrum of <b>8</b> .....	61
<b>Appendix 55.</b>	<sup>1</sup> H NMR spectrum of <b>10</b> .....	62
<b>Appendix 56.</b>	<sup>13</sup> C NMR spectrum of <b>10</b> .....	62
<b>Appendix 57.</b>	<sup>1</sup> H NMR spectrum of <b>11</b> .....	63
<b>Appendix 58.</b>	<sup>13</sup> C NMR spectrum of <b>11</b> .....	63
<b>Appendix 59.</b>	<sup>1</sup> H NMR spectrum of absence of <b>20</b> using catalyst <b>18</b> - KO <sup>t</sup> Bu ....	64
<b>Appendix 60.</b>	<sup>1</sup> H NMR spectrum of absence of <b>20</b> using catalyst <b>18</b> - KHMDS .	64
<b>Appendix 61.</b>	<sup>1</sup> H NMR spectrum of <b>12</b> .....	65
<b>Appendix 62.</b>	<sup>1</sup> H NMR spectrum of <b>12</b> .....	65
<b>Appendix 63.</b>	<sup>77</sup> Se NMR spectrum of <b>12</b> .....	66
<b>Appendix 64.</b>	<sup>1</sup> H NMR spectrum of <b>14</b> .....	66
<b>Appendix 65.</b>	<sup>13</sup> C NMR spectrum of <b>14</b> .....	67
<b>Appendix 66.</b>	<sup>1</sup> H NMR spectrum of <b>21</b> using catalyst <b>14</b> .....	68

## Introduction

Chalcogenides are ubiquitous in biological processes.<sup>1,2,3</sup> They often act as highly nucleophilic and redox active species.<sup>4</sup> Sulfur and selenium possess biologically important antioxidant properties that suppress oxidative stress, which likely plays a significant role in many neurodegenerative diseases.<sup>5,6,7,8</sup> The polarizability of these atoms, not only allows for the stabilization of free radicals, but also for ease of bond making and breaking, which are essential properties of any catalyst. For the present work, a sulfenate anion mediated Baylis-Hillman (BH) reaction is in development as an important step toward the utilization these reactive organocatalysts. Complimentary to sulfenate anions, selenolate anions (Se-, **Figure 1**), specifically bulky *ortho-ortho* di-substituted variants; are investigated herein for their ability to function as organocatalysts.

Organocatalysis has emerged in the past several decades as a powerful method for the construction of C-C bonds.<sup>9</sup> Generally, organocatalysts offer good air and water stability, low manufacturing costs, ease of use, ease of functionalization and low toxicity in exchange for moderately higher loadings.<sup>9</sup> The sulfenate anion is not air stable, preventing isolation and storage.<sup>10,11</sup> Sulfenate anions tend to undergo irreversible disproportionation (dimerization); however, it is not well understood how this process occurs. It is well known that sulfenic (RSOH) and related selenic acids (RSeOH) disproportionate readily, losing water to form oxidized disulfide and diselenide bonds.<sup>8,12,13</sup> Typically large bowl-shaped structures are required to prevent disproportionation, thus making it an ongoing challenge in the scientific community to study these transient species.<sup>12,14,15</sup>

Researchers in the Walsh lab are exploring the use of selenium based catalysts **1,2** (without hinderance) shown in **Figure 1**, for their applications as organocatalysts; hence the study of selenium based catalysts in this work. To study steric effects on the rate of disproportionation, **1,3** in **Figure 1** were synthesized. It was hypothesized that adding steric bulk around the chalcogenide center could result in increased catalyst efficiency (higher turnover number), while allowing the necessary chemistry to occur a few atoms removed from the center.



R= Me  
R'= Mesityl  
M<sup>+</sup>= Li, Na, K

**Figure 1.** 2,6-Hindered variants of seleneolate, selenenate and sulfenate anions

Typically, 2.5 mol % – 20 mol % precatalyst (since it is not air stable) is used in sulfenate anion organocatalysis to produce stilbenes and alkynes (**Scheme 1**).<sup>16,17,18</sup> In **Scheme 1**, the sulfenate anion is introduced via precatalyst benzyl sulfoxide **C**, which is deprotonated by base affording **D**. In the absence of aldehyde, **D** will undergo a benzylation with benzyl chloride **B** via an S<sub>N</sub>2 reaction pathway, generating intermediate **E**. Under basic conditions **E** will undergo E2 elimination from the β-hydrogens to afford stilbene **F** and regenerate sulfenate **A**. In the presence of aldehyde **G**, a competition of rates ensues, with **D** preferring addition to aldehyde **G** over benzyl chloride **B** to afford β-hydroxy sulfoxide **H**. Under basic conditions, **H** is deprotonated in the α-position to afford vinyl sulfoxide **I**. Subsequent elimination of the β-hydrogens of **I** affords alkyne **J** and regenerates sulfenate **A**.

It is advantageous to increase efficiency and decrease loadings, so sulfenate (RSO<sup>-</sup>) and selenenate (RSeO<sup>-</sup>) anions become attractive options to the broader scientific community. It is possible that high precatalyst loadings are due to out of cycle processes that destroy the catalyst, not involving disproportionation; however, given the propensity for such processes it is a likely contributor.

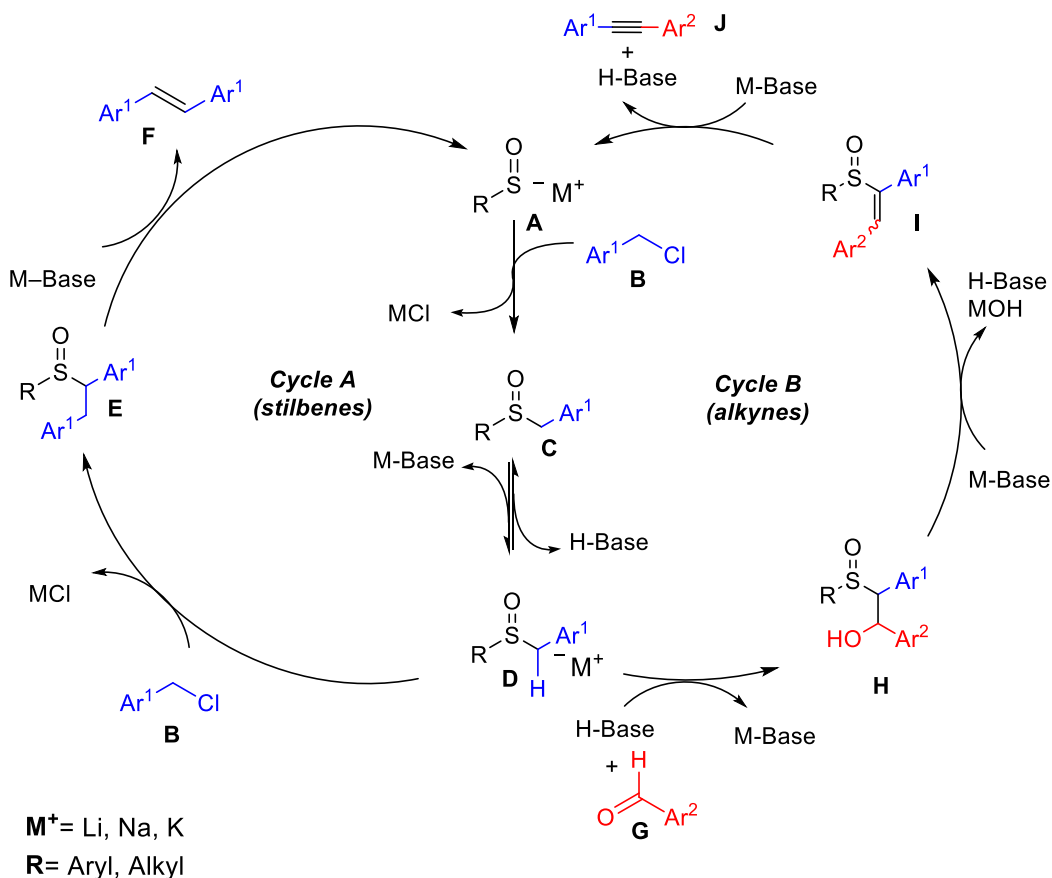
While increasing catalyst efficiency, it is necessary that the steric bulk does not increase the activation energy ( $E_a$ ) of the rate-determining step (RDS), because the reaction will likely stop. In the stilbene synthesis shown in Cycle A of **Scheme 1**, the RDS is known to be the benzylation from intermediate **D** to **E**.<sup>17</sup> Bonding, Not Hydrophobic Effects, Is Implicated.<sup>19</sup> There may be a delicate balance between blocking disproportionation and attenuating catalytic activity, which directed the experimental design to the following approach. Instead of randomly adding different bulky groups and testing results, the experiments were designed to hone in on the solution from established boundaries. Catalysts **1,3** in **Scheme 1** were designed to test small (methyl) and large (mesityl) groups effects in the stilbene reaction.

Depending on the results, either one of three conclusions can be drawn. **1.** If **3** completely shuts down reactivity with small methyl groups then steric protection

is unlikely to yield desired results. **2.** If **1** completely shuts down reactivity with the large mesityl groups, substituent size must be decreased. **3.** If mesityl does not significantly impact reaction yield, the boundary can be increased to include even larger substituents and the process is repeated until an ideal candidate is found. Even though **1** is not an oxide, and does not undergo disproportionation, it can provide valuable information being sterically similar to **2** and still being able to catalyze the stilbene reaction. Experiments show that **1** completely fails to catalyze the reaction and **3** suffers reduced yields at higher loadings, prompting further investigations.

*The objectives are as follows:* To determine if either of the species in **Figure 1** show comparable activity in catalyzing the well-established stilbene reaction at decreased loadings.

**Scheme 1. Previous work using sulfenate anions as organocatalysts by Walsh and co-workers<sup>18</sup>**



There are two ways one can envision the sulfenate and selenenate anion disproportionation's occurring as shown in **Figure 2** and **Figure 3**. In the presence of a proton source (**Figure 2**), the sulfenate could protonate and undergo nucleophilic attack by a second sulfenate to form a thiosulfinate. In the absence of a proton source (**Figure 3**), the two nucleophilic sites, oxygen and

chalcogen combine and disproportionate. Reported sulfenic acid  $pK_a$  values cast doubt upon **Figure 2** as a dominant mechanism; however, there is some literature evidence for such processes.<sup>16,20</sup> The  $pK_a$  of triptycene (alkyl) sulfenic acids are reported to be 12.5 in 4:1 (v:v)  $\text{CH}_3\text{CN}/\text{H}_2\text{O}$ , compared to *tert*-butyl hydroperoxide  $\sim 14$  under the same conditions.<sup>20</sup> Considering a 4:1 (v:v)  $\text{CH}_3\text{CN}/\text{H}_2\text{O}$  is likely increasing the  $pK_a$  in relation to pure  $\text{H}_2\text{O}$  and aromatic sulfenic acids are expected to several orders of magnitude more acidic than alkyl analogues; it is highly unlikely that there will be an acid-base equilibrium between  $\text{H}_2\text{O}$  and an aromatic sulfenate as shown in **Figure 2**.<sup>20</sup>

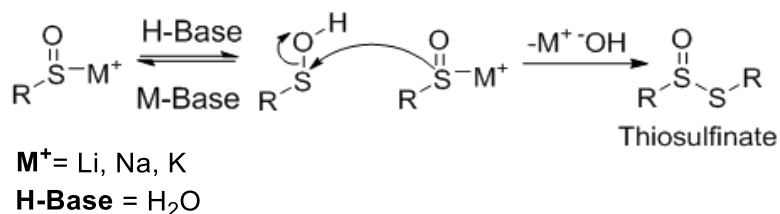
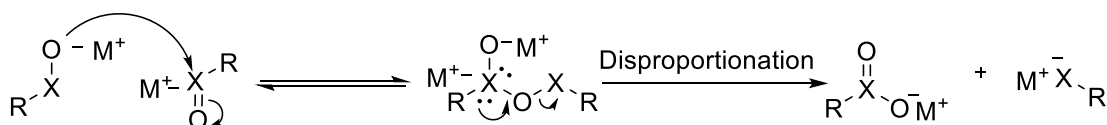


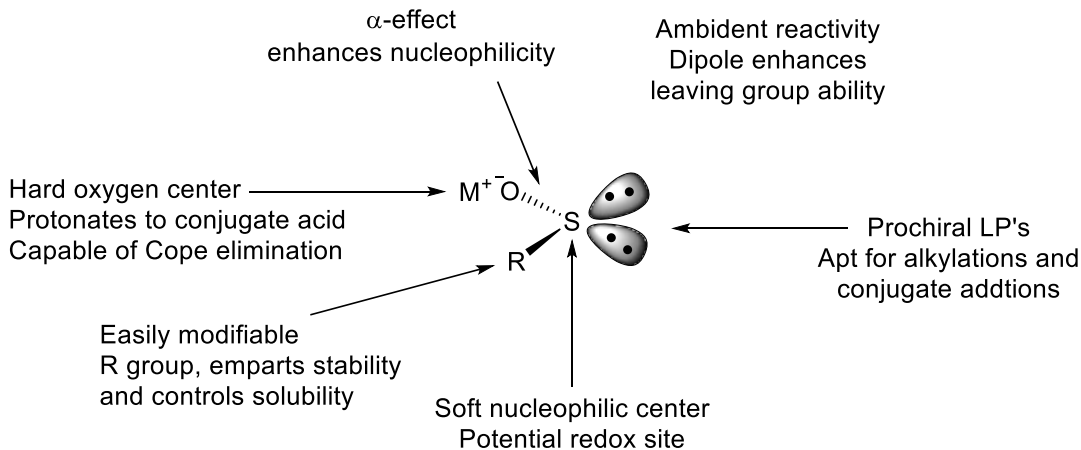
**Figure 2.** Sulfenate anion disproportionation in the presence of a proton source



$\text{X} = \text{S, Se}$   
 $\text{R} = \text{Ar, Alkyl}$   
 $\text{M}^+ = \text{Li, Na, K}$

**Figure 3.** Proposed disproportionation mechanism between two chalcogenide oxyanions

The sulfenate anion possess a plethora of unique and desirable properties for C-C bond formation shown in **Figure 4**. These include a soft nucleophilic sulfur center which readily alkylates and in this work, undergoes conjugate additions. The sulfenate anion possess a strong dipole, often drawn as a zwitterion that enhances its leaving group ability and allows the oxygen to function as proton acceptor and donor. The organic fragment (**R**) offers steric protection and controls solubility in organic media. Unique features include prochiral lone pairs that offer great potential for stereoselective catalysis, and vicinal heteroatoms that enhance reactivity due to an  $\alpha$ -effect.<sup>21</sup> The history of such species has been regarded as esoteric and thus the catalytic potential has largely been overlooked by the broader scientific community.<sup>16,19</sup> This may be, in part, due to the focus on the biologically important sulfenic acids that are used in redox singling processes; however, in recent years there has been a resurgence of sulfenate anion research.<sup>16,17,18,22,23,24,25</sup>



$M^+$  = Li, Na, K

R = Aryl or Alkyl

**Figure 4.** General properties of a sulfenate anion

The combination of sulfenate anion and BH chemistry provides a unique opportunity to explore a prochiral chalcogenide in conjugate addition reactions. Chalcogenides have been utilized with strong Lewis acids to afford BH products with limited success.<sup>26</sup> The first example of a sulfenate anion being utilized as an organocatalyst for stilbene formation was developed by the Walsh lab at the University of Pennsylvania.<sup>17</sup> Walsh and co-workers have shown the sulfenate anion has a dualistic nature, behaving as a good nucleophile and leaving group, similar to an N-heterocyclic carbene.<sup>17,27</sup>

*The objectives aimed to identify ideal conditions of the BH reactions are as follows:* **1.** Find a precatalyst that can introduce the sulfenate anion in a way that diminishes side-reactions and permits straightforward testing of conditions (solvent, temperature and concentration). **2.** Use the identified conditions in the reactions of  $\alpha$ ,  $\beta$ -unsaturated nitriles, ketones and esters with neutral unhindered aldehydes (benzaldehyde). **3.** Complete High-Throughput screening using optimized conditions to develop substrate scope. Developing substrate scope encompasses the possible combinations of activated alkenes and substituted aldehydes that the sulfenate can catalyze.

The optimization of this process was expected to be rather difficult, because it represents a new application of an understudied species on a notoriously difficult reaction that typically takes days to afford products (due to the reversibility of the processes), while introducing extra variables in the form of a precatalyst and any additives that are required for cleavage.

There are a several examples of sulfenate anions generated as reagents to prepare enantioenriched aryl and alkyl-sulfoxides.<sup>23,24,28,29</sup> However, there are only two examples of the sulfenate anion used as an organocatalyst to construct  $sp$  and  $sp^2$  C-C bonds as shown in **Scheme 1**. Using inspiration from previous works in **Scheme 1**, it is proposed that either fluoride or strong base mediated

cleavage of sulfoxide precatalyst shown in **5** yields sulfenate anion **A**.<sup>11</sup> The sulfenate anion **A** performs a reversible conjugate addition onto the  $\beta$ -carbon of the activated alkene **B**. The anionic **A-B** adduct performs a reversible aldol addition to the aldehyde **E** to generate adduct **C**. A reversible proton transfer from a product molecule **4**, to adduct **C** ensues, followed by irreversible E2 elimination of adduct **D** to generate sulfenate **A** and allylic alcohol **4**.<sup>30</sup>

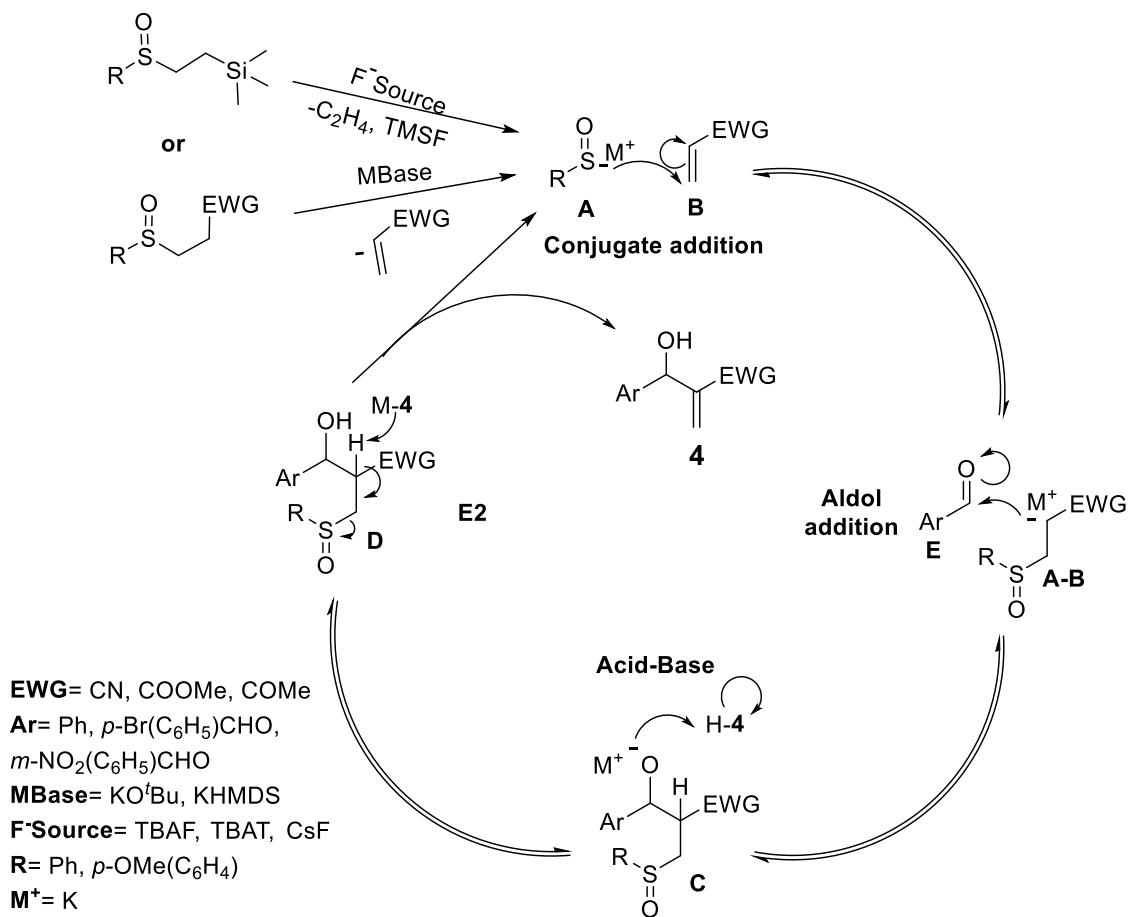
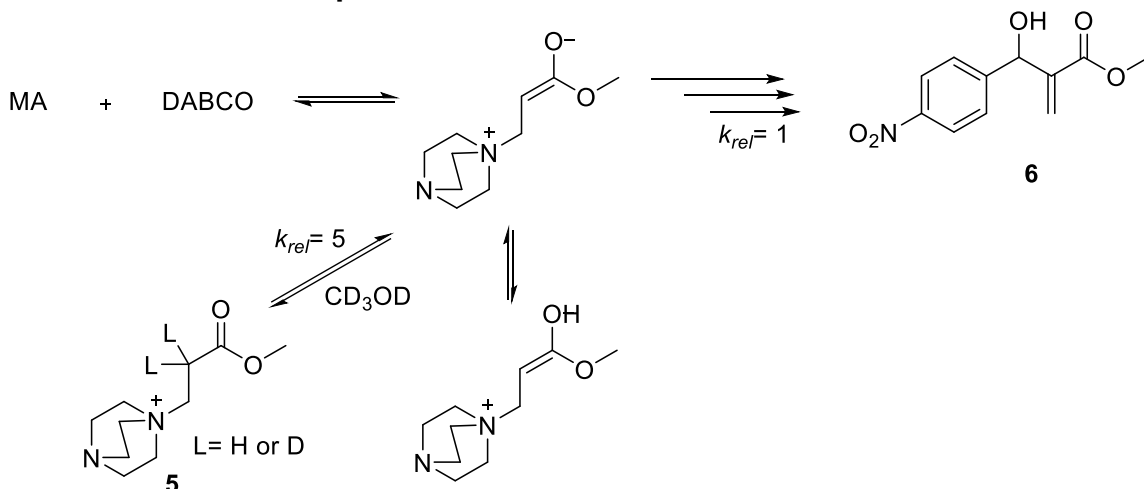


**Figure 5.** Proposed sulfenate anion catalyzed Baylis-Hillman mechanism

In recent literature Singleton and Plata have shown that deuterium incorporation (**Scheme 2**) to unreacted methyl acrylate in *d*<sub>4</sub>-methanol was “extensive”. When product **6** reached in 18% yield, 85% of adduct **5**’s  $\alpha$ -protons were deuterated (followed by <sup>1</sup>H NMR).<sup>31</sup> This is notable when considering a sulfenate anion catalyzed BH reaction, because the sulfenate-acrylic adduct **A-B** in **Figure 3** is not zwitterionic and therefore may be protonated irreversibly; consuming the catalyst.



**Scheme 2. Singleton and Plata show significant deuterium incorporation in intermediate 5 before product 6 is formed**



It was important to investigate whether entering the BH cycle mid-cycle from precatalysts **7.1**, **7.2** is a viable way to introduce the sulfonate anion **Figure 6**. Understanding the proper base and temperature conditions required to cleave **7.1**, **7.2** is integral to being able to complete full BH cycle. The pKa of the  $\alpha$ -hydrogens of **7.1** in **Figure 6** are  $\sim 35$  (DMSO) compared to  $\sim 32.5$  (DMSO) for the  $\beta$ -hydrogens.<sup>32</sup> A strong base such as a *tert*-butoxide or hexamethyldisilazane would be expected to deprotonate the  $\beta$ -hydrogens first, leading to E2 elimination and generation of the sulfonate anion. However, sulfoxides are known to be good alpha directing groups and therefore may play a factor into what conditions are necessary to achieve full deprotonation.<sup>33</sup>

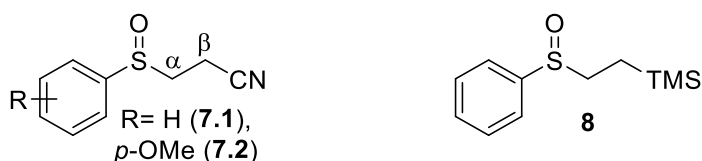


**Figure 6.** Two types of sulfonate anion precatalysts tested in BH reaction

Milder methods, such as introduction by fluoride cleavage using precatalyst **8** in **Figure 6**, are preferable to strong base with **7.1**, **7.2**. Fluoride cleavage studies are subsequently designed to optimize the fluoride source and conditions to cleave precatalyst **8**. Substrates including substituted aldehydes and activated alkenes are tested with the improved conditions generating yield in the BH reaction. Further testing of conditions including temperature, equivalents, solvent and concentration were altered to achieve optimal conditions. These conditions will be used in future experiments to develop a substrate scope and mechanistic study.

## Materials and Methods

**General Methods:** All reactions were carried out under dry nitrogen. Anhydrous grade tetrahydrofuran, dichloromethane, *n*-hexane, dimethylformamide, methanol, and cyclopentyl methyl ether were purchased from Sigma-Aldrich and directly used without purification. Reagents were commercially available and used as purchased without purification unless otherwise noted. Chemicals were purchased from Sigma-Aldrich, Acros, Alfa-Aesar or Matrix Scientific. Benzaldehyde (Sigma-Aldrich, > 99%) and vinyl electrophiles, including methyl acrylate (Sigma-Aldrich, 99%), acrylonitrile (Sigma Aldrich, > 99%) and methyl vinyl ketone (Sigma Aldrich, 99%) were purified by simple distillation prior to use. *p*-Bromobenzaldehyde (Sigma Aldrich, 99%) and *m*-nitrobenzaldehyde (Sigma Aldrich, 99%) were checked for purity by <sup>1</sup>H NMR and used without further purification. The progress of reactions was monitored using thin-layer chromatography using Whatman Partisil K6F 250 μm precoated 60 Å silica gel plates and visualized by short-wave ultraviolet light as well as by treatment with iodine. Flash chromatography was performed with silica gel (230-400 mesh, Silicycle). The NMR spectra were obtained using a Brüker 500 MHz Fourier-transform NMR spectrometer. All <sup>1</sup>H NMR and <sup>13</sup>C NMR were taken in CDCl<sub>3</sub>. Chemical shifts are reported in units of parts per million (ppm) downfield from tetramethylsilane (TMS), and all coupling constants are reported in hertz. The infrared spectra were taken with a Perkin Elmer spectra two FT-IR. High resolution mass spectrometry (HMS) data were obtained on a Waters LC-TOF mass spectrometer (model LCT-XE Premier) using chemical ionization (CI) or electrospray ionization (ESI) in positive or negative mode, depending on the analyte. Melting points were determined on a Unimelt Thomas-Hoover melting point apparatus and were uncorrected.

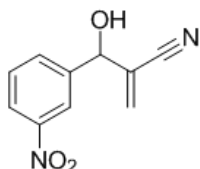
### Determination of crude <sup>1</sup>H NMR allylic alcohol product yields:

Allylic alcohol product yields were determined by integration of the two sp<sup>2</sup> acrylic protons (doublets) and the sp<sup>3</sup> methine (singlet) around 6 ppm against CH<sub>2</sub>Br<sub>2</sub> internal standard. Vinyl electrophiles including acrylonitrile, methyl acrylate and methyl vinyl ketone are evaporated under reduced pressure during normal workup procedures and therefore do not appear in the crude <sup>1</sup>H NMR.

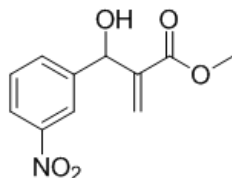
**General procedure for catalysis using precatalysts 7.1 or 7.2 for products 9, 10 and 11:** This Procedure was adapted from the literature.<sup>34</sup> To an oven dried microwave vial equipped with a stir bar was added 2-cyanoethyl phenyl sulfoxide (7.0 mg, 0.033 mmol, 10 mol %), in a nitrogen filled dry box. The microwave vial was sealed with a vial cap with a rubber insert and the sealed vial removed from the dry box. The vial was cooled to -78 °C and stirred. In a separate oven dried microwave vial equipped with a stir bar, base (0.036 mmol) and THF (0.2 mL) were mixed at RT for 5-10 min. The base and THF solution was added dropwise to the sulfoxide at -78 °C and stirred for 20-45 min. To the mixture at -78 °C, benzaldehyde (34.0 μL 0.34 mmol) and acrylonitrile (43.7 μL 0.67 mmol) were added sequentially and stirred for 1.5 h. The mixture was warmed RT and

allowed to stir for 18 h. After 18 h the mixture was diluted in CH<sub>2</sub>Cl<sub>2</sub> (2 mL) and H<sub>2</sub>O (2 mL), shaken and the bottom organic layer was pipetted out of the vial. The volatiles were removed under reduced pressure before acquiring the <sup>1</sup>H NMR spectrum.

**General procedure for catalysis using precatalyst 8 for products 12, 13 or 14:** To an oven dried microwave vial equipped with a stir bar was added phenyl 2-(trimethylsilyl)ethyl sulfoxide (9.0 mg, 0.04 mmol, 20 mol %), tetra-*n*-butylammonium fluoride (0.12 mL, 0.12 mmol, 1 M in THF) and THF (0.38 mL) in a nitrogen filled dry box. The microwave vial was sealed with a vial cap with a rubber insert and the sealed vial removed from the dry box followed by stirring at 40 °C for 30 min. The solution was cooled to RT and transferred via 1 mL plastic syringe into an oven dried microwave vial equipped with a stir bar containing activated alkene (3 equiv., 0.6 mmol) and aldehyde (1 eq, 0.2 mmol). The solution was stirred at RT for 18 h. The sealed vial was opened to air and the reaction mixture was passed through a short pad of silica gel. The pad was then rinsed with 10 mL of a 9:1 dichloromethane:methanol mixture. The volatiles were removed under reduced pressure before acquiring the <sup>1</sup>H NMR spectrum.



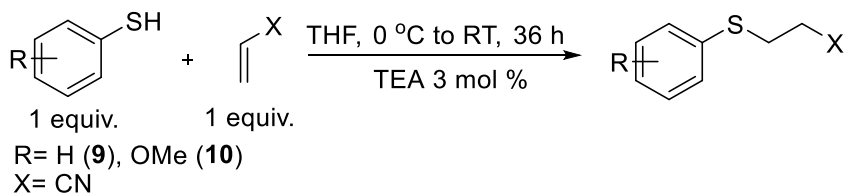
**2-[Hydroxy-(3-nitro-phenyl)-methyl]-acrylonitrile 13:** The crude oil was purified by column chromatography to yield 2-[hydroxy-(3-nitro-phenyl)-methyl]-acrylonitrile as a yellow oil (106.0 mg, 0.52 mmol, 47%). The spectroscopic data match the previously reported data.<sup>48</sup>



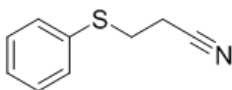
**2-[Hydroxy-(3-nitro-phenyl)-methyl]-methyl acrylate 14:** The crude oil was purified by column chromatography to yield 2-[hydroxy-(3-nitro-phenyl)-methyl]-methyl acrylate as a light-yellow oil (96.0 mg, 0.40 mmol, 37.0% yield). The spectroscopic data match the previously reported data.<sup>50</sup>

## Sulfide preparation

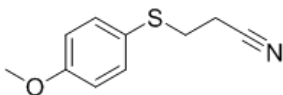
### Scheme 3. General sulfide preparation



This Procedure was adapted from the literature.<sup>35</sup> To an oven-dried 8 mL vial equipped with a stir bar, was added tetrahydrofuran (1 mL), acrylonitrile (196.5  $\mu$ L, 3.0 mmol), and thiol (3.0 mmol). The mixture was stirred and cooled to 0 °C. To the mixture at 0 °C, triethylamine (12.5  $\mu$ L, 0.09 mmol) was added. The solution was warmed to RT and stirred for 36 h. After 36 h, the solution was diluted in EtOAc (30 mL) and extracted with 5% aqueous NaOH (1x 30 mL), H<sub>2</sub>O (2x 30 mL), and brine (1x 30 mL). The organic phase was dried over MgSO<sub>4</sub> and concentrated under reduced pressure.



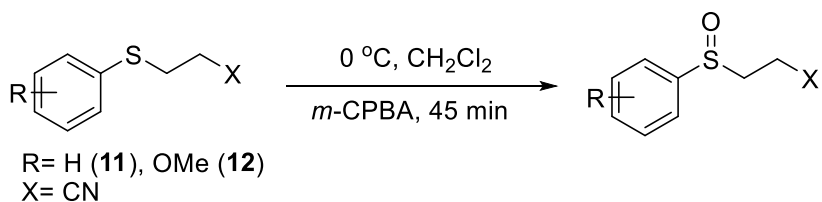
**2-Cyanoethyl phenyl sulfide 7.1 a:** The product, 2-cyanoethyl phenyl sulfide was obtained as a colorless oil (570.0 mg, 116.5% yield\*) and did not require further purification. The spectroscopic data match the previously reported data.<sup>36</sup>  
\* The product is > 99% pure by <sup>1</sup>H NMR. Excess yield resulted from using a plastic mL syringe to measure several hundred  $\mu$ L amounts. After realizing the accuracy was not ideal, the 100  $\mu$ L syringe was utilized successively thereafter for amounts over 100  $\mu$ L. This error was an isolated incident.



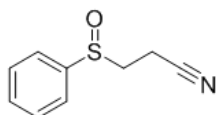
**2-Cyanoethyl *p*-methoxyphenyl sulfide 7.2 a:** The crude oil was purified by column chromatography to yield 2-cyanoethyl *p*-methoxyphenyl sulfide as a colorless oil (450.0 mg, 77.7% yield). <sup>1</sup>H-NMR (CDCl<sub>3</sub>):  $\delta$ = 7.40 (d, 2H, *J*=8.75 Hz) 6.87 (d, 2H, *J*=8.75Hz) 3.79 (s, 3H) 2.98 (t, 2H *J*=7.31, 6.8 Hz) 2.51 (t, 2H *J*=7.31, 6.8 Hz) ppm. <sup>13</sup>C-NMR (CDCl<sub>3</sub>):  $\delta$ = 160.01, 135.03, 123.28, 118.21, 115.01, 55.41, 31.84, 18.21 ppm. IR (cm<sup>-1</sup>): 2939, 2250 1590 1570 1592 1243. MS (EI) *m/z* = Calculated for C<sub>10</sub>H<sub>11</sub>NOS, 194.1 Found: 194.1.

## Sulfoxide precatalyst preparation

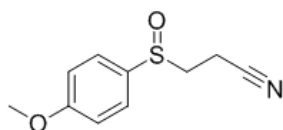
### Scheme 4. General sulfide oxidation preparation



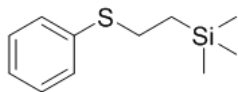
This Procedure was adapted from the literature.<sup>37</sup> To an oven-dried 20 mL vial equipped with a stir bar was added sulfide (1.0 mmol) and CH<sub>2</sub>Cl<sub>2</sub> (10 mL). The mixture was stirred and cooled to 0 °C in air. *Meta*-chloroperoxybenzoic acid 72.5% in H<sub>2</sub>O (241.0 mg, 1.39 mmol) was added over the course of 2 min. After the addition was complete, the solution was allowed to warm to RT over the course of 45 min. After 45 min mixing, the solution was diluted with 30 mL CH<sub>2</sub>Cl<sub>2</sub> and extracted with 30 mL NaOH (0.5 M). The organic layer was separated and set aside. The aqueous layer was extracted twice more with CH<sub>2</sub>Cl<sub>2</sub> (30 mL) before combining the organic layers. The organic layers were dried over MgSO<sub>4</sub> and evaporated to dryness.



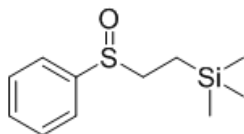
**2-Cyanoethyl phenyl sulfoxide 7.1:** The crude oil was purified by column chromatography to yield 2-cyanoethyl phenyl sulfoxide as a white solid (100.0 mg, 0.56 mmol, 56% yield). The spectroscopic data match the previously reported data.<sup>38</sup>



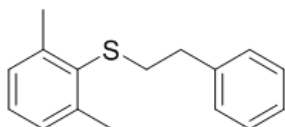
**2-Cyanoethyl *p*-methoxyphenyl sulfoxide 7.2:** The crude oil was purified by column chromatography to yield 2-cyanoethyl *p*-methoxyphenyl sulfoxide as a colorless oil (145.0 mg, 0.69 mmol, 69% yield). <sup>1</sup>H-NMR (CDCl<sub>3</sub>): δ= 7.53 (d, 2H, *J*=8.74 Hz), 7.07 (d, 2H, *J*=8.79 Hz) 3.86 (s, 3H) 3.15 (m, 1H) 2.87 (m, 2H) 2.52 (m, 1H) ppm. <sup>13</sup>C-NMR (CDCl<sub>3</sub>): δ= 162.55, 132.13, 125.83, 117.32 115.21, 55.62, 50.56, 9.75 ppm. MS (EI) *m/z* = Calculated for C<sub>10</sub>H<sub>11</sub>NO<sub>2</sub>S, 210.0 Found: 210.0.



**2-(Trimethylsilyl)ethyl sulfide 8 a:** This Procedure was adapted from the literature.<sup>39</sup> To an oven-dried 20 mL vial equipped with a stir bar, azobisisobutyronitrile (57.0 mg, 0.35 mmol) was added in a nitrogen filled dry box. To the vial under nitrogen a RT was added vinyl trimethylsilane (4.77 mL, 32.8 mmol), and thiophenol (3.0 mL, 29.3 mmol). The neat mixture was heated to reflux at 65 °C under nitrogen for 18 h. The mixture was cooled to RT, exposed to air and transferred into a 25 mL RBF. Excess vinyl trimethylsilane was distilled off by short path distillation at 65 °C. A colorless oil was recovered (6.15 g, 29.3 mmol) and was used without further purification. The spectroscopic data match the previously reported data.<sup>39</sup>

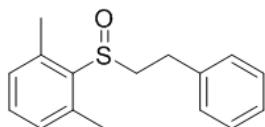


**2-(Trimethylsilyl)ethyl sulfoxide 8:** In an oven-dried 250 mL round bottom flask equipped with a stir bar, was added 2-(trimethylsilyl)ethyl sulfide (6.15 g, 29.3 mmol) and methanol/H<sub>2</sub>O 95:5 (101 mL : 5.4 mL). The solution was stirred and cooled to 0 °C in air. At 0 °C sodium periodate (6.63 g, 31.0 mmol) was added over the course of 2 min, forming a white suspension. After the addition was complete, the suspension was allowed to warm to RT for 18 h. The white suspension was transferred to a 500 mL separatory funnel. In the 500 mL separatory funnel the reaction mixture was diluted with CH<sub>2</sub>Cl<sub>2</sub> (50 mL) and extracted with aqueous sodium thiosulfate (50 mL). The organic layer was set aside and the aqueous layer was extracted with CH<sub>2</sub>Cl<sub>2</sub> (50 mL). The combined organic layers were extracted with sodium thiosulfate (1x 50 mL) and brine (2 x 50 mL). The organic layer was dried over MgSO<sub>4</sub> and evaporated to dryness. A pale-yellow oil, 2-(trimethylsilyl)ethyl sulfoxide was isolated (6.38 g, 28.2 mmol, 96.3% yield over two steps). The spectroscopic data match the previously reported data.<sup>40</sup>



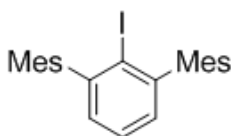
**2,6-Me<sub>2</sub>C<sub>6</sub>H<sub>3</sub>S(C<sub>2</sub>H<sub>4</sub>)Ph 21 a :** To an oven-dried 20 mL vial equipped with a stir bar was added 2,6-dimethylbenzenethiol (199.8 mg, 1.5 mmol), potassium *tert*-butoxide (179.5 mg, 1.6 mmol) and dimethylformamide (7.5 mL) in a nitrogen

filled dry box. The vial was removed from the dry box and stirred at RT. To the mixing solution 2-bromoethybenzene (409.7  $\mu$ L, 3 mmol) was added. The mixture was heated to reflux for 18 hours. After 18 h, the mixture was cooled to RT. The mixture was diluted in EtOAc (30 mL). Dimethylformamide was extracted into the aqueous layer with H<sub>2</sub>O (3x 30 mL). The organic layer was dried over MgSO<sub>4</sub> and evaporated under reduced pressure. The crude oil, 2,6-Me<sub>2</sub>C<sub>6</sub>H<sub>3</sub>S(C<sub>2</sub>H<sub>4</sub>)Ph (269.0 mg, 1.11 mmol, 74.1% yield) was used without further purification.



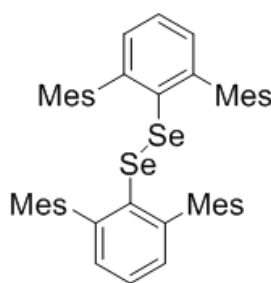
**2,6-Me<sub>2</sub>C<sub>6</sub>H<sub>3</sub>SO(C<sub>2</sub>H<sub>4</sub>)Ph 21:** To an oven-dried 20 mL vial equipped with a stir bar was added 2,6-Me<sub>2</sub>C<sub>6</sub>H<sub>3</sub>S(C<sub>2</sub>H<sub>4</sub>) Ph (269.0 mg, 1.11 mmol) and CH<sub>2</sub>Cl<sub>2</sub> (13.3 mL). The mixture was cooled to 0 °C and mixed in air. To the mixture at 0 °C was added *meta*-chloroperoxybenzoic acid 72.5% in H<sub>2</sub>O (320.5 mg, 1.44 mmol) over 2 min. After the addition was complete, the solution was allowed to warm to RT over the course of 1 h. After 1 h the solution was diluted with 30 mL CH<sub>2</sub>Cl<sub>2</sub> and extracted with 30 mL aqueous NaOH (0.5 M). The organic layer was separated and set aside. The aqueous layers were extracted twice more with CH<sub>2</sub>Cl<sub>2</sub> (30 mL) before combining the organic layers. The organic layers were dried over MgSO<sub>4</sub> and evaporated to dryness. The crude oil 2,6-Me<sub>2</sub>C<sub>6</sub>H<sub>3</sub>SO(C<sub>2</sub>H<sub>4</sub>)Ph was purified by column chromatography to yield a colorless oil (191.0 mg, 0.74 mmol, 67% yield). <sup>1</sup>H-NMR (CDCl<sub>3</sub>):  $\delta$ = 7.28 (m, 2H) 7.22 (m, 4H) 7.02 (d, 2H, *J*= 8.4 Hz) 3.53 (m, 1H) 3.15 (m, 1H) 3.03 (m, 2H) 2.53 (s, 6H) ppm. <sup>13</sup>C-NMR (CDCl<sub>3</sub>):  $\delta$ = 138.77, 138.21, 137.94, 130.75, 130.16, 128.67, 128.40, 126.65, 53.65, 29.95, 19.11 ppm.

### Selenide catalyst preparation



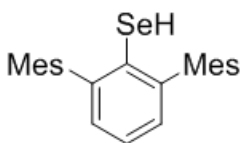
**2,6-Dimesityliodobenzene 16:** This Procedure was adapted from the literature.<sup>41</sup> In an oven-dried 3 neck 250 mL flask equipped with a stir bar and reflux condenser, was added freshly distilled 1,3-dichlorobenzene (1.48 mL, 13 mmol) and THF (40.5 mL) under nitrogen. The solution was cooled to -78 °C and *n*-BuLi (2.5 M in hexanes, 5.4 mL, 13.5 mmol) was added over 30 min via 6 mL plastic syringe under positive nitrogen pressure. The resulting white suspension was then stirred for 90 min at -78 °C. To the white suspension at -78 °C was added 2-mesitylmagnesium bromide (1M in THF, 32.5 mL, 32.5 mmol) via three 12 mL syringes to the suspension at -78 °C under positive nitrogen pressure over

2 h. The resulting brown suspension was warmed to RT for 18 h. After 18 h, the solution was refluxed for 2 h, then cooled to 0 °C. At 0 °C iodine (8.25 g, 32.5 mmol) in 32.5 mL of THF was added via three 12 mL syringes over 1 h to the solution. The solution was allowed to warm to RT and stirred 18 h. After 18 h, the reaction was quenched with a saturated aqueous solution of sodium thiosulfate (50 mL). The solution was transferred to a 250 mL separatory funnel. The organic layer was extracted and set aside. The aqueous layer was extracted with diethyl ether 3x (50 mL). The combined organic phases were dried over MgSO<sub>4</sub>. Removal of the solvent under vacuum gave the crude product as a white solid that was recrystallized from approximately 500 mL ethanol (> 99.5%). The product 2,6-dimesityliodobenzene was obtained as a white crystalline solid in 52.4% yield (3.0 g, 6.81 mmol). The spectroscopic data match the previously reported data.<sup>41</sup>

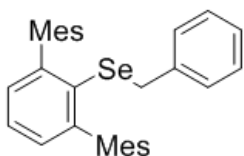


**(2,6-Mes<sub>2</sub>C<sub>6</sub>H<sub>3</sub>Se)<sub>2</sub> 17:** This procedure was adapted from the literature.<sup>42</sup> In an oven-dried Schleck flask (100 mL) equipped with a stir bar was added 2,6-dimesityliodobenzene (1.23 g, 2.8 mmol) and hexanes (30 mL) under nitrogen. To the solution at RT was added *n*-BuLi (2.5 M in hexanes, 1.15 mL, 2.85 mmol) via 6 mL syringe under positive nitrogen pressure and stirred 18 h. After 18 h, the volume of the suspension was reduced to 15 mL under reduced pressure and the white solid was filtered off via cannula filtration. The remaining white solid was dissolved in THF (20 mL), and cooled to -78 °C. At -78 °C selenium powder was added through a funnel into the septa opening with nitrogen backflow. The black suspension was stirred 18 h and allowed to warm to RT. After 18 h, aqueous hydrochloric acid (7.5 mL, 5%) was added to the suspension and the stirring was extended for another 2 h. After 2 h, the mixture was extracted with CHCl<sub>3</sub> (3 x 25 mL). The organic phases were combined and extracted with H<sub>2</sub>O (1 x 25 mL) and brine (1 x 25 mL). The organic phase was dried over MgSO<sub>4</sub> and evaporated under reduced pressure. The crude product (2,6-Mes<sub>2</sub>C<sub>6</sub>H<sub>3</sub>Se)<sub>2</sub> an orange waxy solid (0.70 g, 0.89 mmol, 63.6% yield) was used without further purification.





**2,6-Mes<sub>2</sub>C<sub>6</sub>H<sub>3</sub>SeH 18:** This Procedure was adapted from the literature.<sup>42</sup> In an oven-dried Schleck flask (100 mL) equipped with a stir bar was added crude (2,6-Mes<sub>2</sub>C<sub>6</sub>H<sub>3</sub>Se)<sub>2</sub> (0.70 g, 0.89 mmol) under nitrogen. To the solid was added THF (20 mL) via cannula. The mixing solution was added via cannula over 2 min to a solution of LiAlH<sub>4</sub> (152.0 mg, 4.0 mmol) in THF (10 mL) under nitrogen at 0 °C. The resulting grey suspension was stirred for 1 h at 0 °C. After 1 h, the solution was exposed to air and cautiously poured onto ice-water. The ice was cautiously melted using a heat gun and extracted with CHCl<sub>3</sub> (3 x 25 mL). The organic layers were combined and extracted with H<sub>2</sub>O (1 x 25 mL) and brine (1 x 25 mL). The organic phase was dried over MgSO<sub>4</sub> and evaporated under reduced pressure. The crude product was recrystallized from *n*-hexane to afford yellow crystals and further purified by column chromatography using pure hexanes to yield a white solid 2,6-Mes<sub>2</sub>C<sub>6</sub>H<sub>3</sub>SeH (91.0 mg, 0.23 mmol, 12.9% yield). The spectroscopic data match the previously reported data.<sup>42</sup>



**2,6-Mes<sub>2</sub>C<sub>6</sub>H<sub>3</sub>SeBn 19:** To an oven-dried microwave vial equipped with a stir bar was added 2,6-Mes<sub>2</sub>C<sub>6</sub>H<sub>3</sub>SeH (39.3 mg, 0.1 mmol), KO<sup>t</sup>Bu (11.8 mg, 0.105 mmol) and DMF (1 mL) in a dry box under nitrogen. The solution was stirred for 10 minutes and then removed from the dry box. After 10 min, benzyl chloride (23.0  $\mu$ L, 0.2 mmol) was added and the solution was mixed at RT under N<sub>2</sub> for 17.5 hours. After 17.5 h, a capillary spotter was entered into the solution under positive nitrogen pressure and a TLC was taken. TLC confirmed no SM had remained. After 17.5 h, the mixture was diluted with EtOAc (15 mL), extracted with H<sub>2</sub>O (3 x 10 mL) and brine (1 x 25 mL). The organic phase was dried over MgSO<sub>4</sub> and evaporated under reduced pressure. The crude product was recrystallized from ethanol (> 99.5%) to afford tan crystals of 2,6-Mes<sub>2</sub>C<sub>6</sub>H<sub>3</sub>SeBn (39.0 mg, 0.08 mmol, 80% yield). <sup>1</sup>H-NMR (CDCl<sub>3</sub>):  $\delta$ = 7.39 (t, 1H, *J*= 7.5 Hz), 7.08 (d, 2H, *J*= 7.5 Hz) 7.04 (m, 3H) 6.95 (s, 4H), 6.77 (d, 2H, *J*= 1.9 HZ), 6.76 (d, 1H, *J*=1.4 Hz) 3.37 (s, 1H) 2.34 (s, 6H) 2.05 (s, 12H) ppm. <sup>13</sup>C-NMR (CDCl<sub>3</sub>):  $\delta$ = 144.04, 137.90, 136.23, 135.07, 134.11, 130.31, 127.51, 127.47, 126.68, 126.45, 124.89, 28.77, 19.50, 19.07 ppm. <sup>77</sup>Se-NMR (C<sub>6</sub>D<sub>6</sub>):  $\delta$ = 314.29 ppm. MS (EI) *m/z* = Calculated for C<sub>31</sub>H<sub>32</sub>Se, 484.17 Found: 484.17.

## High Throughput Screening of 2,6-Me<sub>2</sub>C<sub>6</sub>H<sub>3</sub>SO(C<sub>2</sub>H<sub>4</sub>)Ph:

Procedure adapted from the literature.<sup>18</sup>

### Set up:

Experiments were setup in a glove box under nitrogen atmosphere. A 24-well aluminum block containing 1 mL glass vials was dosed with 1 μmol 2,6-Me<sub>2</sub>C<sub>6</sub>H<sub>3</sub>SO(C<sub>2</sub>H<sub>4</sub>)Ph in THF. The solvent was removed to dryness using a Gene Vac. Base (30 μmol) in THF was added to the vials. The solvent was again removed to dryness using a GeneVac and a parylene stir bar was then added to each reaction vial. Benzyl chloride (10 μmol/vial) and biphenyl (1 μmol/vial, used as an internal standard to measure HPLC yields) were then dosed together into each reaction vial as a solution in each solvent (100 μL, 0.1 M). The 24-well plate was then sealed and stirred for 14 h at 80 °C.

### Work up:

The plate was cooled to room temperature. Upon opened the plate to air, 500 μL of acetonitrile was added into each vial. The plate was covered again and the vials stirred for 10 min to ensure good homogenization. Into a separate 24-well LC block was added 700 μL of acetonitrile, followed by 40 μL of the diluted reactions mixtures. The LC block was then sealed with a silicon-rubber storage mat and mounted on an automated HPLC instrument for analysis.

## Results and Discussion

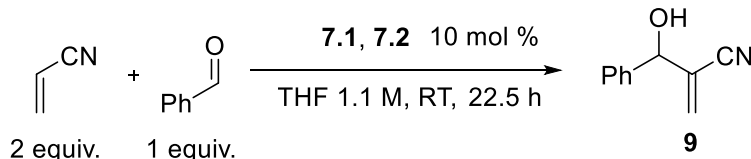
To explore precatalysts that would be compatible with BH conditions, the reaction discovery process was initiated with sulfoxides **7.1** and **7.2** in **Figure 6**. A series of reactions were conducted that aimed at coupling benzaldehyde and acrylonitrile in tetrahydrofuran (THF) at RT for 22.5 h with **7.1** and **7.2** (**Table 1**). Several conditions below were utilized as controls to ensure that the precatalyst would not cleave or undergo chemical reactions in the presence of BH reagents.

In **Table 1**, precatalysts **7.1** and **7.2** were tested without additives, 2,4-dinitrophenol (2,4-DNP, p*K*<sub>a</sub> 4.1) and H<sub>2</sub>O. 2,4-DNP, a weak Brønsted acid that was added to activate the nitriles α-hydrogens via hydrogen bond activation.<sup>43</sup> Hydrogen bonding activation lowers the LUMO (e.g. C-O or C-N π\*) of a hydrogen bond acceptor, such as the Brønsted basic nitrogen of a nitrile by forming an acid-base pair.<sup>44</sup> This places a positive charge through resonance on the carbon of nitrile, which stabilizes anions alpha to the positive carbon, thus decreasing the p*K*<sub>a</sub> of the nitriles α-hydrogens (**Figure 6**). Similarly, water was added to achieve activation unsuccessfully. <sup>1</sup>H NMR peaks corresponding to precatalysts **7.1** and **7.2** had remained, and no peaks of allylic alcohol **9** were observed in the 6-ppm region. It is unknown if any sulfenate anion was cleaved into the reaction under the conditions employed in **Table 1**, since precatalysts **7.1**

and **7.2** remained (as determined by  $^1\text{H}$  NMR spectroscopy). It is not clear whether the reaction did not proceed because the sulfenate failed to catalyze the reaction or was never generated in the first place. Based on these results, it was decided that, establishing precatalyst cleavage conditions was a priority. This experimental uncertainty is addressed below in **Scheme 6**, with experiments designed to test optimal cleavage conditions of **7.2** with strong bases.

As described previously Singleton and Plata have shown that during the BH cycle, the catalyst-methyl acrylate adduct in **Scheme 2** (acrylonitrile in this case) is likely to protonate. Given that the conditions in **Table 1** were unsuccessful in enacting cleavage, it is likely that stronger bases will be needed to activate the precatalysts **7.1** and **7.2**, and prevent the catalyst from being taken out of cycle via protonation; due to the relatively high  $pK_a$  of the  $\beta$ -hydrogens (**Scheme 6**).

**Table 1. BH reaction of acrylonitrile and benzaldehyde with 7.1, 7.2 at RT**



Entry	Vinyl Electrophile	Aldehyde	Additive	Catalyst	Yield of 9 <sup>c</sup> %
1	Acrylonitrile	Benzaldehyde	None	7.1	0
2	Acrylonitrile	Benzaldehyde	None	7.2	0
3	Acrylonitrile	Benzaldehyde	2,4-DNP <sup>a</sup>	7.1	0
4	Acrylonitrile	Benzaldehyde	2,4-DNP	7.2	0
5	Acrylonitrile	Benzaldehyde	H <sub>2</sub> O <sup>b</sup>	7.1	0

[a] 2,4-dinitrophenol 10 mol % [b] 0.1 mL H<sub>2</sub>O [c] Yield based on crude  $^1\text{H}$  NMR

Strong bases including, potassium *tert*-butoxide (KO<sup>t</sup>Bu) and potassium bis(trimethylsilyl)amide (KHMDS) were tested in the BH reaction at RT and 50 °C with **7.1** as shown in **Table 1**. The solvent was changed to cyclopentyl methyl ether (CPME) to avoid evaporation due to the higher temperature and small reaction volumes. As described previously, (**Figure 6**) the base must show a preference for the  $\beta$ -hydrogens over the  $\alpha$ -hydrogens. Reactions at 50 °C (entries 2 and 4) were conducted to push the equilibrium of that process, since cleavage results in an increase in entropy (increase in number of molecules).

Under all conditions tested in **Table 2**, Peaks corresponding to precatalyst **7.1** were not present by  $^1\text{H}$  NMR (entries 1-4). However, it was unclear whether the precatalyst was consumed (deprotonation/alkylation) or cleaved in the process. Product **9** was not observed in the  $^1\text{H}$  NMR either; however, there were peaks corresponding to several other products. Two triplets in low concentration at 2.6 ppm, 3.1 ppm suggested a Stetter reaction between benzaldehyde and vinyl cyanide.<sup>45</sup> The triplet peaks were observed in a BH reaction at 50 °C (**Scheme 5**) to be significant by-products along with a singlet at 6 ppm, likely corresponding to a benzoin product; matching literature chemical shifts.<sup>46</sup> However, LC-MS and

GC-MS of the reaction sample could not confirm the identity products **10** and **11**. A scaled-up isolation of these products are necessary to determine their identity.

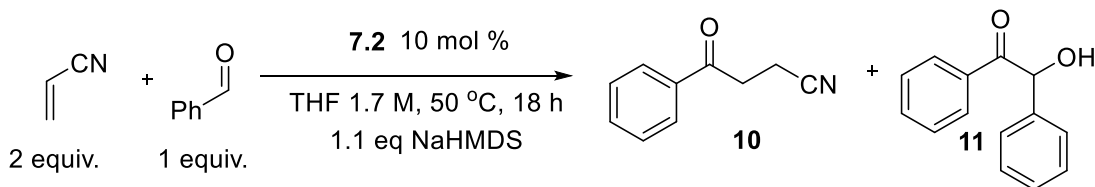
**Table 2. BH reaction of acrylonitrile, benzaldehyde and 7.1 at RT / 50 °C**

3 equiv.      1 equiv.      **9**

Entry	Vinyl Electrophile	Aldehyde	Base <sup>b</sup>	Temperature °C	Yield of 9 <sup>a</sup> %
1	Acrylonitrile	Benzaldehyde	KO <sup>t</sup> Bu	25	0
2	Acrylonitrile	Benzaldehyde	KO <sup>t</sup> Bu	50	0
3	Acrylonitrile	Benzaldehyde	KHMDS	25	0
4	Acrylonitrile	Benzaldehyde	KHMDS	50	0

[a] Yield based on crude <sup>1</sup>H NMR [b] 10 mol %

**Scheme 5. Possible Stetter/Benzoin product in BH at 50 °C**

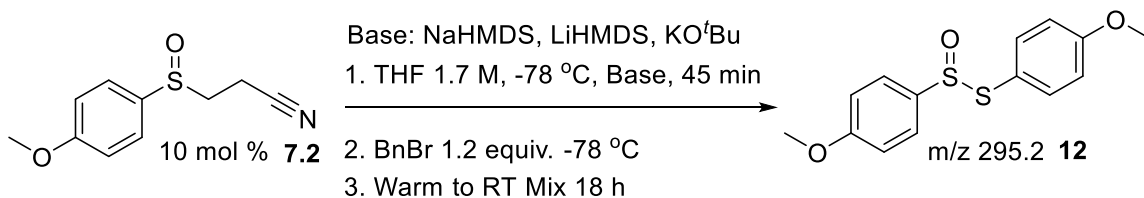


As previously stated, sulfoxides are good directing groups and therefore conditions, such as temperature may need to be altered to achieve deprotonation of either set of methylene protons shown in **Scheme 6**. Since temperatures at RT to 50 °C enacted cleavage of **7.1**, but also afford undesired side-products, the temperature was lowered to -78 °C. By lowering the temperature, it may be possible to favor only the desired transition state (the TS leading to β-elimination), affording sulfenate liberation. Precatalyst **7.2** was utilized to easily distinguish aromatic peaks in the product by its characteristic doublet of doublets pattern (*para*-substitution). This <sup>1</sup>H NMR pattern was helpful in determining the sulfenate preference for alkylation or disproportionation.

Using conditions in **Scheme 6**, sodium bis(trimethylsilyl)amide and lithium bis(trimethylsilyl)amide resulted in consumption of **7.2** as judged by the absence of the methylene protons around 2.8 ppm in crude <sup>1</sup>H NMR. Interestingly, no incorporation of benzyl bromide was observed in either product; however, a thiosulfinate **12** is observed by <sup>1</sup>H NMR that matches previously reported chemical shifts.<sup>47</sup> A molecular ion of *m/z* 295.2 (100% relative abundance) corresponding to thiosulfinate **12** was found using LC-MS. The concentration of reaction in **Scheme 6** is 1.7 M with respect to 1 equivalent of aldehyde (theoretically; however absent), given that **7.2** is at 10 mol %. Under these

conditions potassium *tert*-butoxide was unable to enact cleavage of sulfoxide **7.2**. This finding is concerning, because during the course of a BH reaction (typically without strong base present), there would be no base sufficient to regenerate the sulfenate anion if precatalyst **7.2** reformed during the course of the reaction.

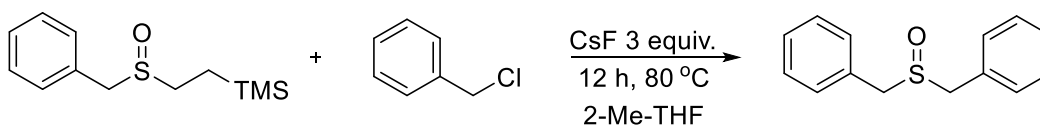
### Scheme 6. Strong base testing cleavage of sulfoxide precatalyst



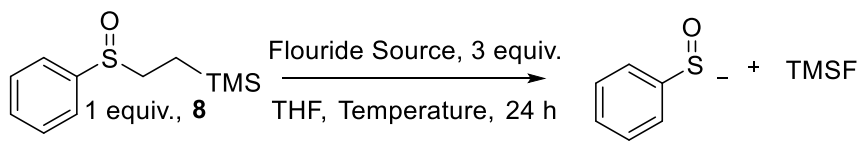
It is a highly likely scenario wherein **7.2** reforms after cleavage via Na or LiHMDS base and the allylic alkoxide (anion of the product) is insufficiently basic (similar to *tert*-butoxide) to regenerate the sulfenate anion, effectively quenching the reaction. The observance of disproportionation product over alkylation under the low temperature conditions (**Scheme 6**), the need to reduce the temperature to enact cleavage and the affinity of the sulfenate for side reactions in the presence of strong base caused us to change our strategy.

The Walsh Lab previously reported palladium-catalyzed arylation of alkyl sulfenate anions utilizing 2-(trimethylsilyl)ethyl sulfoxide (**Scheme 7**). In this work, the sulfenate anion was introduced under mildly basic conditions with fluoride mediated cleavage of the precatalyst.<sup>22</sup> Based on these results, we set out to investigate the fluorine mediated cleavage of 2-(trimethylsilyl)ethyl sulfoxides to introduce the highly reactive sulfenate anion.

### Scheme 7. Palladium catalyzed arylation of sulfenate anions



In palladium catalyzed arylation of sulfenate anions (**Scheme 7**), the Walsh group added 3 equivalents of cesium fluoride to cleave 2-(trimethylsilyl)ethyl benzyl sulfoxide over a 12 h period at 80 °C in 2-Me-THF. Under these conditions, only 15% benzylated product was obtained. Regardless, the conditions were subsequently used to search for a palladium-ligand combination.<sup>22</sup> Similar results were obtained in the present work in **Table 3**. Instead of determining the amount of sulfenate anion generated by trapping with benzyl halides, it is more accurate to measure percent remaining of precatalyst. This is due to the competing disproportionation generating a thiosulfinate, that is not easily observable in <sup>1</sup>H NMR, unless the aryl sulfoxide is substituted (e.g. 4-methoxy).

**Table 3. Cleavage of 2-(trimethylsilyl)ethyl sulfoxide **8** with fluoride**

Entry	F- Source	Temp °C	Time min	Remaining ( <b>8</b> ) <sup>a</sup> %
1	CsF	40	30	84
2	CsF	40	60	93
3	CsF	80	30	96
4	CsF	80	60	76
5	TBAF	40	30	0
6	TBAF	40	60	0
7	TBAF	80	30	0
8	TBAF	80	60	0
9	TBAT	40	30	73
10	TBAT	40	60	43
11	TBAT	80	30	0
12	TBAT	80	60	0

[a] Percent remaining of **8** determined by <sup>1</sup>H NMR of the crude reaction mixture using CH<sub>2</sub>Br<sub>2</sub> as internal standard [b] All reactions were in THF at 0.4 M with respect to a 1 mmol scale of limiting reagent

Three different fluoride sources, including cesium fluoride (CsF), tetra-*n*-butylammonium fluoride (TBAF) and tetrabutylammonium difluorotriphenylsilicate (TBAT) were screened at 40 °C for 30min, 40 °C for 60 min, 80 °C for 30 min and 80 °C for 60 min. The percentage remaining of precatalyst **8** was determined by integration of methylene protons in <sup>1</sup>H NMR thereafter. The fluoride source screen (**Table 3**) showed a high percentage remaining of CsF (entries 1–4), presumably due to poor solubility in THF. Both TBAF (entries 5–8) and TBAT (entries 9–12) showed promising results at elevated temperatures giving complete cleavage.

Although TBAF showed complete cleavage at 80 °C and 40 °C, it is not ideal to use because it is sold as the hydrate (in THF) from Sigma Aldrich. This limits reaction solvent choices, especially when at 3 equivalents loading, because the reaction is essentially always in THF. It is more desirable to have TBAT, a white powder that can be easily dosed, cleaves slowly throughout the reaction, is anhydrous and cost-effective. It was not evident that TBAF would be less desirable prior to testing, and since it cleaved the precatalyst completely under all conditions tested, it was utilized. The concentration was chosen to be 0.4 M, because it allowed for accurate transfer of the TBAF and precatalyst mixture into the reaction vial at mmol scales.

Electron-withdrawing aldehydes showed the most promise in the BH reaction. Furthermore, various proton sources including phenols have been utilized in BH reactions serving to both activate electrophile and to as a proton source for acid-

base equilibrium step **C-D** in **Figure 5**.<sup>43</sup> Initial success was achieved using 3-nitrobenzaldehyde with 4-bromophenol as additive (**Scheme 8**). Under the conditions in **Scheme 8**, precatalyst **8** (20 mol %) was cleaved at 40 °C prior to addition to the reaction mixture, which was heated to 40 °C for 18 h. Under identical conditions without the phenolic additive, the yield remained similar (51.5 vs. 54%), therefore the 4-bromophenol was not necessary as previously thought.

A scaled-up reaction at 1.1 mmol (compared to 0.2 mmol) was conducted utilizing identical conditions as in **Scheme 8**. This afforded a crude (two product) isolated yield (47%). By relative integration of <sup>1</sup>H NMR peaks yield of product **13** were, 35% and byproduct 12% (identity confirmed by <sup>1</sup>H, <sup>13</sup>C NMR).<sup>48</sup> The column conditions need to be optimized further; however, the byproduct in 15% yield appears as two triplets at 2.8 ppm and 3.4 ppm. These peaks likely correspond to sulfone **7.3**.<sup>49</sup> The sulfenate anion is extremely air sensitive and thus likely to oxidize during the course of the reaction.<sup>10</sup> The identity of the triplet byproducts will need to be investigated further to determine the exact structure. It is possible that the oxidation took place during the workup and therefore difficult to know whether or not oxidation is a significant issue in these reactions.

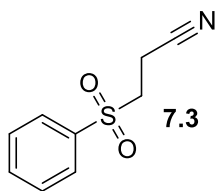
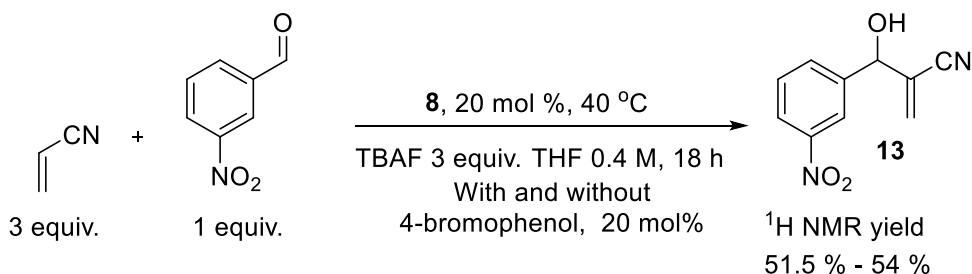


**Figure 7:** Oxidation product of sulfenate anion upon workup

**Scheme 8. BH reaction with **8** to produce nitrile **13****



Vinyl esters were also tested with electron deficient aldehydes as seen in **Scheme 9**. When the reaction was conducted with 3-nitrobenzaldehyde, the yield was 51%, with *para*-bromobenzaldehyde 10% and benzaldehyde <1%. This data suggests that reactions with more electron withdrawing aldehydes resulted in higher yields, most likely due to increased electrophilicity of the aldehydes. A scaled-up reaction at 1.1 mmol (compared to 0.2 mmol) was conducted utilizing identical conditions as in **Scheme 9**, affording a 37% isolated yield of product **14** (identity confirmed by <sup>1</sup>H, <sup>13</sup>C NMR).<sup>50</sup>

### Scheme 9. BH using sulfoxide **8** to produce ester **14**

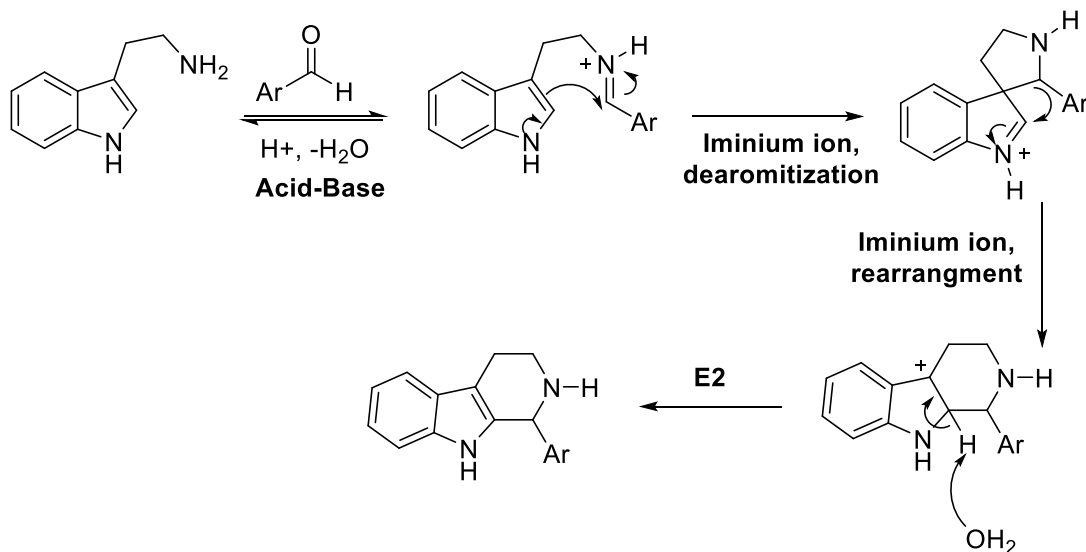
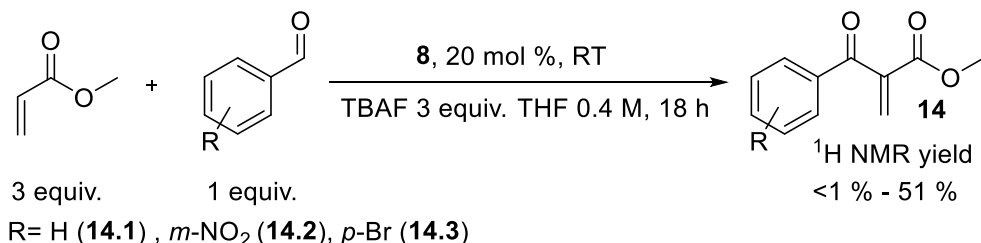


**Figure 8.** Generic Pictet Spengler reaction with iminium cation activation

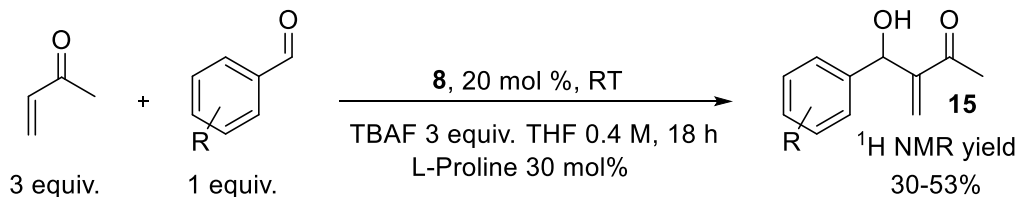
To activate substrates such as ketones and aldehydes L-proline was utilized to create an iminium cation. Iminium cations are intermediates in many reactions, such as the Mannich and Pictet-Spengler (**Figure 8**).<sup>51,52</sup> By introduction of the iminium species the electrophilicity of the aldehyde or ketone is increased, generally resulting in faster reaction rates. Using conditions in **Scheme 10**, benzaldehyde was coupled with acrylonitrile in the presence of L-proline; expecting iminium ion activation. Surprisingly, a decreased <sup>1</sup>H NMR yield of 27% was obtained. The combination of methyl vinyl ketone (MVK) and benzaldehyde is difficult to activate; however, a moderate 30% <sup>1</sup>H NMR yield was obtained with L-proline as additive (**Scheme 10**). Similarly, promising yields were obtained using MVK with 4-bromobenzaldehyde 31%, and 3-nitrobenzaldehyde 53% (**Scheme 10**). Its noteworthy the 30% yield matched the 30 mol % loading of L-proline and therefore additional experiments should be run at higher loadings of L-proline.

Polar solvents are thought to increase the rate of BH reactions by stabilizing the zwitterionic catalyst-vinyl-EWG adduct formed upon conjugate addition of a typical neutral phosphine or amine catalyst.<sup>53</sup> The sulfoxide adduct **A-B** in **Scheme 3** is a highly polar adduct that could potentially benefit from such stabilization. Under identical conditions as in **Scheme 10**, the solvent was



changed to dimethylformamide and methanol. The  $^1\text{H}$  NMR yields decreased significantly to 18% (DMF) and <1% (MeOH) for the methyl vinyl ketone/benzaldehyde combination. Considering increased polarity was not beneficial to the reaction conditions, it may be advantageous to explore less polar conditions. This is however complicated by the fact that TBAF is essentially always in THF/H<sub>2</sub>O. The alternative solid fluoride source, TBAT was explored for its compatibility in the sulfenate catalyzed BH reaction.

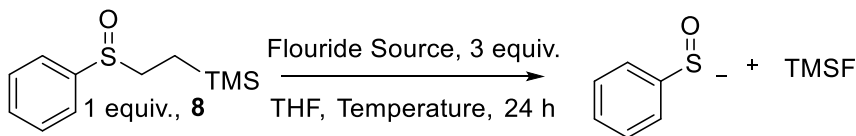
### Scheme 10. BH reaction with L-proline to product ketone 15



R = H (**15.1**), *m*-NO<sub>2</sub> (**15.2**), *p*-Br (**15.3**)

TBAT is an organic soluble hygroscopic white crystalline powder that may allow for further screening of reaction solvents based on results in **Table 4** (entries 9-12). Cleavage conditions were further optimized with TBAT at RT since reactions in **Scheme 9** and **Scheme 10** were conducted at RT. All reactions were run at RT for 24 hours using 1, 2 and 3 equivalents of TBAT at 0.4 M and 1 M concentrations. As shown in **Table 4**, the strategy of increasing the time and decreasing the temperature yielded mixed results. Concentration had little effect on the extent of cleavage, while it is clear in **Table 4** (entries 5 and 6) that 3 equivalents of TBAT were necessary to achieve maximum cleavage around 31–43 %.

**Table 4. Cleavage of 2-(trimethylsilyl)ethyl sulfoxide with TBAT at RT**



Entry	Equivalents of F-	Remaining ( <b>8</b> ) <sup>b</sup> %	Concentration <sup>a</sup> M
1	1	88	0.4
2	1	94	1
3	2	80	0.4
4	2	53	1
5	3	31	0.4
6	3	43	1

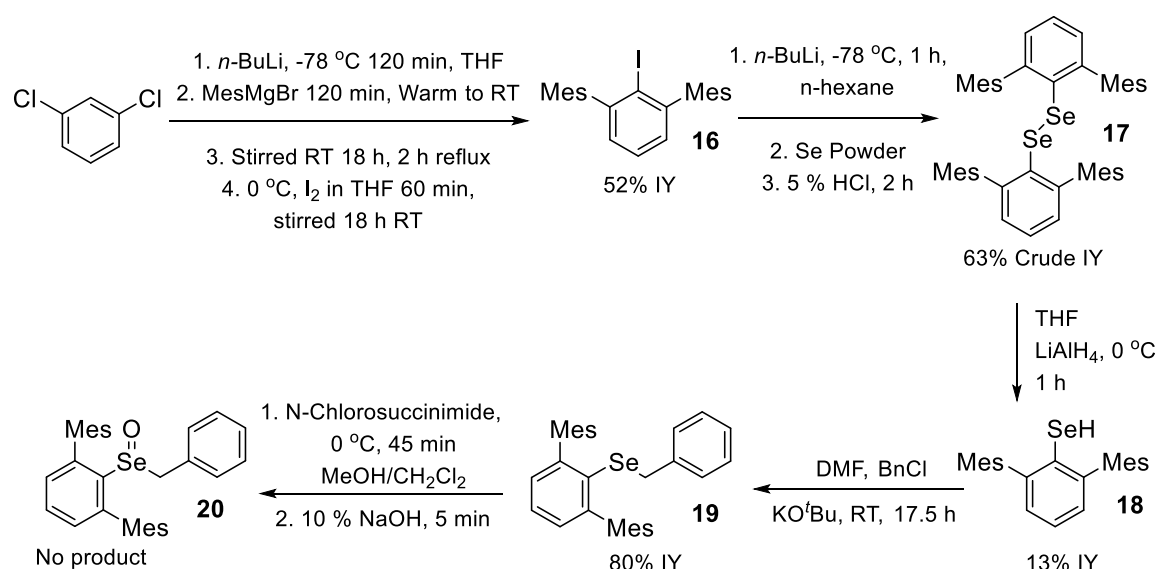
[a] Concentration in THF with respect to a 1 mmol scale of limiting reagent [b] Percent remaining of **8** determined by  $^1\text{H}$  NMR of the crude reaction mixture using CH<sub>2</sub>Br<sub>2</sub> as internal standard

Optimal cleavage conditions in **Table 4** for TBAT mediated cleavage will need to be adapted and utilized in a BH reaction such as in **Scheme 9**. These cleavage conditions will likely serve as a basis for future optimization in the BH reaction. The optimization of sulfenate anion catalyzed BH conditions has not been straightforward thus far. However, with the initial optimization of cleavage conditions complete, and two different vinyl electrophiles generating yield, it is likely that reaction optimization will proceed more readily in future work.

### Synthesis and implementation of hindered chalcogenides as catalysts

To disfavor the disproportionation pathway between two sulfenate anions as observed by thiosulfinate **12** in **Scheme 6**, steric bulk was added to the *ortho*-positions of the catalysts. Adding bulk, such as mesityl, to the *ortho*-positions should increase activation energy ( $E_a$ ) of the disproportionation relative to that of the benzylation.

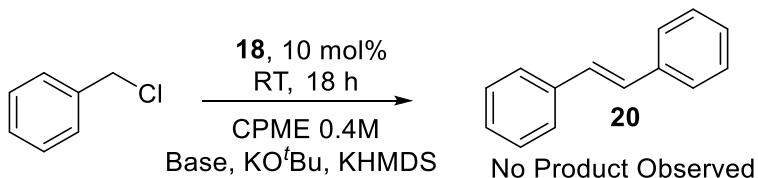
### Scheme 11. Synthesis progress of ortho-ortho hindered chalcogenides <sup>41,42</sup>



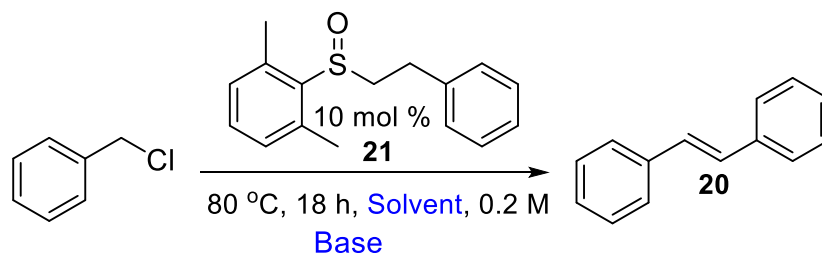
Synthesis of selenide **18**, was conducted according to a known preparation wherein 2,6-dimesityliodobenzene is lithiated with *n*-BuLi via lithium halogen exchange. A benzyne forms which undergoes a nucleophilic attack by MesMgBr, forming **16**. The resulting **16** is lithiated followed by nucleophilic attack on selenium <sup>0</sup>.<sup>41,42</sup> The resulting RSe-SeR product is reduced via LiAlH<sub>4</sub> to afford **18** (**Scheme 11**).<sup>42</sup> The exact structure of RSe-SeR is unknown. Selenide catalyst **18** was tested in a general stilbene reaction (**Scheme 12**), and did not afford any of the desired product **20** with either KO<sup>t</sup>Bu or KHMDS at RT. This may be due to the steric bulk of the catalyst increasing the kinetic barrier ( $E_a$ ) of the RDS. The complete neutralization of the selenium catalyst was a surprise; however, it provided valuable information about how much bulk the catalyst can tolerate before losing activity. Although **18** is not an oxide, it can still provide valuable

information about the stilbene reaction, since selenolates are currently being investigated in the Walsh lab as highly active organocatalysts.

### Scheme 12. Hindered selenide stilbene experiment using **17**



To access selenoxide **20**, an oxidation using N-chlorosuccinimide was conducted. After oxidation of **19** with N-chlorosuccinimide, product **20** did not show the expected methylene doublet of doublets around 4 ppm in the crude <sup>1</sup>H NMR. This may be due to selenide **19** having different sterics and electronics than a typical benzyl phenyl selenide. Oxidation by *meta*-chloroperoxybenzoic acid (*m*-CPBA) is likely to yield better results in the future, as the mild conditions (weak base workup) are unlikely to cause any issues.



### 2,6-dimethylbenzenesulfenate HTE screen

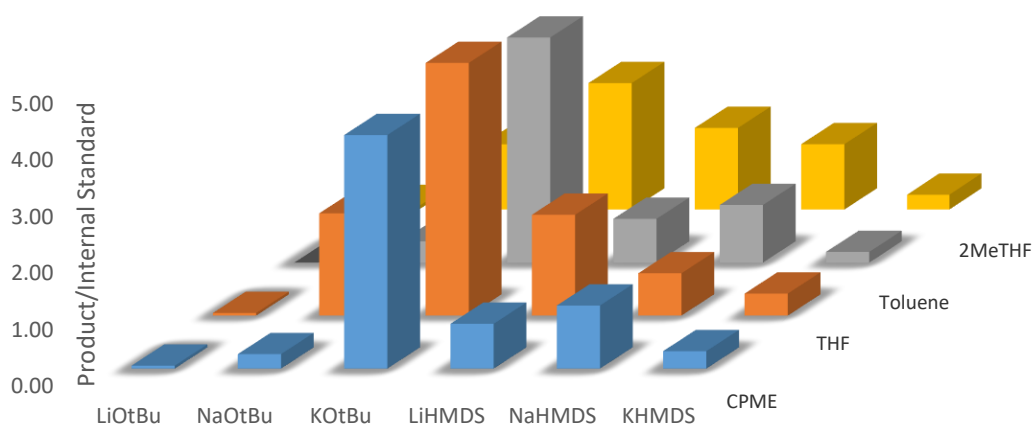
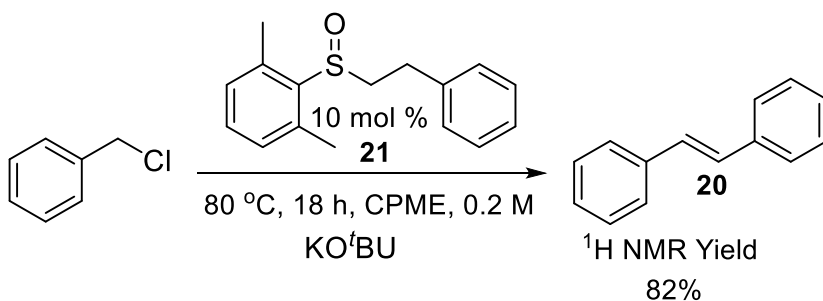


**Figure 9.** High throughput screening results for stilbene formation catalyzed by 2,6-dimethylbenzenesulfenate

Variables such as solvent and base were screened in **Figure 9**, using High Throughput Experimentation. The conditions using KO<sup>t</sup>Bu and CPME were identified to be ideal, shown in the blue column. These conditions were used in a scaled-up reaction (**Scheme 13**) to afford the product **20** in 82% <sup>1</sup>H NMR, yield. More optimization is needed to achieve excellent yields with a sterically hindered catalyst. The transition state for the RDS may be more crowded and therefore more sensitive to solvent and base effects. Yields are typically 99% at 2.5 mol % precatalyst loading using conditions optimized for benzyl phenyl sulfoxide. This work has not matured enough to reach any definitive conclusions and is still ongoing.

### Scheme 13. Stillbene catalysis using **21** at 10 mol % loading



### Conclusion and Future Work

Steady progress has been made towards optimizing the BH conditions and understanding the reactivity of the sulfenate anion. From concept to experimentation, several objectives were met along the way. The objective of finding a suitable precatalyst that diminishes side reactions, and provides uncomplicated testing of reactions has been met. The successive cleavage experiments provided valuable information, that will be utilized in High Throughput Screening.

The objective of generating yield on  $\alpha,\beta$ -unsaturated nitriles, ketones and esters with activated aldehydes and unactivated aldehydes has also been met. Future work will mainly consist of using High-Throughput Screening results to obtain optimal conditions and applying those conditions to develop scope. While the scope is being developed, a mechanistic study will likely ensue. Due to the unique character of the sulfenate anion it is expected to operate similarly to **Figure 5**, but with some interesting differences. Once the first general sulfenate anion catalyzed BH is developed, an enantioselective version will most likely be pursued.

The sulfenate anion has proven to be a difficult species to handle and develop, mainly due to lack of methods for facile catalyst introduction. While initial attempts to introduce the catalyst with strong base in the BH reaction proved troublesome, eventually fluoride mediated cleavage was satisfactory. Low BH

isolated yields were generated on acrylonitrile and methyl acrylate substrates, proving the sulfenate anions capacity for organocatalysis. Exploring the sulfenate anion in the BH reaction is an important step towards realizing the potential of this new class of organocatalysts.

The future of bulky sulfenate catalyst is uncertain. More conditions for the oxidation of the hindered selenide **19** can be explored, as the steric bulk proved to be troublesome. If testing of hindered catalysts at lower loadings does not show comparable catalytic activity, there will be no further investigation into hindered catalyst substrates.

## References

1. McGrath, A. J.; Garrett, G. E.; Valgimigli, L.; Pratt, D. A. The Redox Chemistry of Sulfenic Acids. *J. Am. Chem. Soc.* **2010**, *132* (47), 16759-16761.
2. Devarie-Baez, N. O.; Silva Lopez, E. I.; Furdui, C. M. Biological Chemistry and Functionality of Protein Sulfenic Acids and Related Thiol Modifications. *Free Radic. Res.* **2016**, *50*, 172-194.
3. Chen, T.; Wong, Y.S.; Selenocystine Induces Reactive Oxygen Species-Mediated Apoptosis in Human Cancer Cells. *Biomed. Pharmacother.* **2009**, *63*, 105-113.
4. Arnér, E. S. J.; Selenoproteins—What Unique Properties Can Arise With Selenocysteine in Place of Cysteine? *Exp. Cell Res.* **2010**, *316*, 1296-1303.
5. Rotruck, J. T.; Pope A. Al.; Ganther, H. E.; Swanson, A. B.; Hafeman, D. G.; Hoekstra, W. G. Selenium: Biochemical Role as a Component of Glutathione Peroxidase. *Science* **1973**, *179*, 588-590.
6. Barnham, K. J.; Masters, C. L.; Bush, A. I. Nuerodegenerative Diseases and Oxidative Stress. *Nat. Rev. Drug Discov.* **2004**, *3*, 205-214.
7. Rossato, J. I.; Ketzer, L. A.; Centuriao, F. B.; Silva, S. J. N.; Ludtke, D. S.; Zeni, G.; Braga, A. L.; Rubin, N. A.; Rocha, J. B. T. Antioxidant Properties of New Chalcogenides Against Lipid Peroxidation in Rat Brain. *Neuro. Chem. Res.* **2002**, *27*(4), 297-303.
8. Vaidya, V.; Ingold, K. U.; Pratt, D. A. Garlic: Source of the Ultimate Antioxidants - Sulfenic acids. *Angew. Chemie Int. Ed.* **2009**, *48*, 157-160.
9. MacMillan, D. W. C. The Advent and Development of Organocatalysis. *Nature*, **2008**, *455*, 304-308.
10. Furukawa, N.; Konno, Y.; Tsuruoka, M.; Fujihara, H.; Ogawa, S. Generation of Sulfenate Salts via Ipso-substitution of Azaheterocyclic Sulfoxides. First Preparation and Characterization of Sodium 2-Pyridinesulfenate. *The Chem. Soc. of Jap.* **1989**, 1501-1504.
11. Foucoin, F.; Caupene, C.; Lohier, J.; Santos, J. S. O.; Perrio, S.; Metzner, P. 2-(Trimethylsilyl)ethyl Sulfoxides as a Convenient Source of Sulfenate Anions. *Synthesis (Stuttg)*, **2007**, *9*, 1315-1324.
12. Ishii, A.; Matsubayashi, S.; Takahashi, T.; Nakayama, J. Preparation of a Selenenic Acid and Isolation of Selenoseleninates. *J. Org. Chem.* **1999**, *64*, 1084-1085.
13. Davis, F. A.; Billmers, R. L. Chemistry of Sulfenic Acids. 4. The First Direct Evidence for the Involvement of Sulfenic Acids in the Oxidation of Thiols. *J. Am. Chem. Soc.* **1981**, *103*, 7016-7018.
14. Goto, K.; Naghama, M.; Mizushima, T.; Shimada, K.; Kawashima, T.; Okazaki, R. The First Direct Oxidative Conversion of a Selenol to a Stable Selenenic Acid: Experimental Demonstration of Three Processes Included in the Catalytic Cycle of Glutathione Peroxidase. *Org. Lett.* **2001**, *3* (22), 3569-3572.
15. Goto, K.; Tokitoh, N.; Okazaki, R. Synthesis of a Stable Arenesulfenic Acid

- Bearing a Bowl-Shaped Macrobicyclic Cyclophane Skeleton. *Angew. Chemie Int. Ed. English* **1995**, 34, 1124–1126.
16. O'Donnel, J. S.; Schwan, A. L. Generation, Structure and Reactions of Sulfenic Acid Anions. *J. Sulfur Chem.* **2004**, 25, 183–211.
  17. Zhang, M.; Jia, T.; Yin, H.; Carroll, P. J.; Scheleter, E. J.; Walsh, P. J. A New Class of Organocatalysts: Sulfenate Anions. *Angew. Chemie* **2014**, 126, 10931–10934.
  18. Zhang, M.; Jia, T.; Wang, C. Y.; Walsh, P. J. Organocatalytic Synthesis of Alkynes. *J. Am. Chem. Soc.* **2015**, 137, 10346–10350.
  19. Schwan, A. L. A New Role for Sulfenate Anions: Organocatalysis. *Chem. Cat. Chem.* **2015**, 7, 226–227.
  20. McGrath, A. J.; Garrett, G. E.; Valgimigli, L.; Pratt, D. A. The Redox Chemistry of Sulfenic Acids. *J. Am. Chem. Soc.* **2010**, 132 (47), 16759–16761.
  21. Edwards, J. O.; Pearson, R. G. The Factors Determining Nucleophilic Reactivities. **1962**, *J. Am. Chem. Soc.* 84, 16–24.
  22. Jia, T.; Zhang, M.; Jiang, H.; Wang, C. Y.; Walsh, P. J. Palladium-Catalyzed Arylation of Alkyl Sulfenate Anions. *J. Am. Chem. Soc.* **2015**, 137, 13887–13893.
  23. Maitro, G.; Vogel, S.; Prestat, G.; Madec, D.; Poli, G. Aryl Sulfoxides via Palladium-Catalyzed Arylation of Sulfenate Anions. *Org. Lett.* **2006**, 8 (26), 5951–5954.
  24. Caupène C.; Boudou C.; Perrio, S.; Metzner, P. Remarkably Mild and Simple Preparation of Sulfenate Anions from  $\beta$ -Sulfinylesters: A New Route to Enantioenriched Sulfoxides. *J. Org. Chem.* **2005**, 70 (7), 2812–2815.
  25. Zong, L.; Ban, X.; Kee, C. W.; Tan, C. H.; Catalytic Enantioselective Alkylation of Sulfenate Anions to Chiral Heterocyclic Sulfoxides Using Halogenated Pentanidium Salts. *Angew. Chemie Int. Ed.* **2014**, 53, 11849–11853.
  26. Kataoka, W.; Iwama, T.; Tsuijiyama, S. The Chalcogeno-Baylis–Hillman Reaction: the First Examples Catalysed by Chalcogenides in the Presence of Lewis Acids. *Chem. Commun.* **1998**, 197–198.
  27. Jia, T.; Bellomo, A.; Montel, S.; Zhang, M.; Baina, K. E.; Zheng, B.; Walsh, P. J. Diaryl sulfoxides from aryl benzyl sulfoxides: A single Palladium-Catalyzed Triple Relay Process. **2014**, *Angew. Chemie Int. Ed.* 53, 260–264.
  28. Sandrinelli, F.; Perrio, S.; Averbuch-Pouchot, M. T.; Novel Approach to the Synthesis of Enantioenriched Sulfoxides. Highly Diastereoselective Alkylation of Sulfenate Anions with 1,4-Asymmetric Induction. *Org. Lett.* **2002**, 4(21), 3619–3622.

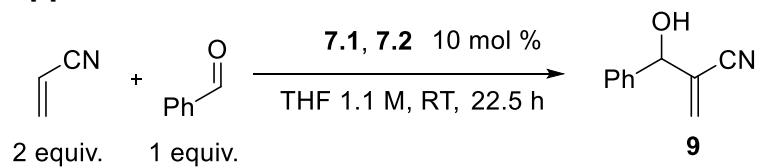
29. Gong, H.; Andrews, R. S.; Zuccarello, J. L.; Lee, S. J.; Gagne, M. R. Sn-free Ni-Catalyzed Reductive Coupling of Glycosyl Bromides with Activated Alkenes. **2009** *Org. Lett.* **11**, 879–882.
30. Aggarwal, V. K.; Fulford, S. Y.; Lloyd-Jones, G. C. Reevaluation of the Mechanism of the Baylis-Hillman Reaction: Implications for Asymmetric Catalysis. *Angew. Chemie*, **2005**, **117**, 1734–1736.
31. Plata, R. E. & Singleton, D. A. A Case Study of the Mechanism of Alcohol-Mediated Morita Baylis– Hillman Reactions. The Importance of Experimental Observations. *J. Am. Chem. Soc.*, **2015**, **137** (11), 3811–3826.
32. pKa's of Inorganic and Oxo-Acids. Available at: [http://evans.rc.fas.harvard.edu/pdf/evans\\_pKa\\_table.pdf](http://evans.rc.fas.harvard.edu/pdf/evans_pKa_table.pdf). (Accessed: 28th July 2017)
33. Nobushige, K.; Hirano, K.; Satoh, T.; Miura, M. Rhodium(III)-Catalyzed Ortho-Alkenylation through C–H Bond Cleavage Directed by Sulfoxide Groups. *Org. Lett.*, **2014**, **16** (4), 1188–1191.
34. Caroline Caupène, Cédric Boudou, Stéphane Perrio, and Metzner, P. Remarkably Mild and Simple Preparation of Sulfenate Anions from  $\beta$ -Sulfinylesters: A New Route to Enantioenriched Sulfoxides. (2005).
35. Bakuzis, P.; Bakuzis, M. L. F. Oxidative Functionalization of the Beta.-Carbon in .Alpha.,.Beta.-Unsaturated systems. Preparation of 3-Phenylthio Enones, Acrylates, and Other Vinyl Derivatives. **1981** *J. Org. Chem.* **46**, 235–239.
36. Gholinejad, M.; Firouzabadi, H. One-pot Odorless Thia-Michael Reaction by Copper Ferrite Nanoparticle-Catalyzed Reaction of Elemental Sulfur, Aryl Halides and Electron-Deficient Alkenes. **2015**, *New J. Chem.* **39**, 5953–5959.
37. Pospíšil, J.; Markó, I. E. Metathesis-Based Synthesis of 3-methoxy a,b-Unsaturated Lactones: Total Synthesis of (R)-Kavain and of the C1–C6 Fragment of Jerangolid D. *Tett. Lett.* **2007**, **49** (9) 1523–1526.
38. Yue, H. L.; Klusmann, M. Acid-Catalyzed Oxidative Addition of Thiols to Olefins and Alkynes for a One-Pot Entry to Sulfoxides. *Synlett*, **2016**, **27**, 2505–2509.
39. Lai, M.; Oh, E.; Shih, Y.; Liu, H.; Synthesis of Enantiomerically Pure [(Methylenecyclopropyl)acetyl]-CoA: The Causative Agent of Jamaican Vomiting Sickness. *J. Org. Chem.* **1991**, **57**, 2471–2476.
40. Schwan, A. L.; Dufault, R. The Reaction of 2-Trimethylsilylethyl Sulfoxides with Sulfuryl Chloride. A Fragmentation Route to Sulfinyl Chlorides. *Tetrahedron Lett.* **1992**, **33**, 3973–3974.
41. Borger, J. E.; Ehlers, A. W.; Lutz, M.; Slootweg, J. C.; Lammertsma, K. Functionalization of P<sub>4</sub> Using a Lewis Acid Stabilized Bicyclo[1.1.0]tetraphosphabutane Anion. *Angew. Chemie Int.* **2014**, **53**, 12836–12839.
42. Mallow, O.; Khanfar, M. A.; Malischewski, M.; Finke, P.; Heese, M.; Lork, E.; Augenstein, T.; Breher, F.; Harmer, J. R.; Vasilieva, N. V.; Zibarev, A.; Bogomyakov, A. S.; Seppelt, K.; Beckmann, J. Diaryldichalcogenide



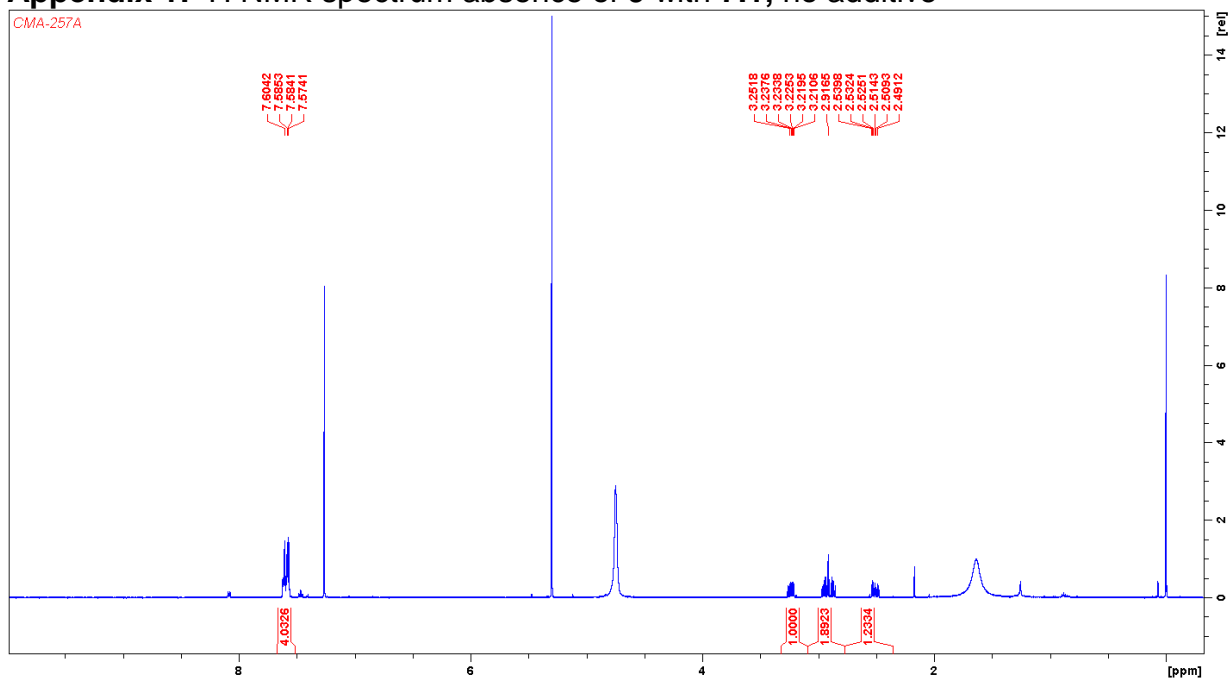
- Radical Cations. *Chem. Sci.* **2015**, *6*, 497–504.
43. Akiyama, T.; Itoh, J.; Fuchibe, K.; Recent Progress in Chiral Brønsted Acid Catalysis. *Adv. Synth. Catal.* **2006**, *348*, 999–1010.
  44. Taylor, M. S.; Jacobsen, E. N. Asymmetric Catalysis by Chiral Hydrogen-Bond Donors. *Angew. Chemie Int. Ed.* **2006**, *45*, 1520–1543.
  45. Wang, G.-Z.; Shang, R.; Cheng, W.-M.; Fu, Y. Decarboxylative 1,4-Addition of  $\alpha$ -Oxocarboxylic Acids with Michael Acceptors Enabled by Photoredox Catalysis. *Org. Lett.* **2005**, *17*, 4830–4833.
  46. Donohoe, T. J.; Jahanshahi, A.; Tucker, M. J.; Bhatti, F. L.; Roslan, I. A.; Kabeshov, M.; Wrigley, G. Exerting Control Over the Acyloin Reaction. *Chem. Commun.* **2011**, *47*, 5849.
  47. Clennan, E. L.; Stensaas, K. L.; Reactions of Bis(*p*-methoxyphenyl)trisulfane and Its Oxides with Dimethyldioxirane and (Trifluoromethyl)methyldioxirane. *J. Org. Chem.* **1996**, *61*,(22) 7911-7917.
  48. Barbosa, T. P.; Junior, C. G. L.; Silva, F. P. L.; Lopes, H. M.; Figueirdo, L. R. F.; Sousa, S. C. O.; Batista, G. N.; Silva, T. G.; Silva T. M. S.; Oliveira, M. R.; Vasconcellos, M. L. A. A. Improved Synthesis of Seven Aromatic Baylisse-Hillman adducts (BHA): Evaluation Against *Artemia Salina* Leach. and *Leishmania Chagasi*. *Eur. J. Med. Chem.* **2008**, *44*, 1726–1730.
  49. Jana, N. K.; Verkade, J. G. Phase-Vanishing Methodology for Efficient Bromination, Alkylation, Epoxidation, and Oxidation Reactions of Organic Substrates. *Org. Lett.* **2003**, *5*(21) 3787-3790.
  50. Dordonne, S.; Crousse, B.; Bonnet-Delpon, D.; Legros, J. Fluorous Tagging of DABCO Through Halogen Bonding: Recyclable Catalyst for the Morita–Baylis–Hillman Reaction. *Chem. Commun.* **2011**, *47*, 5855.
  51. Taylor, M. S.; Tokunaga, N.; Jacobsen, E. N. Enantioselective Thiourea-Catalyzed Acyl-Mannich Reactions of Isoquinolines. *Angew. Chemie* **2005**, *117*, 6858–6862.
  52. Seayad, J.; Seayad A. M.; List, B. Catalytic Asymmetric Pictet–Spengler Reaction. *J. Am. Chem. Soc.* **2006**, *128* (4), 1086-1087.
  53. Aggarwal, V. K.; Dean, D. K.; Mereu, A.; Williams, R. Rate Acceleration of the Baylis-Hillman Reaction in Polar Solvents (Water and Formamide). Dominant Role of Hydrogen Bonding, Not Hydrophobic Effects, Is Implicated. *J. Org. Chem.* **2002**, *67* (2), 510-514.

## Appendices

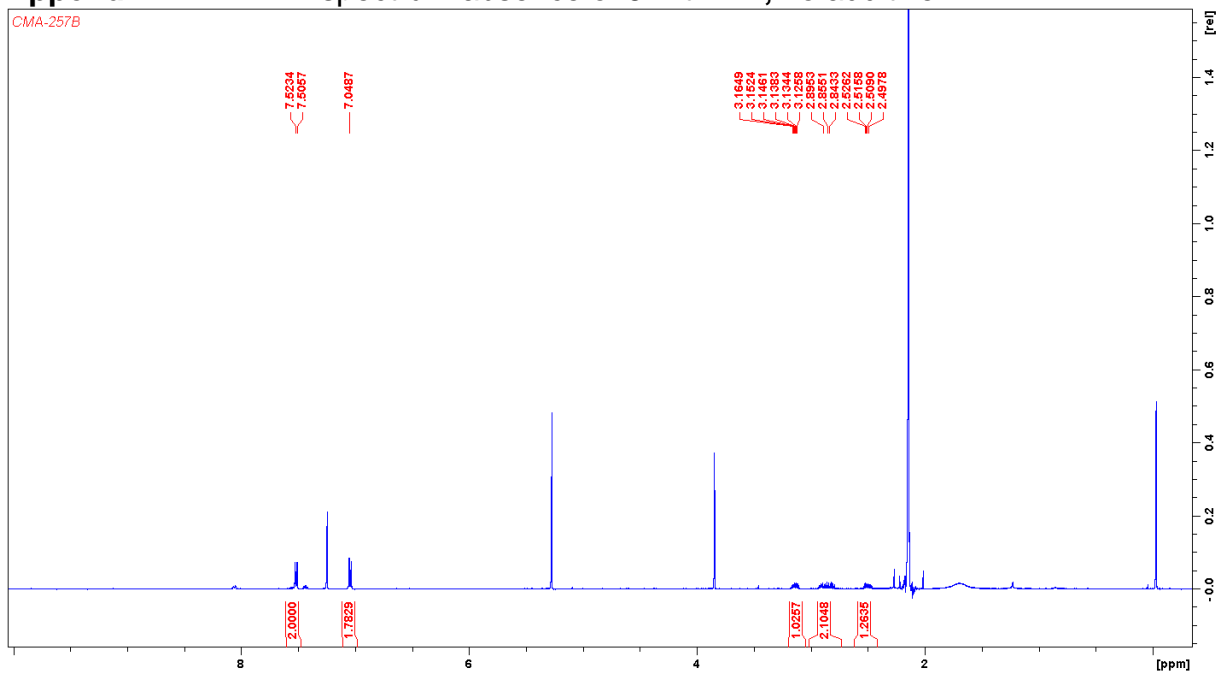
### Appendix 1-5



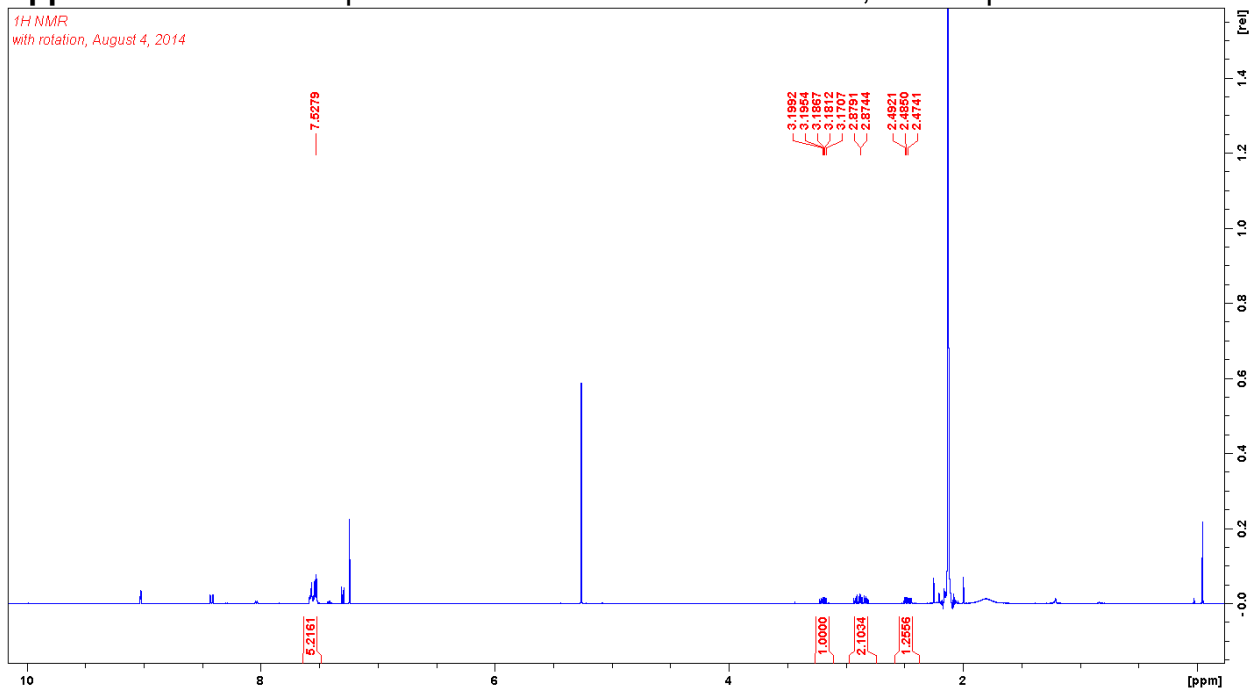
### Appendix 1: $^1\text{H}$ NMR spectrum absence of **9** with **7.1**, no additive



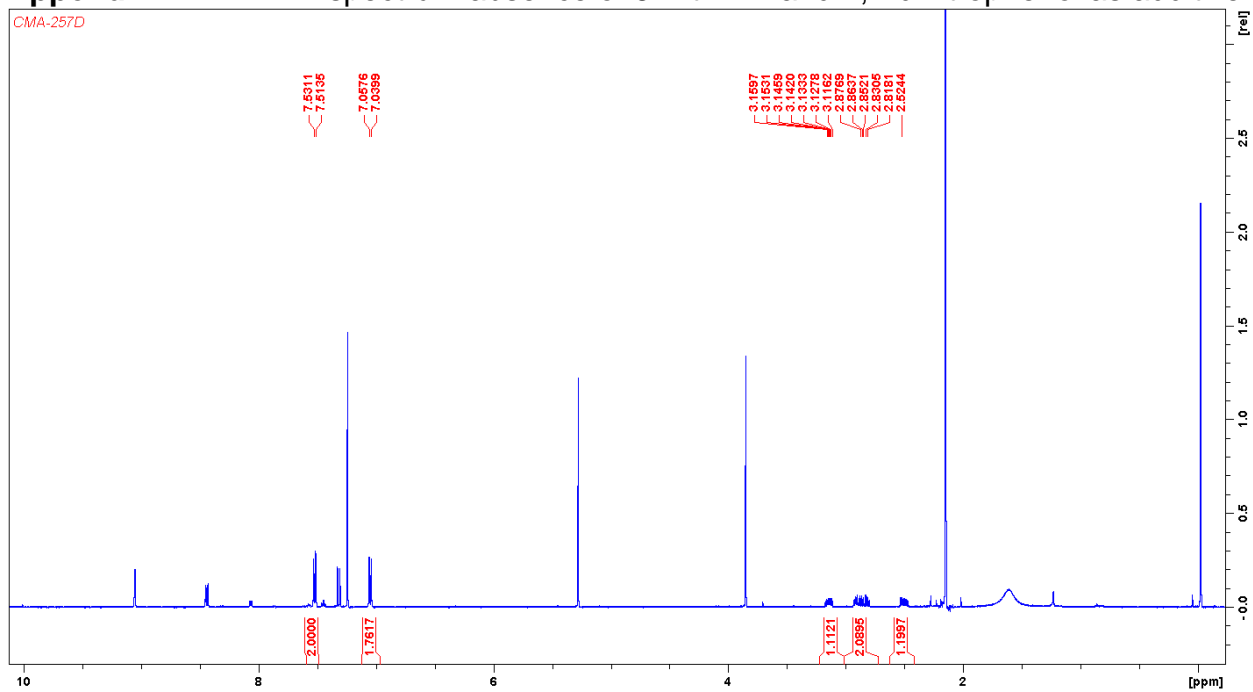
### Appendix 2: <sup>1</sup>H NMR spectrum absence of 9 with 7.2, no additive



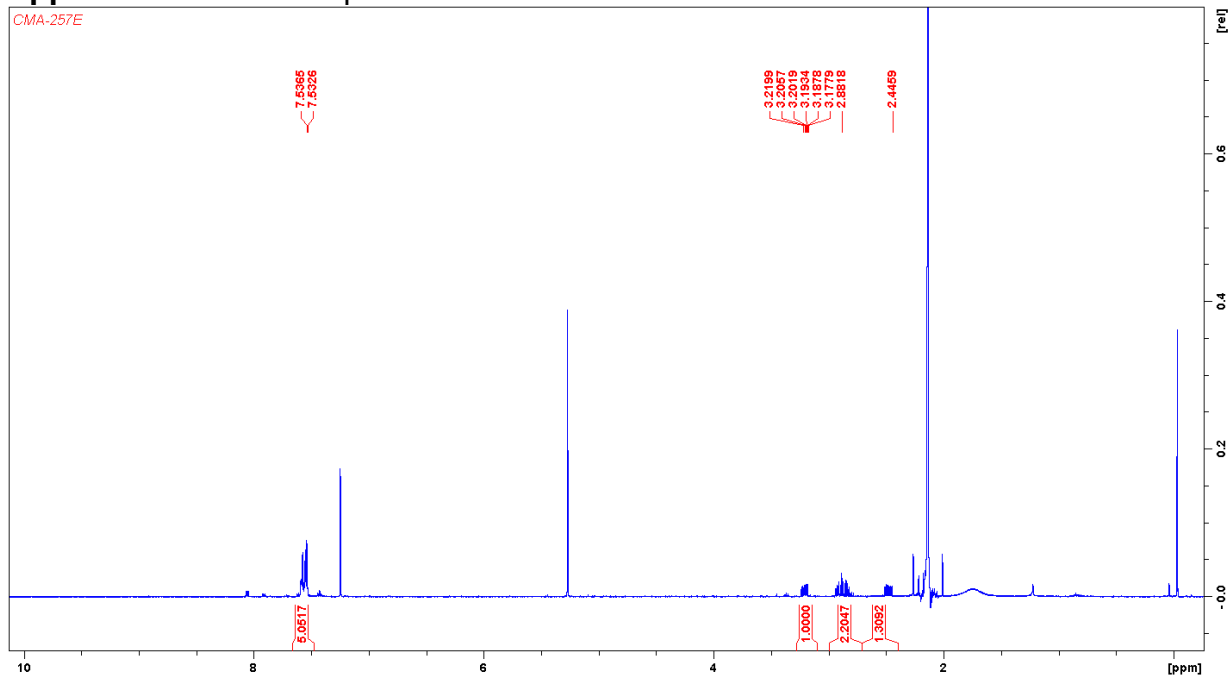
### Appendix 3: <sup>1</sup>H NMR spectrum absence of 9 with 7.1 and 2,4-dinitrophenol as additive



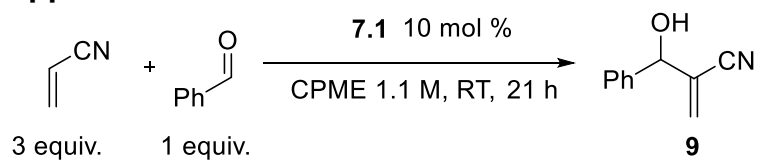
#### Appendix 4: <sup>1</sup>H NMR spectrum absence of **9** with 7.2 and 2,4-dinitrophenol as additive



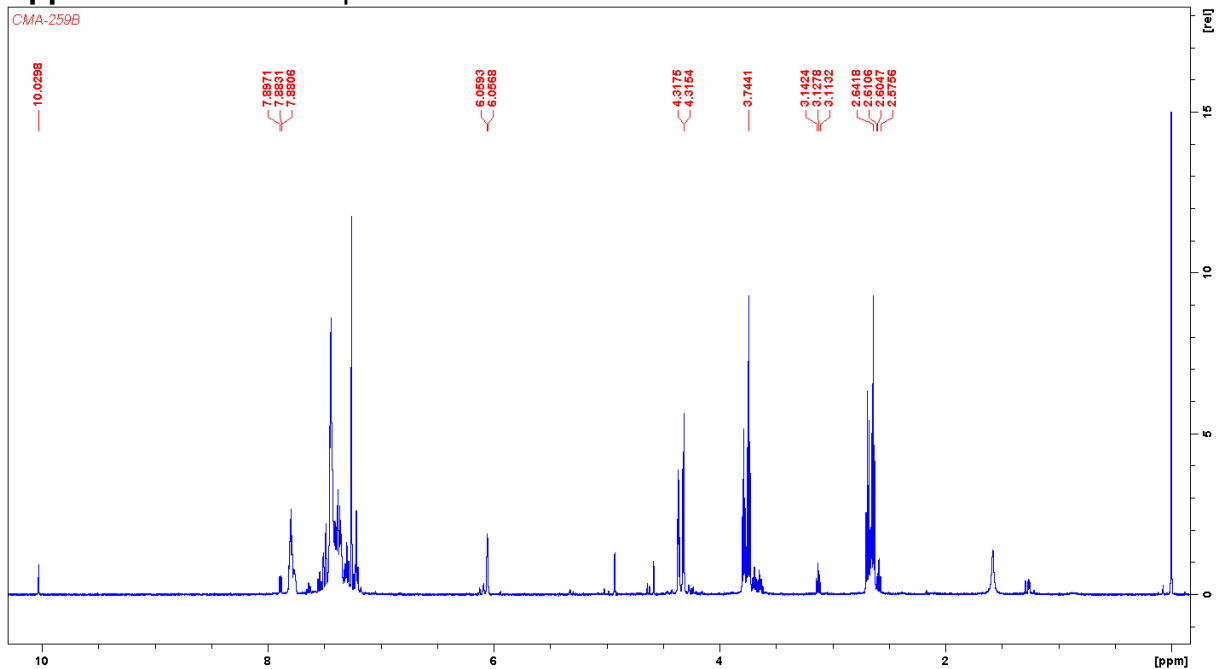
#### Appendix 5: <sup>1</sup>H NMR spectrum absence of **9** with 7.1 and deionized water as additive



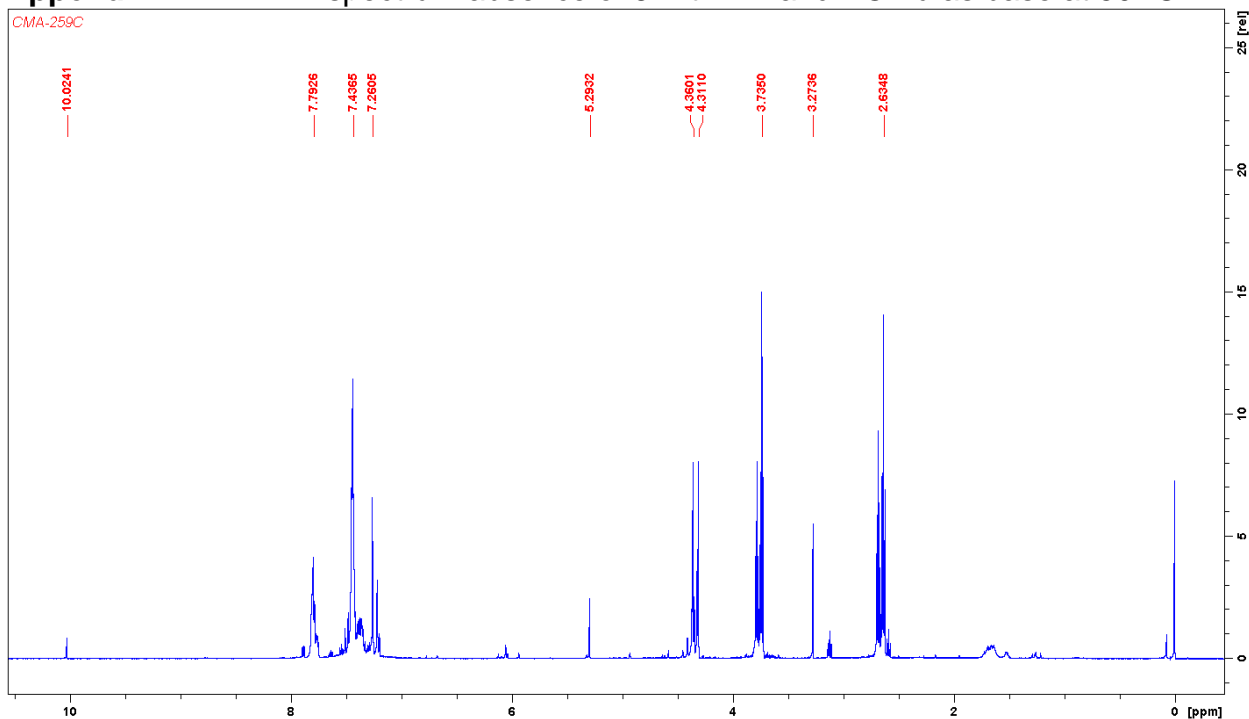
## Appendix 6-10



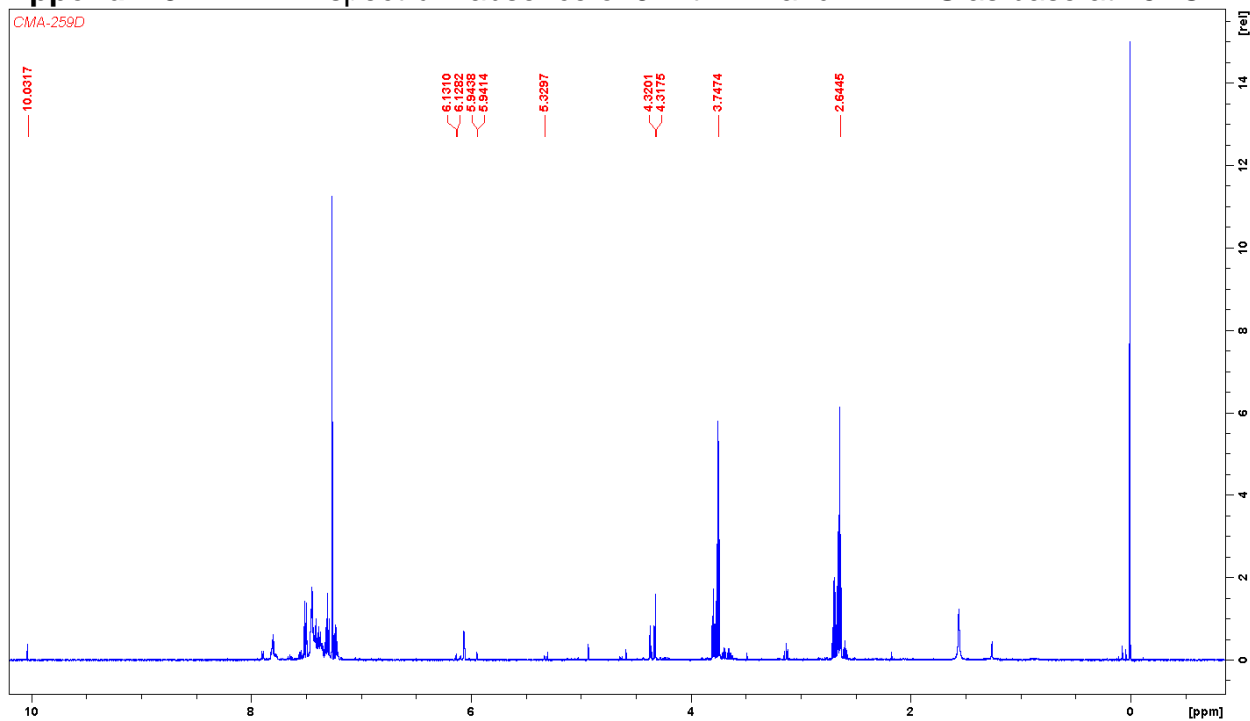
## Appendix 6: $^1\text{H}$ NMR spectrum absence of **9** with **7.1** and $\text{KO}^t\text{Bu}$ as base at 25 °C



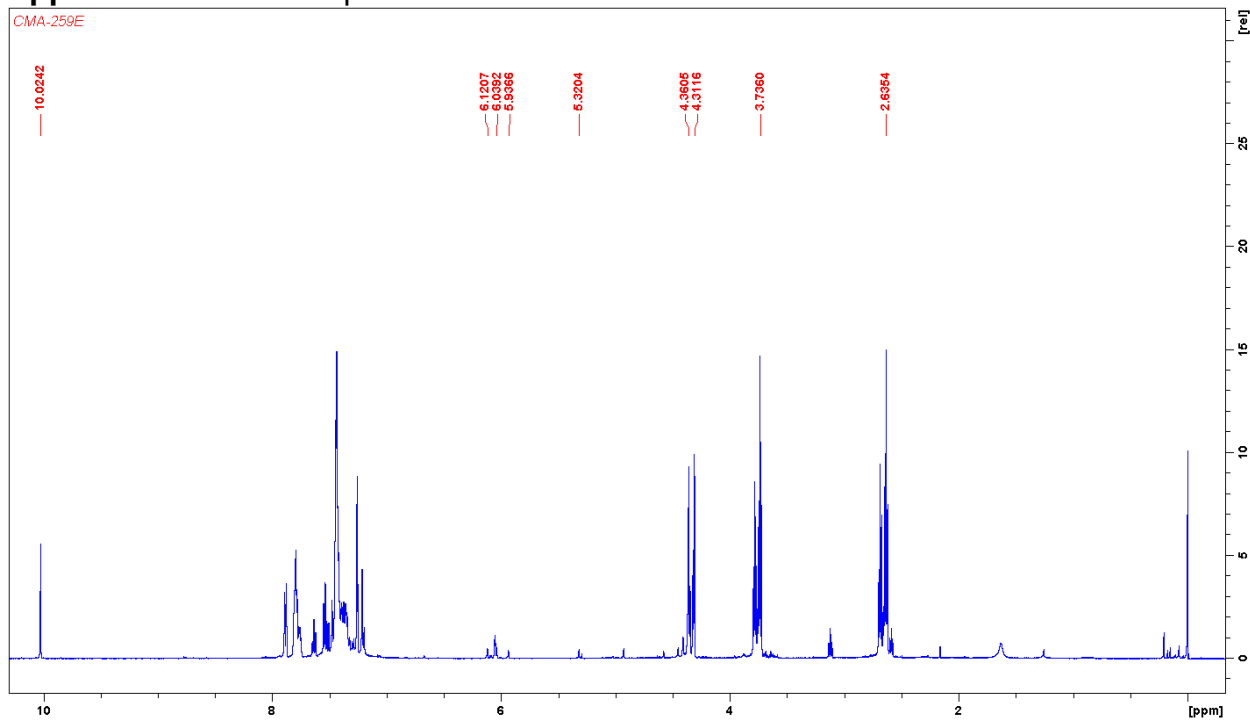
## Appendix 7: $^1\text{H}$ NMR spectrum absence of **9** with **7.1** and $\text{KO}^t\text{Bu}$ as base at 50 °C



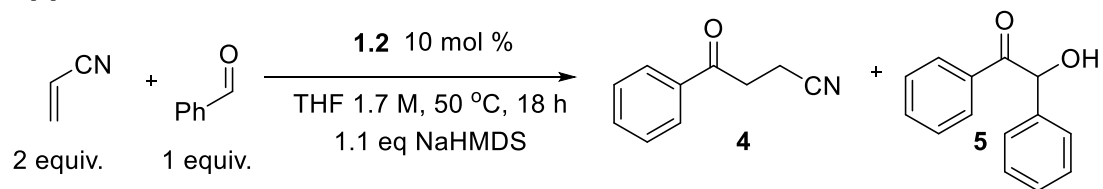
**Appendix 8:**  $^1\text{H}$  NMR spectrum absence of **9** with **7.1** and KHMDS as base at 25 °C



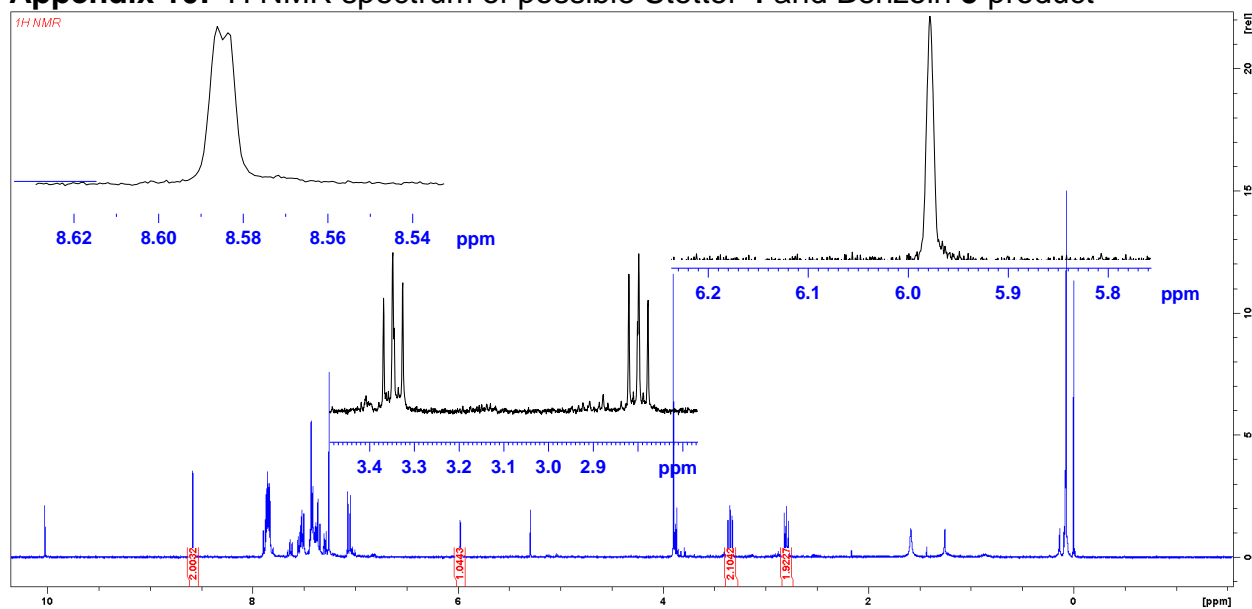
**Appendix 9:**  $^1\text{H}$  NMR spectrum absence of **9** with **7.1** and KHMDS as base at 50 °C



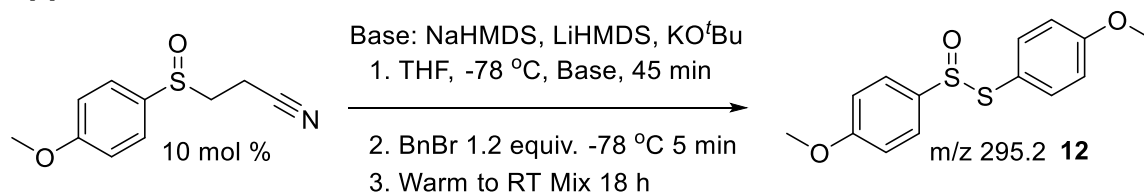
## Appendix 10



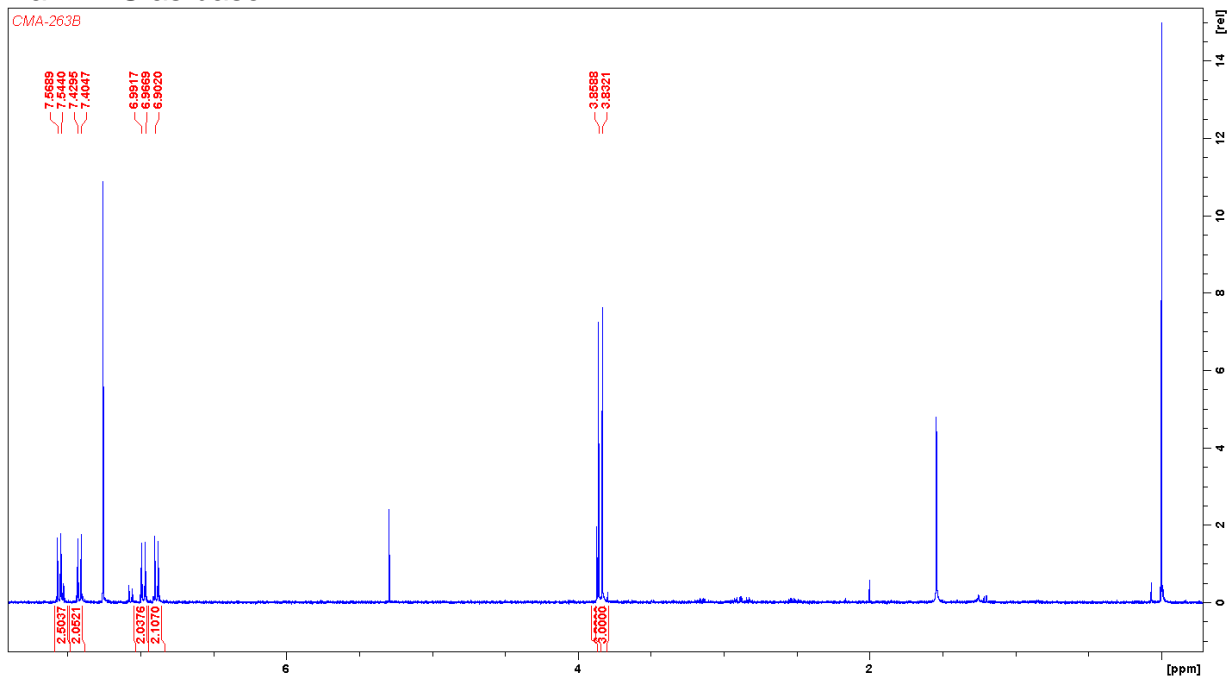
### Appendix 10: <sup>1</sup>H NMR spectrum of possible Stetter 4 and Benzoin 5 product



## Appendix 11-13

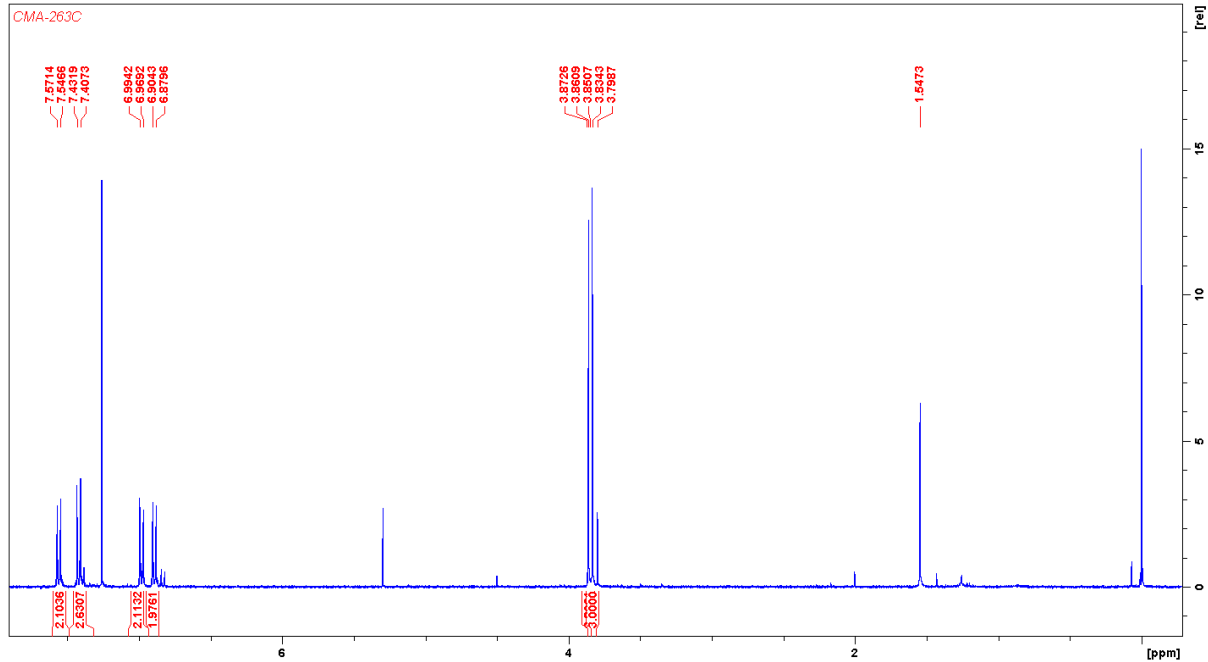


## Appendix 11: <sup>1</sup>H NMR spectrum absence of **4** with **1.2** and presence of **5** with NaHMDS as base

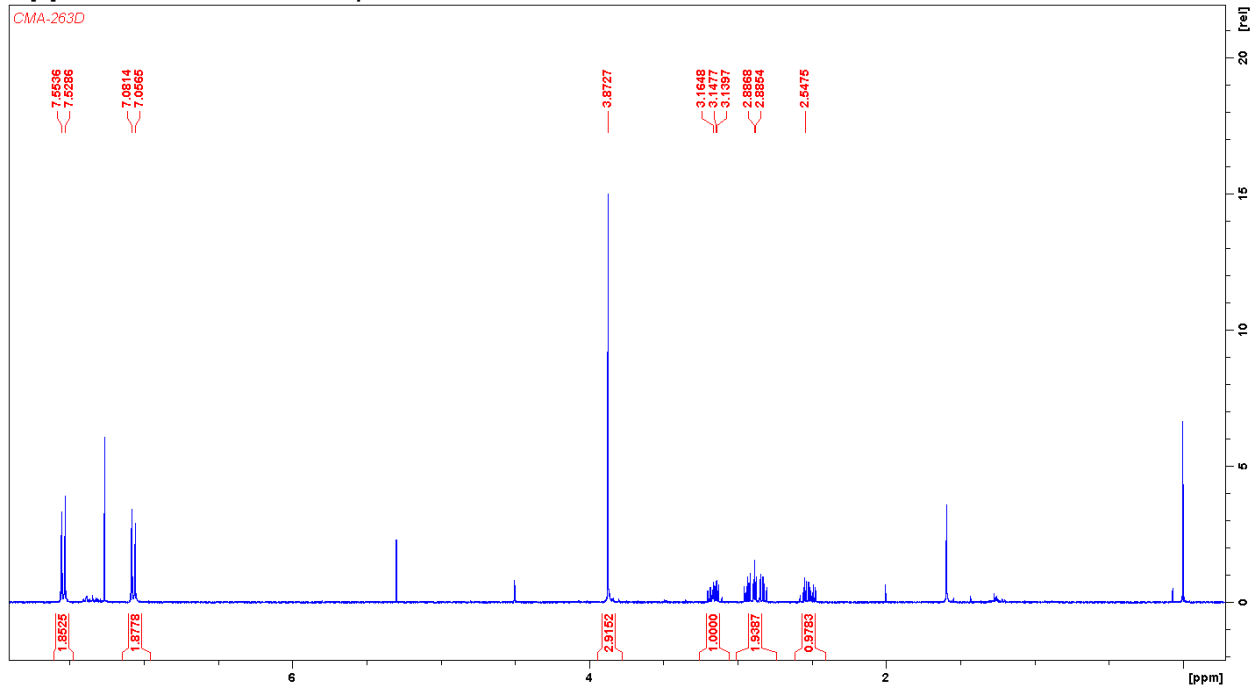




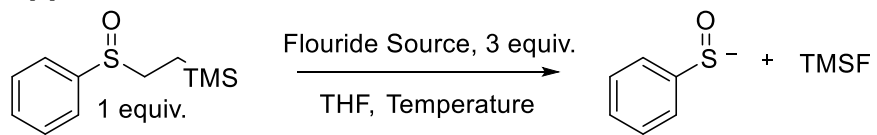
**Appendix 12: <sup>1</sup>H NMR spectrum absence of 4 with 1.2 and presence of 5 with LiHMDS as base**



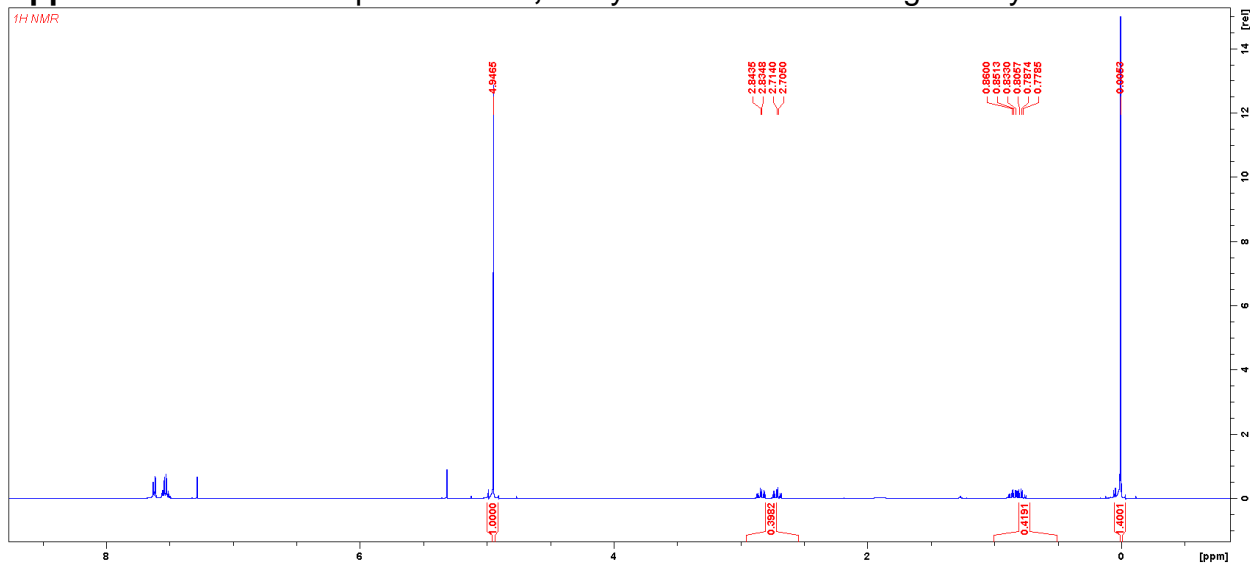
**Appendix 13: <sup>1</sup>H NMR spectrum absence of 4 with 1.2 and KO<sup>t</sup>Bu as base**



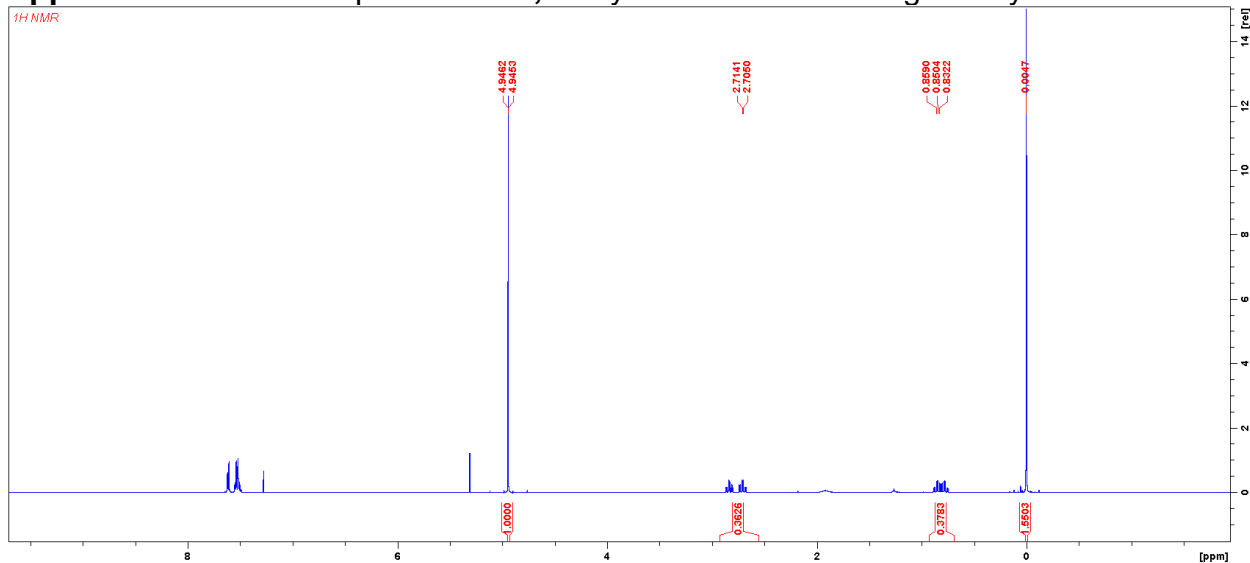
## Appendix 14-25



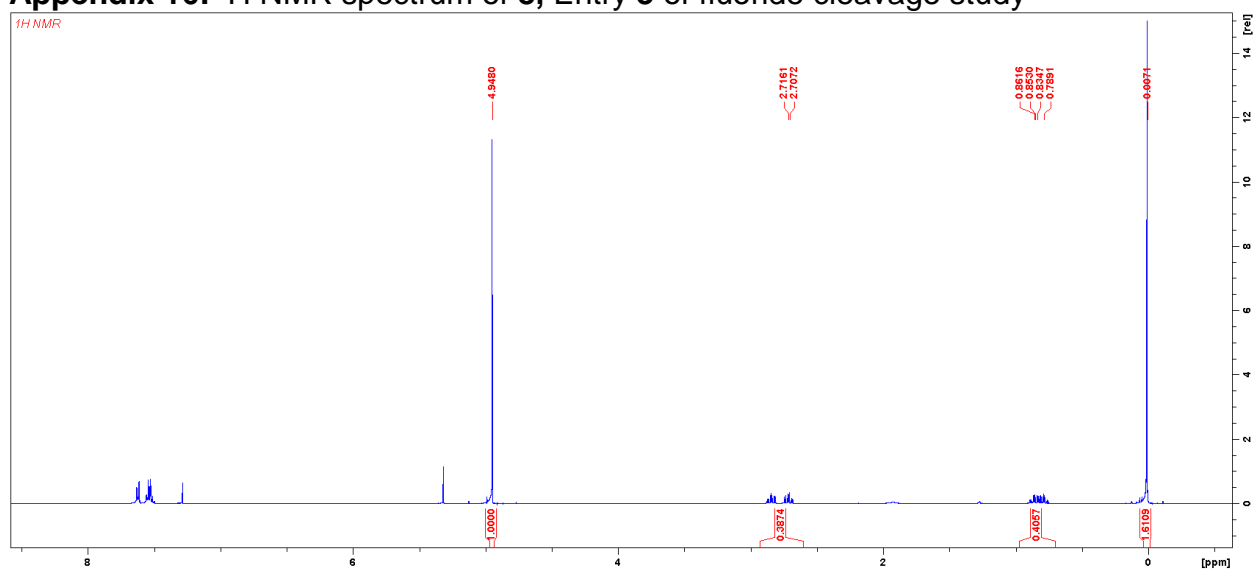
## Appendix 14: $^1\text{H}$ NMR spectrum of **8**, Entry 1 of fluoride cleavage study



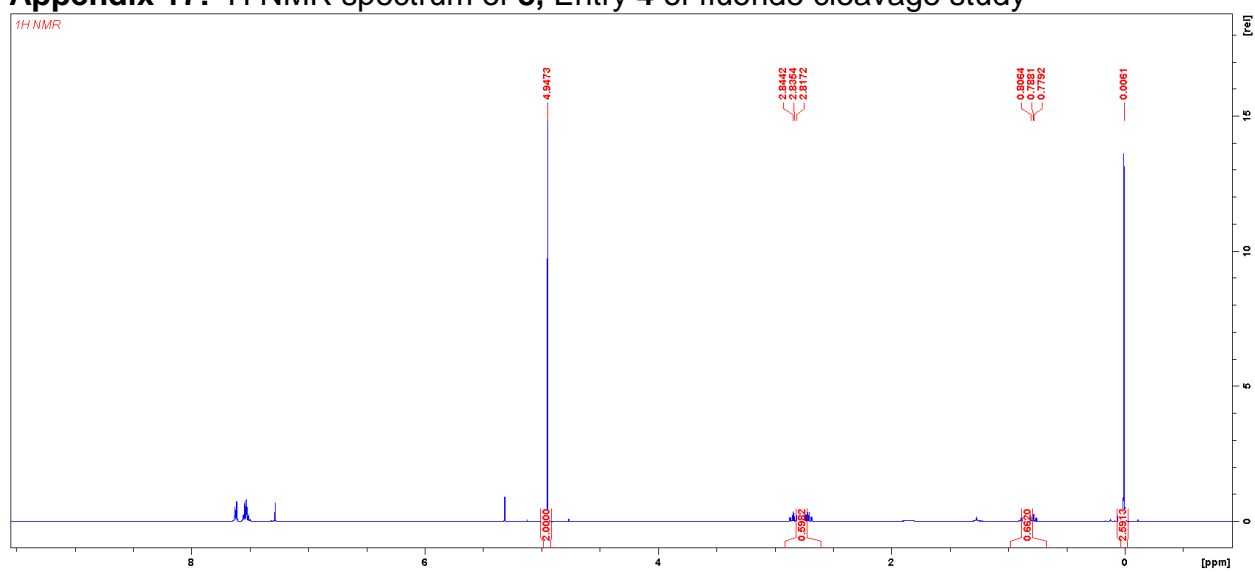
## Appendix 15: $^1\text{H}$ NMR spectrum of **8**, Entry 2 of fluoride cleavage study



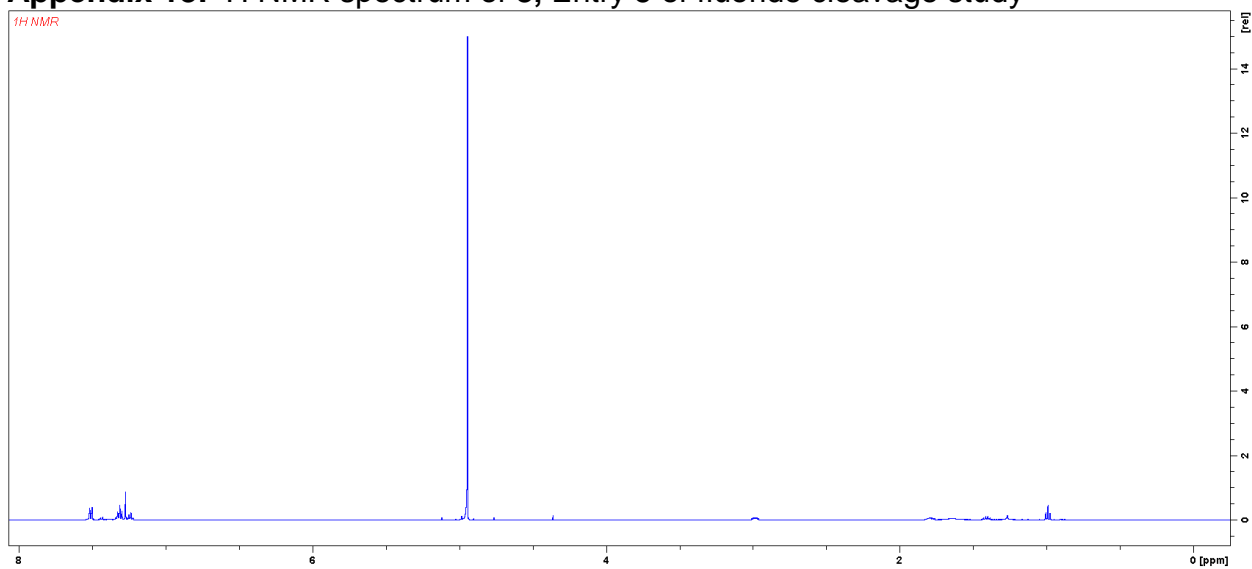
### Appendix 16: <sup>1</sup>H NMR spectrum of **8**, Entry 3 of fluoride cleavage study



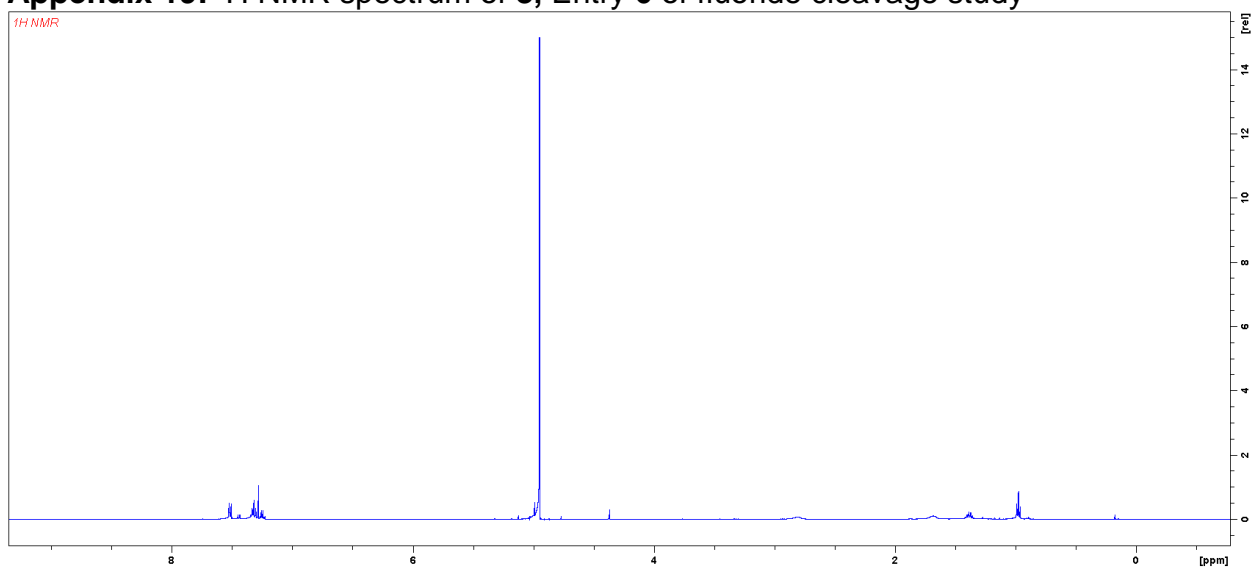
### Appendix 17: <sup>1</sup>H NMR spectrum of **8**, Entry 4 of fluoride cleavage study



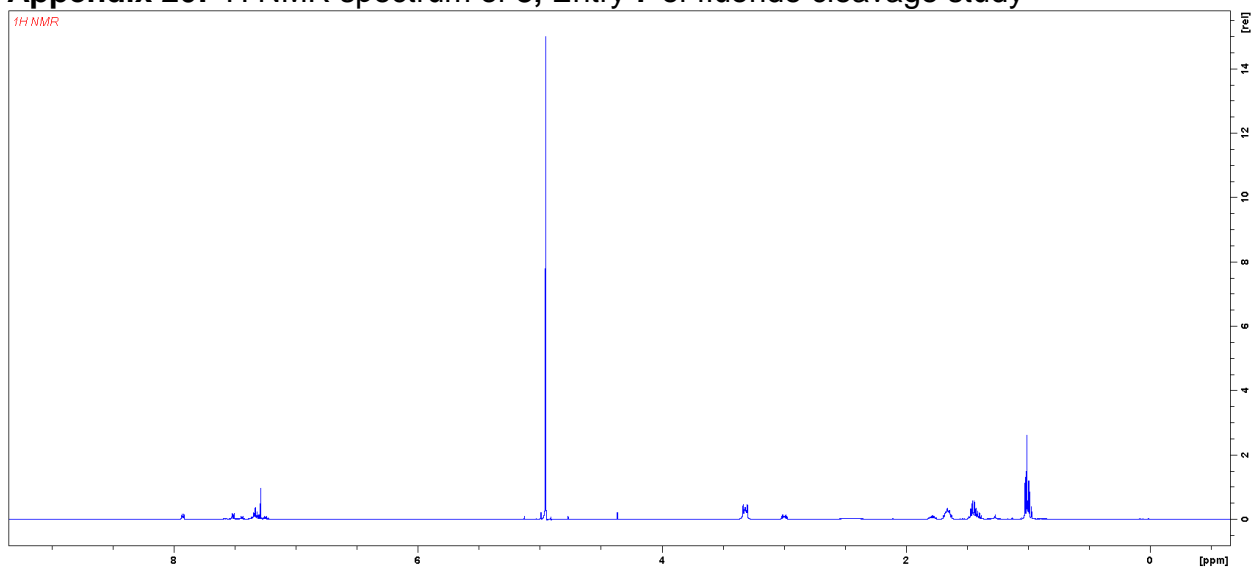
**Appendix 18:**  $^1\text{H}$  NMR spectrum of **8**, Entry **5** of fluoride cleavage study



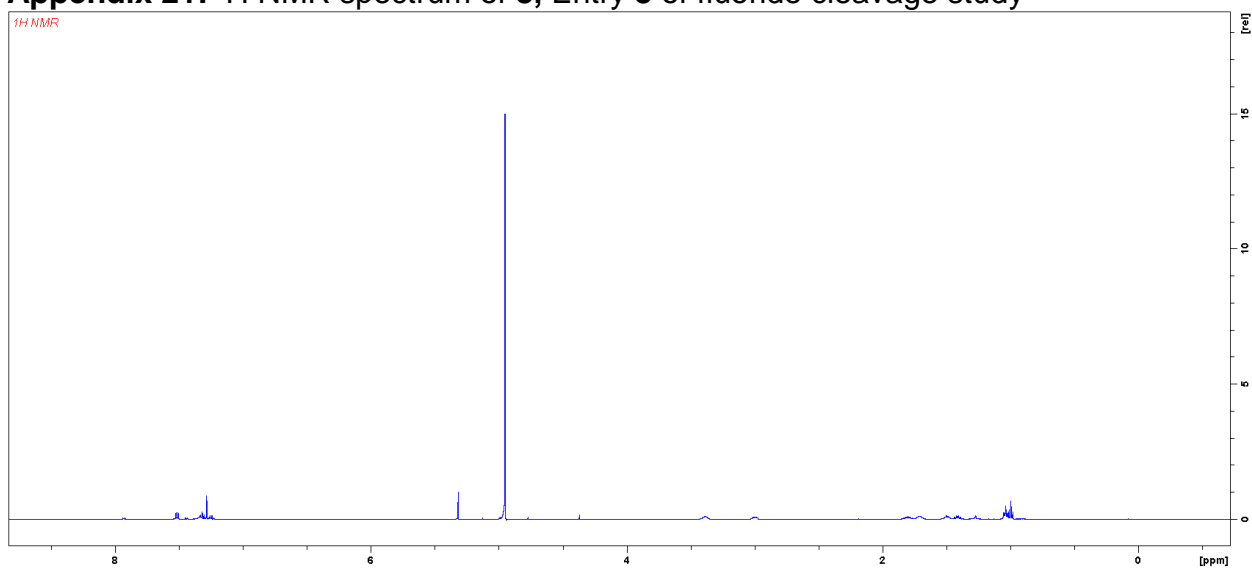
**Appendix 19:**  $^1\text{H}$  NMR spectrum of **8**, Entry **6** of fluoride cleavage study



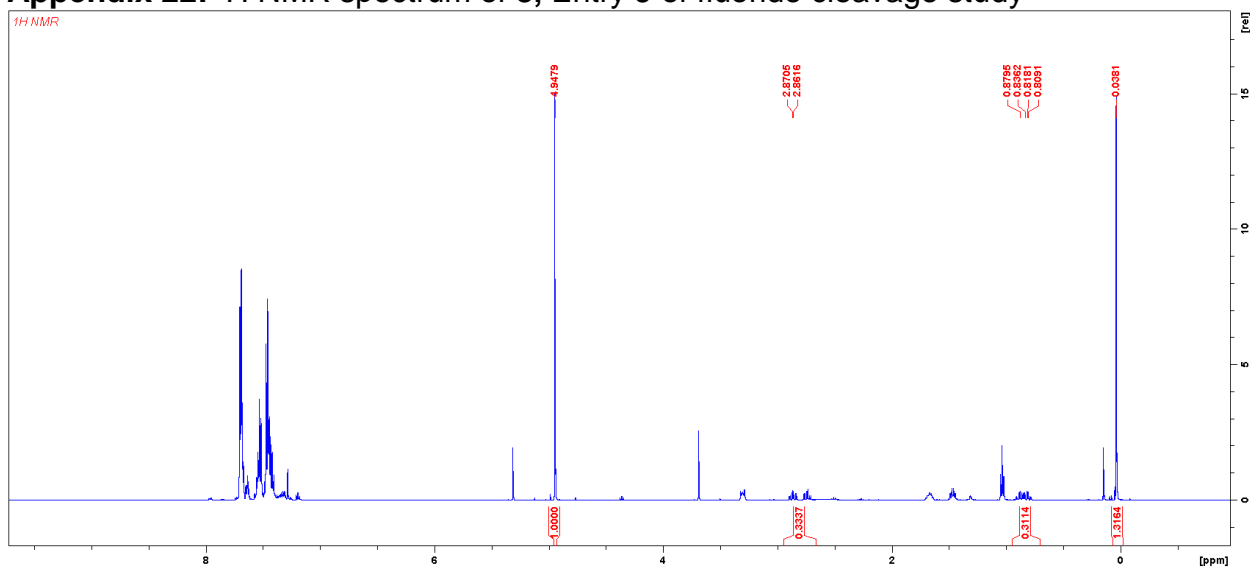
**Appendix 20:  $^1\text{H}$  NMR spectrum of **8**, Entry 7 of fluoride cleavage study**



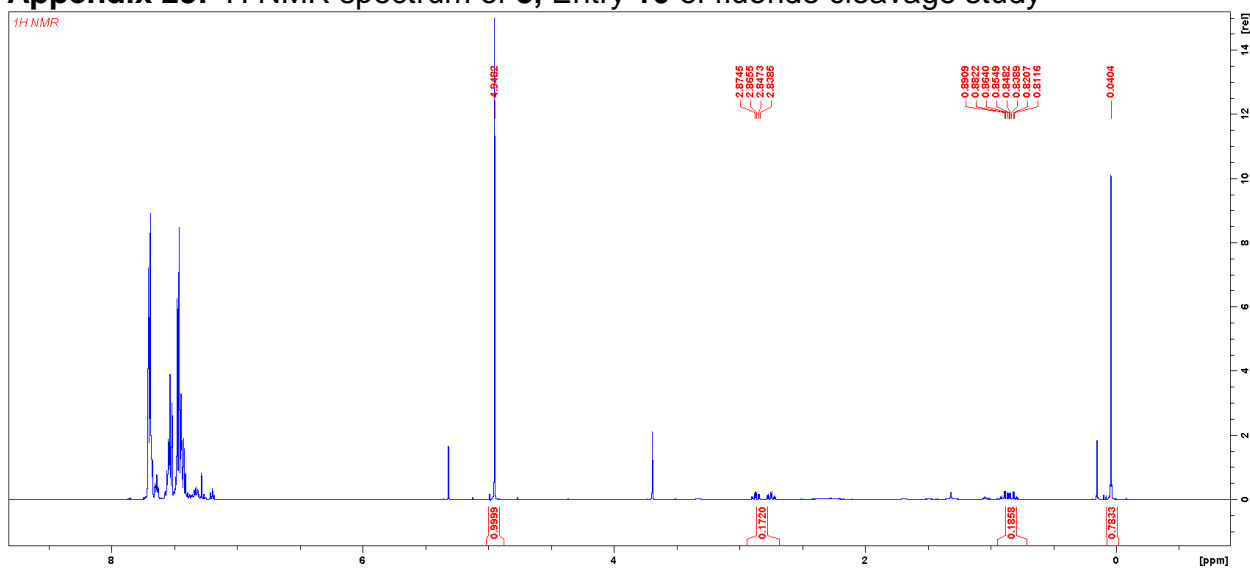
**Appendix 21:  $^1\text{H}$  NMR spectrum of **8**, Entry 8 of fluoride cleavage study**



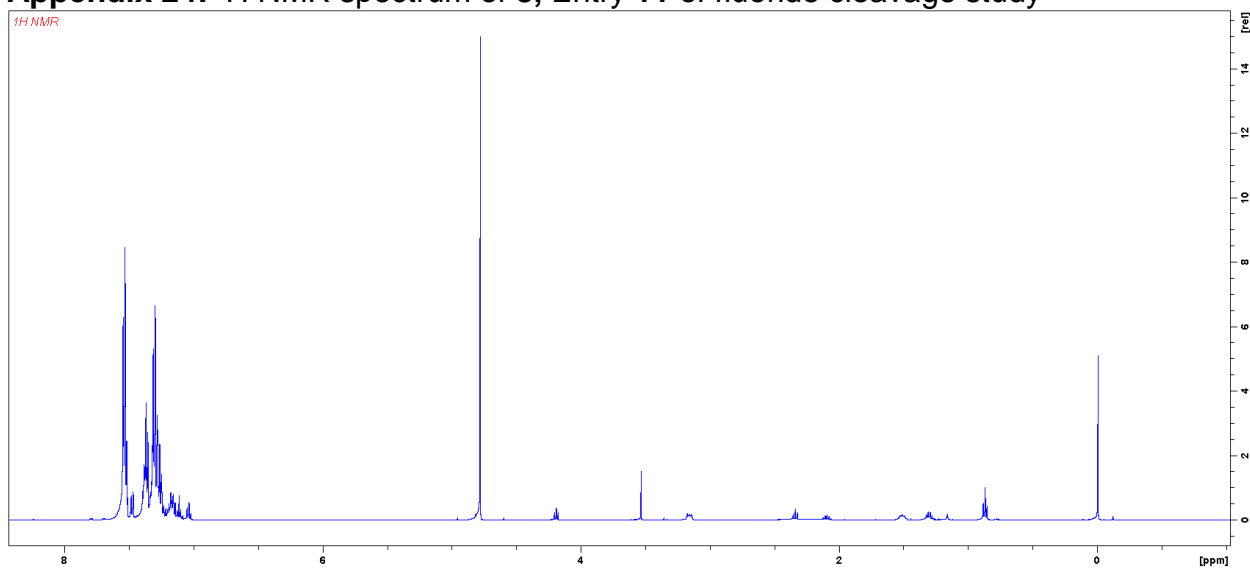
**Appendix 22: <sup>1</sup>H NMR spectrum of 8, Entry 9 of fluoride cleavage study**



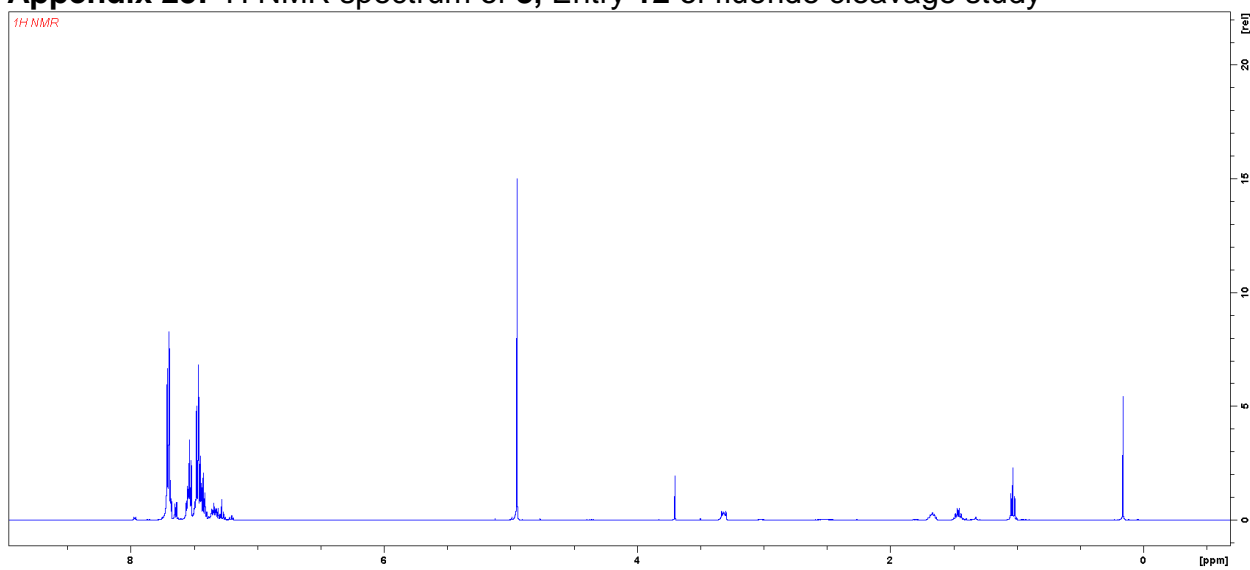
**Appendix 23: <sup>1</sup>H NMR spectrum of 8, Entry 10 of fluoride cleavage study**



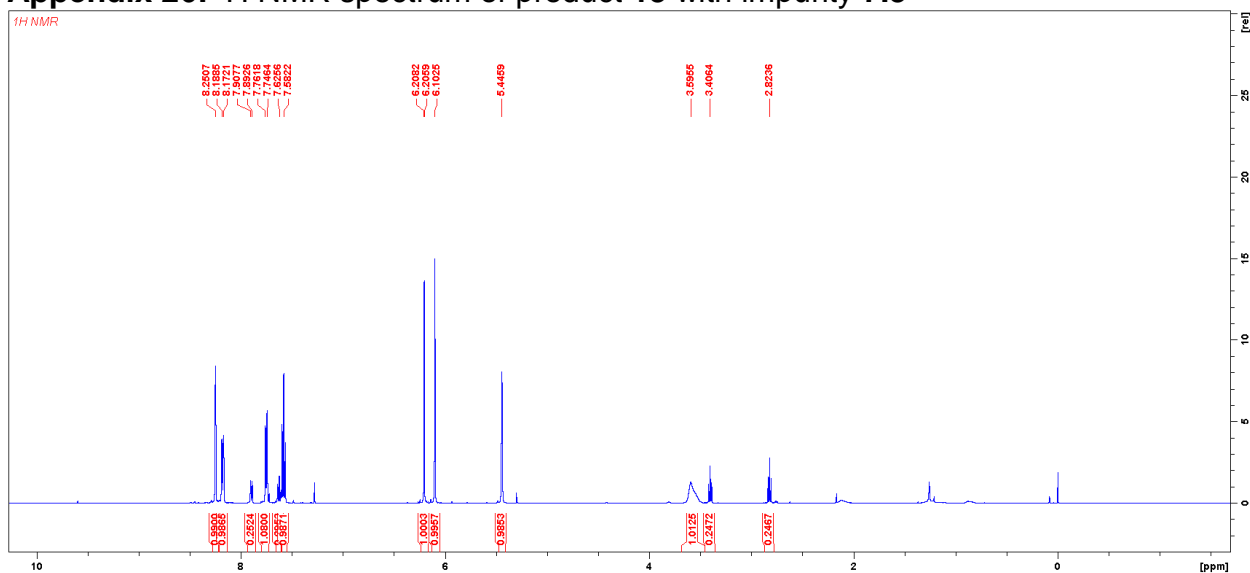
**Appendix 24:  $^1\text{H}$  NMR spectrum of **8**, Entry 11 of fluoride cleavage study**



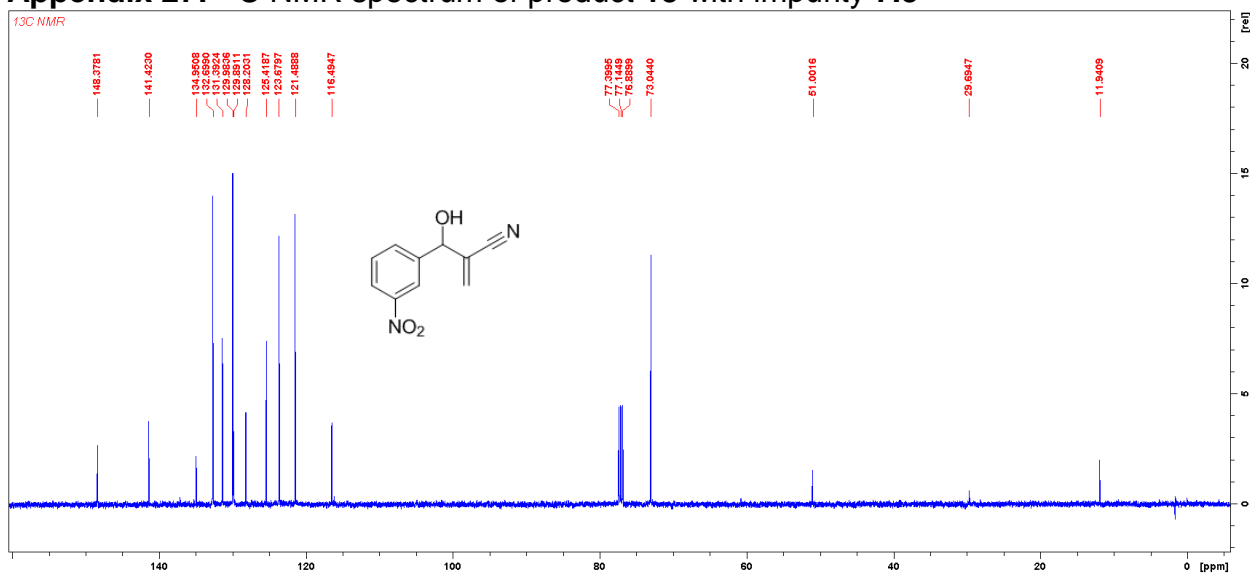
**Appendix 25:  $^1\text{H}$  NMR spectrum of **8**, Entry 12 of fluoride cleavage study**



## Appendix 26: <sup>1</sup>H NMR spectrum of product 13 with impurity 7.3

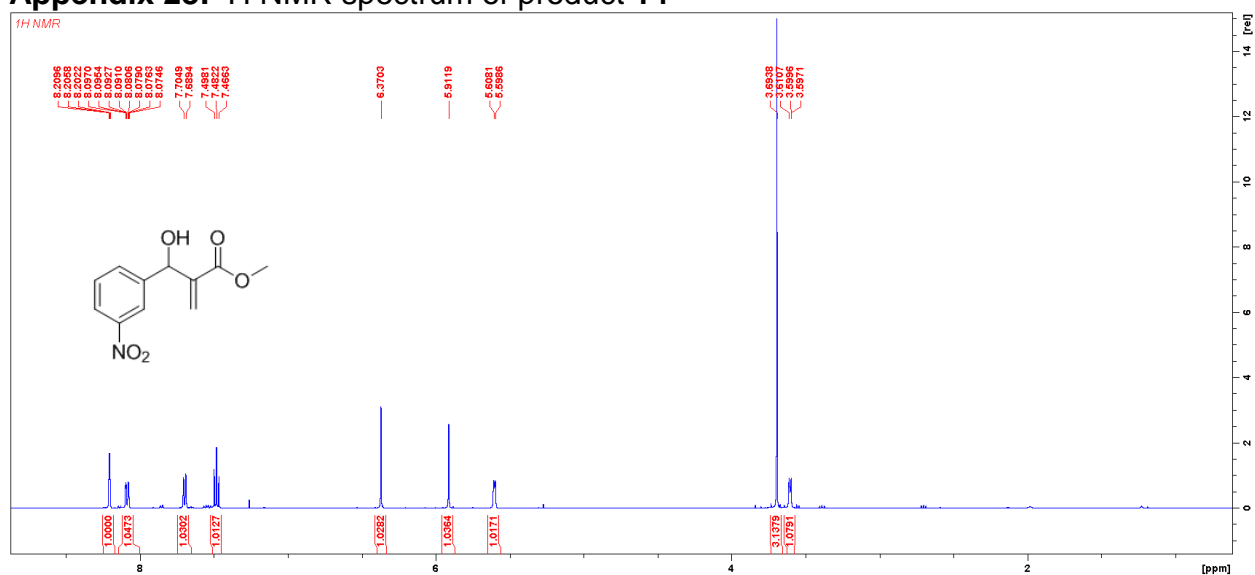


## Appendix 27: <sup>13</sup>C NMR spectrum of product 13 with impurity 7.3

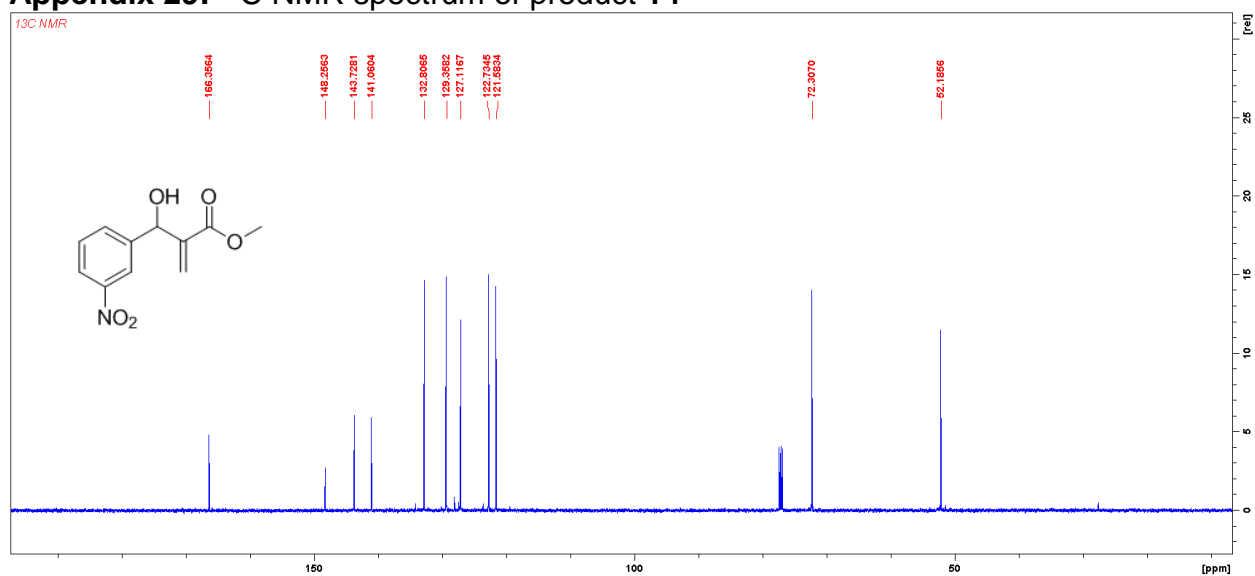




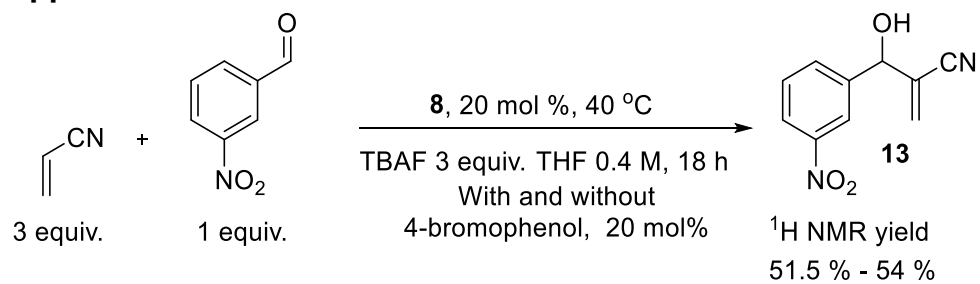
## Appendix 28: <sup>1</sup>H NMR spectrum of product 14



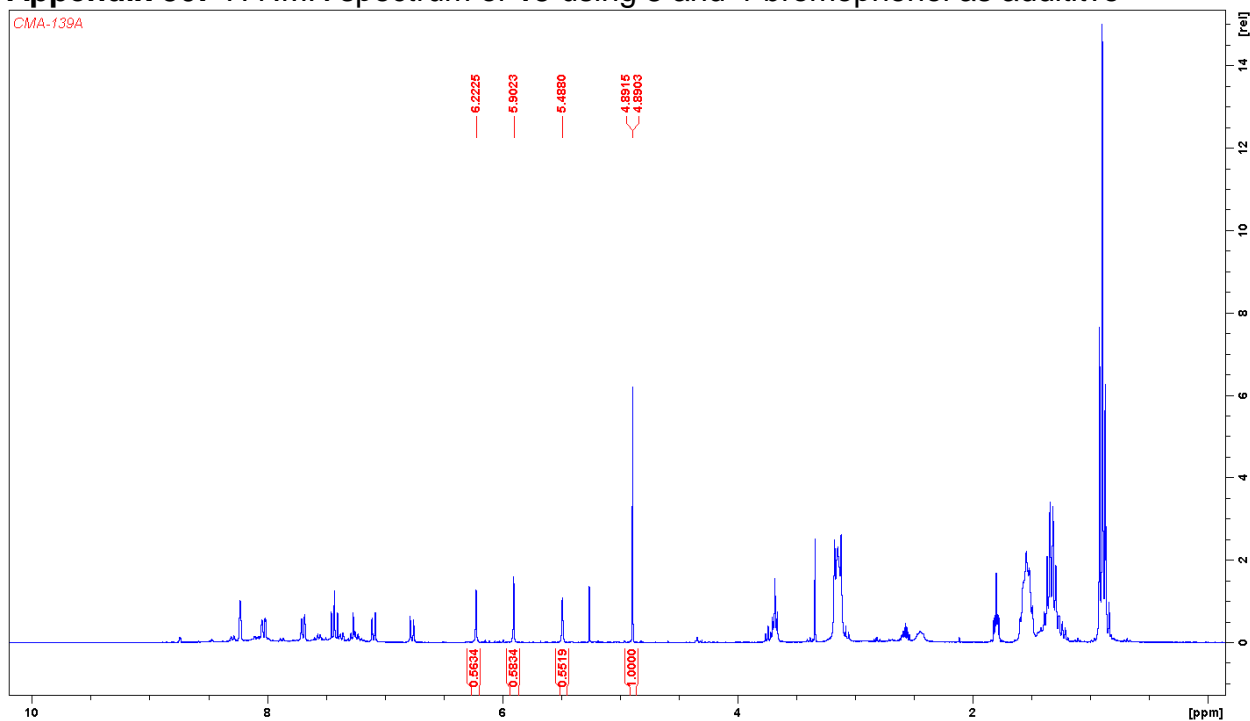
## Appendix 29: <sup>13</sup>C NMR spectrum of product 14



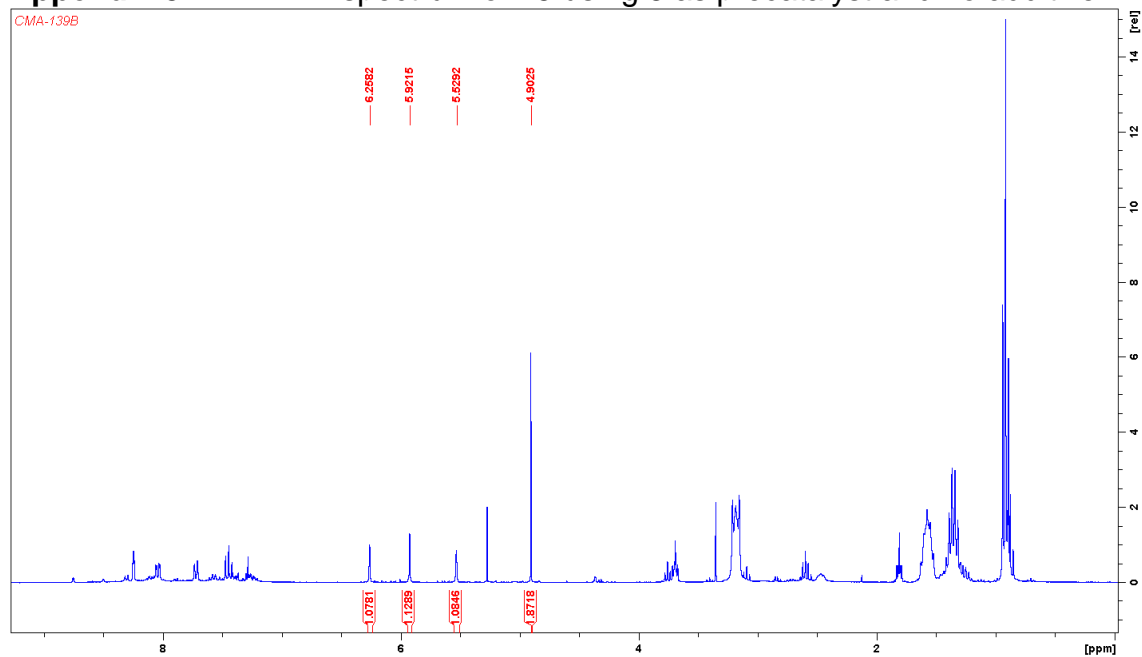
### Appendix 30-31



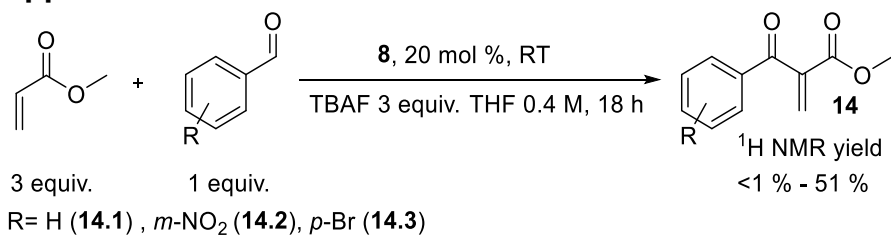
### Appendix 30: $^1\text{H NMR}$ spectrum of **13** using **8** and 4-bromophenol as additive



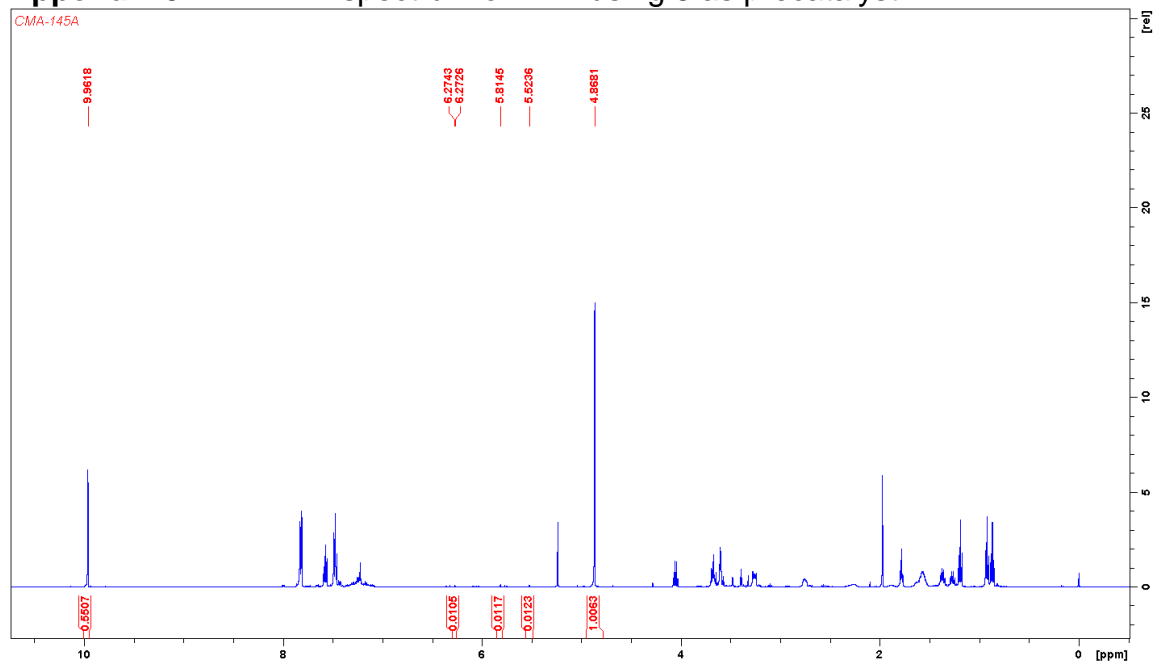
# Appendix 31: $^1\text{H}$ NMR spectrum of **13** using **8** as precatalyst and no additive



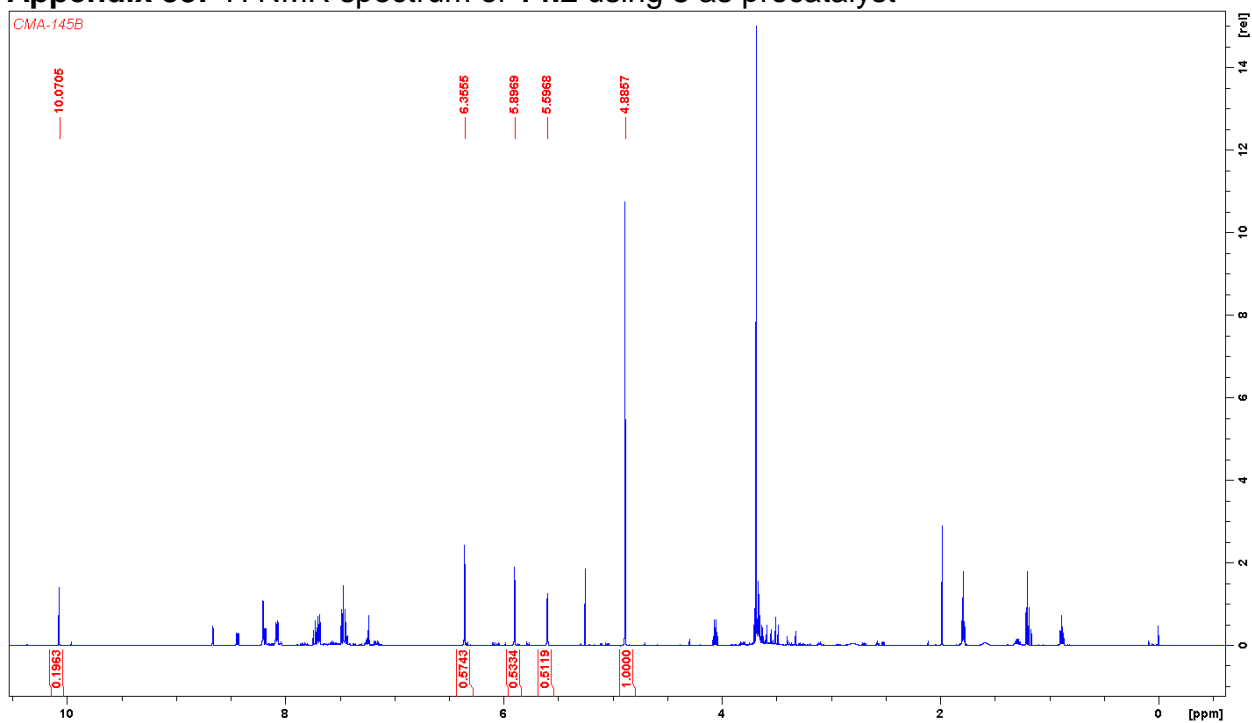
## Appendix 32-34



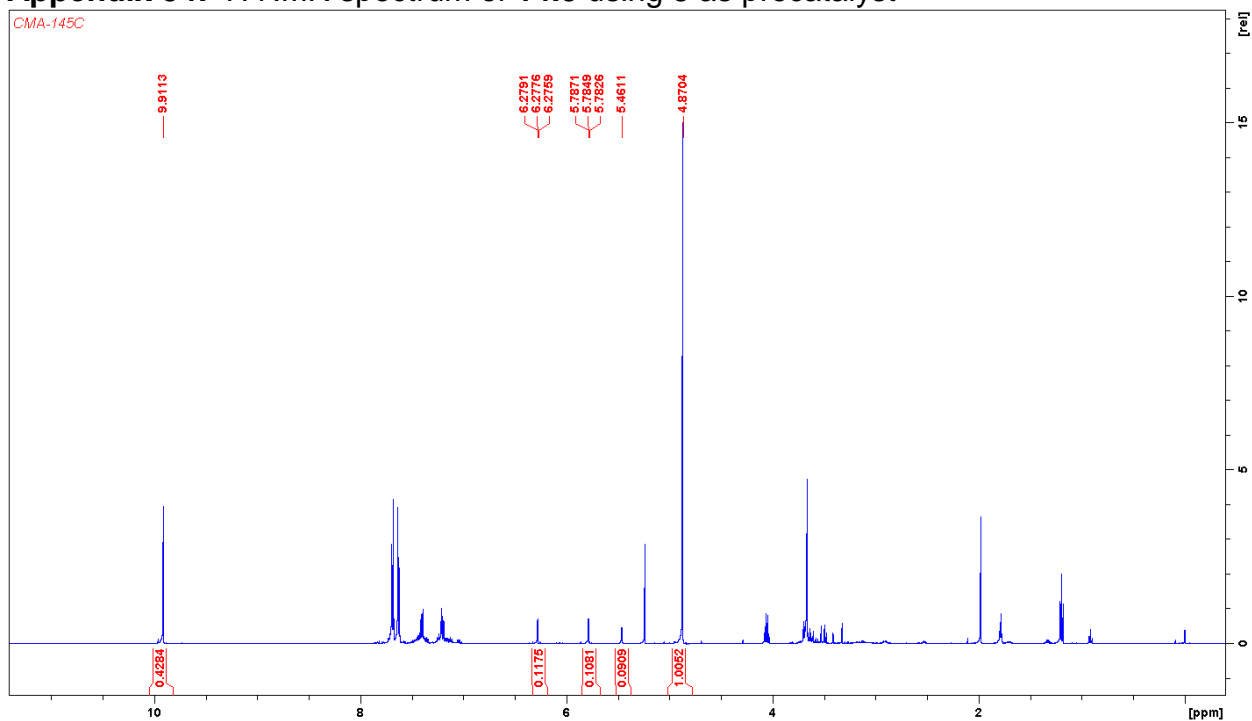
## Appendix 32: <sup>1</sup>H NMR spectrum of **14.1** using **8** as precatalyst



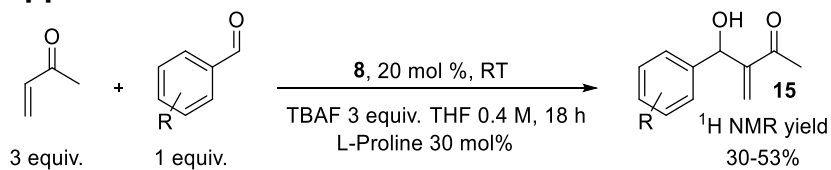
### Appendix 33: <sup>1</sup>H NMR spectrum of 14.2 using 8 as precatalyst



### Appendix 34: <sup>1</sup>H NMR spectrum of 14.3 using 8 as precatalyst

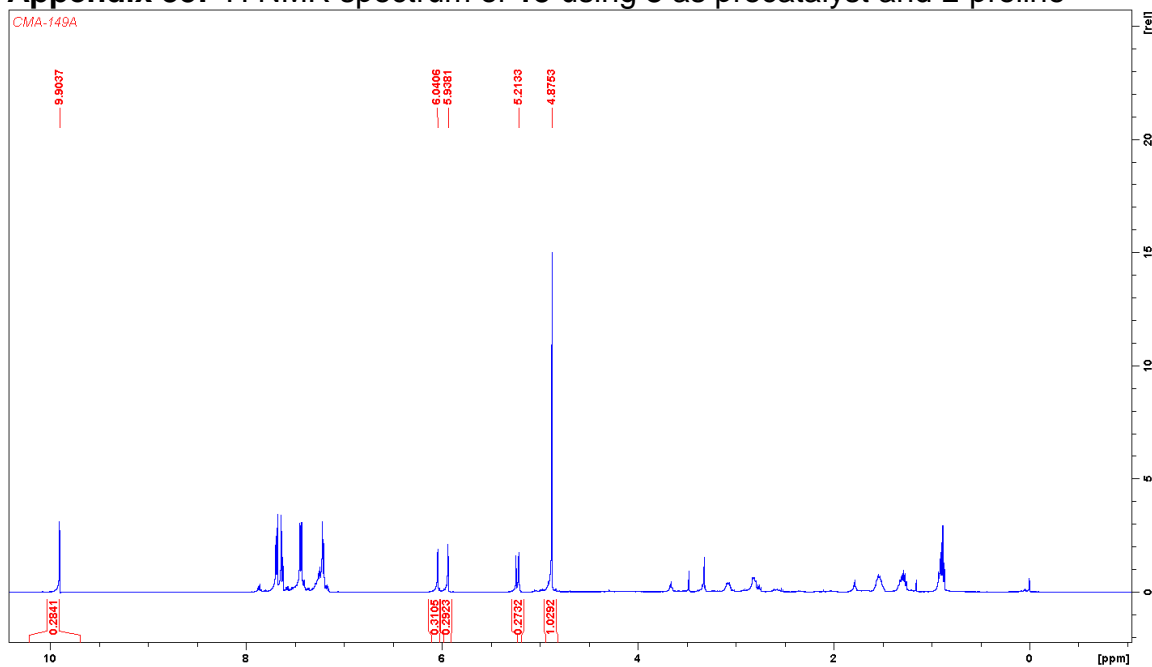


## Appendix 35-40

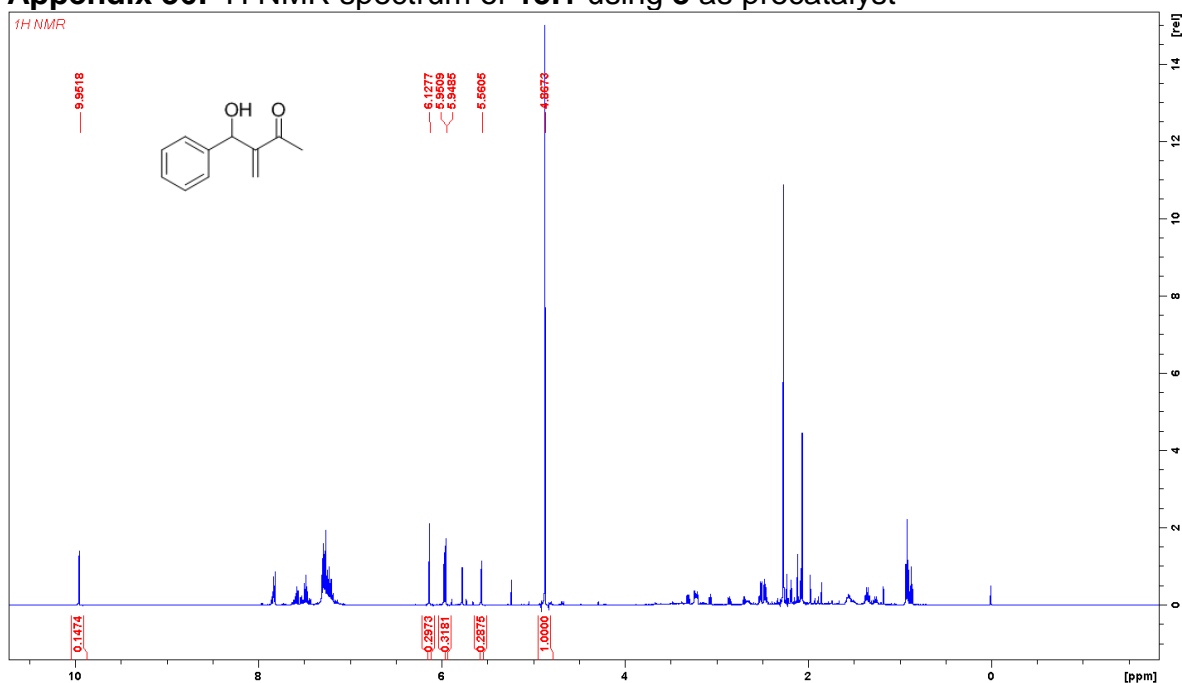


R = H (**15.1**), *m*-NO<sub>2</sub> (**15.2**), *p*-Br (**15.3**)

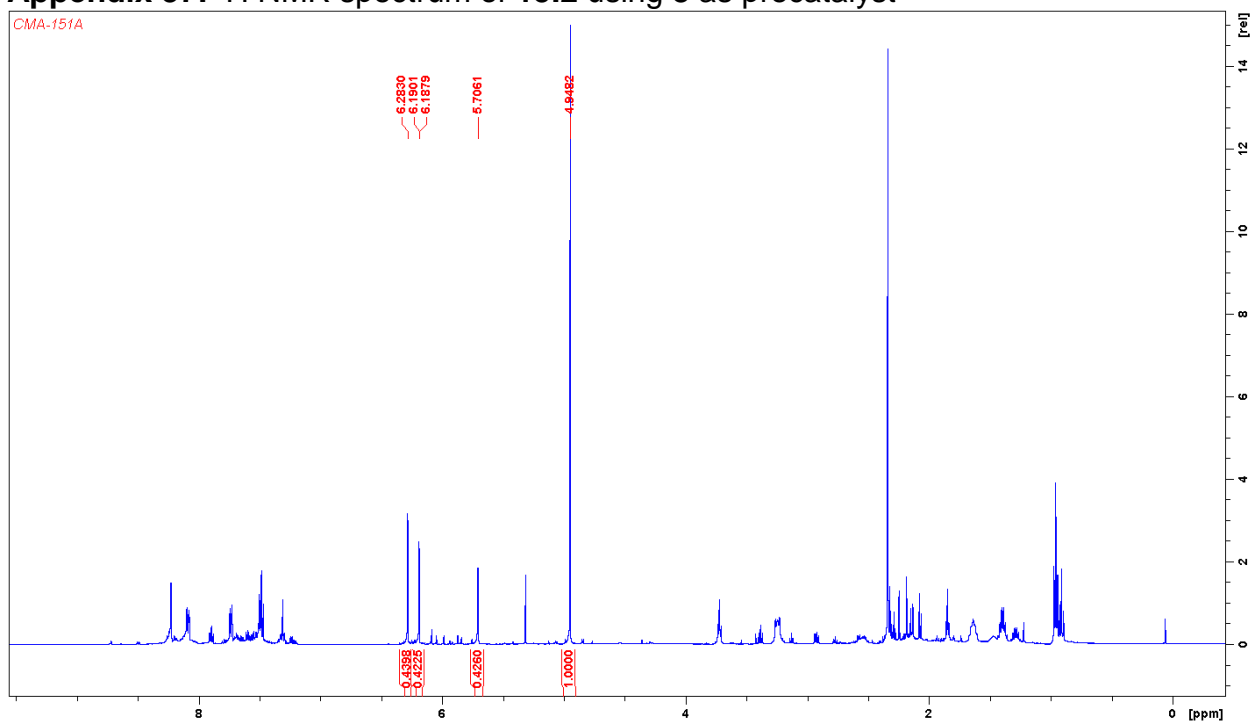
## Appendix 35: $^1\text{H NMR}$ spectrum of **15** using **8** as precatalyst and L-proline



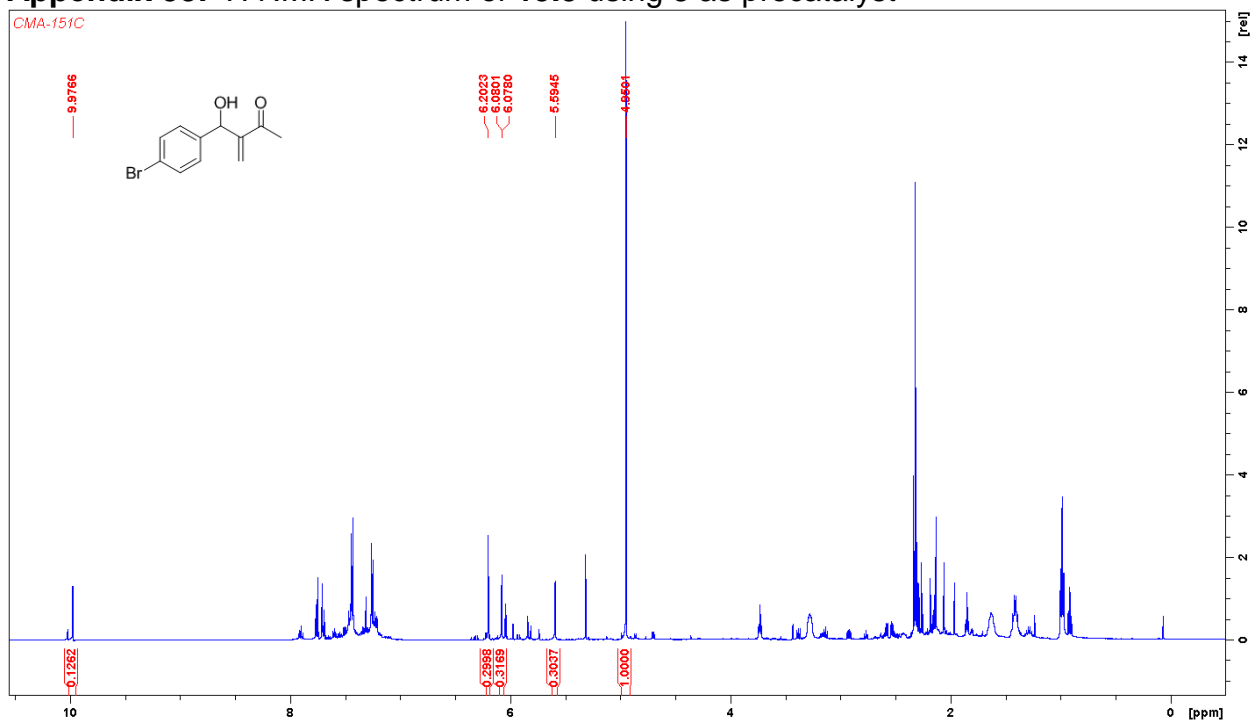
## Appendix 36: $^1\text{H NMR}$ spectrum of **15.1** using **8** as precatalyst



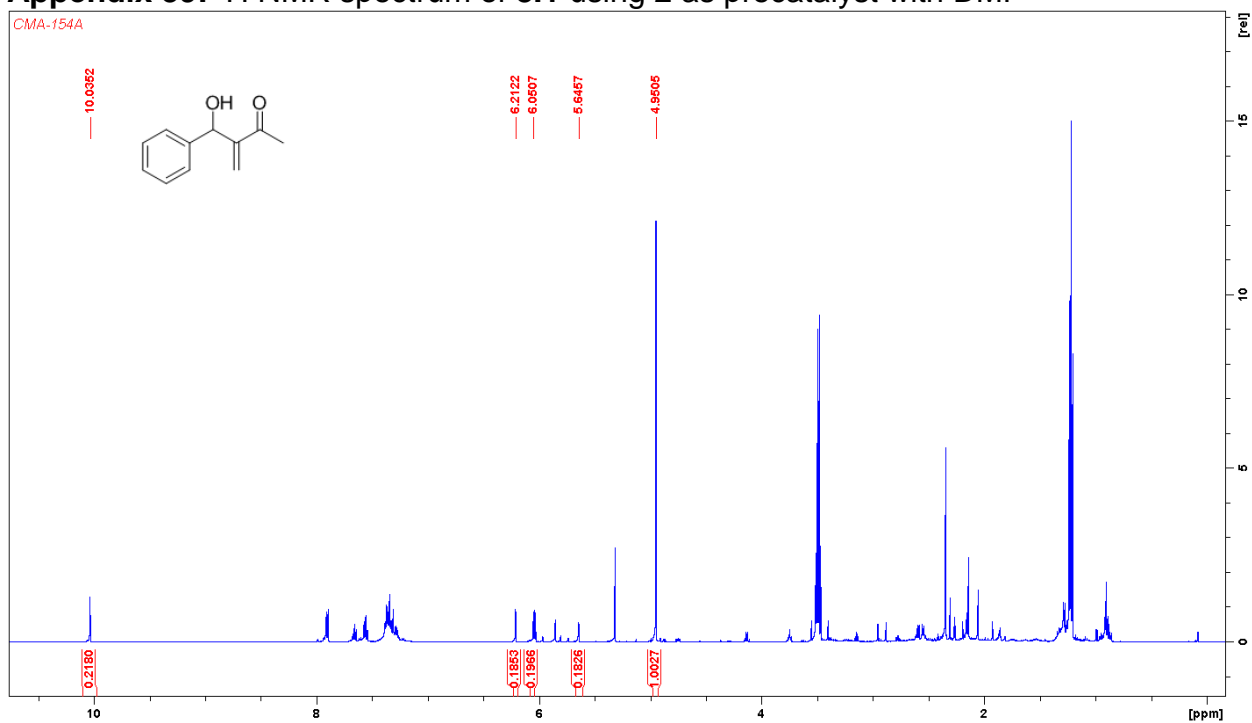
### Appendix 37: <sup>1</sup>H NMR spectrum of 15.2 using 8 as precatalyst



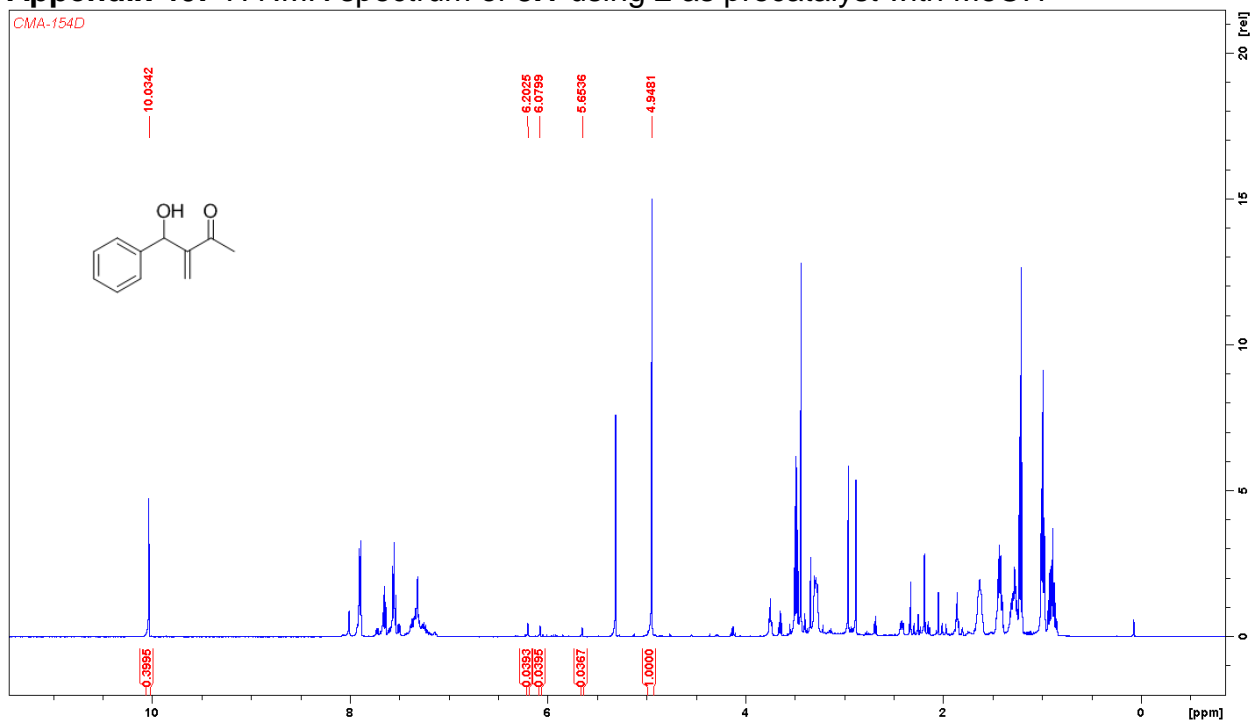
### Appendix 38: <sup>1</sup>H NMR spectrum of 15.3 using 8 as precatalyst



### Appendix 39: <sup>1</sup>H NMR spectrum of **8.1** using **2** as precatalyst with DMF

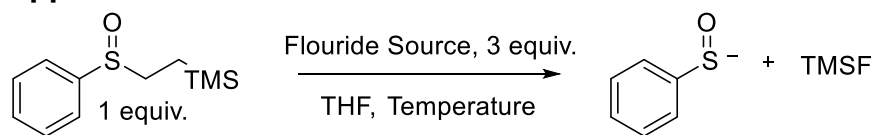


### Appendix 40: <sup>1</sup>H NMR spectrum of **8.1** using **2** as precatalyst with MeOH

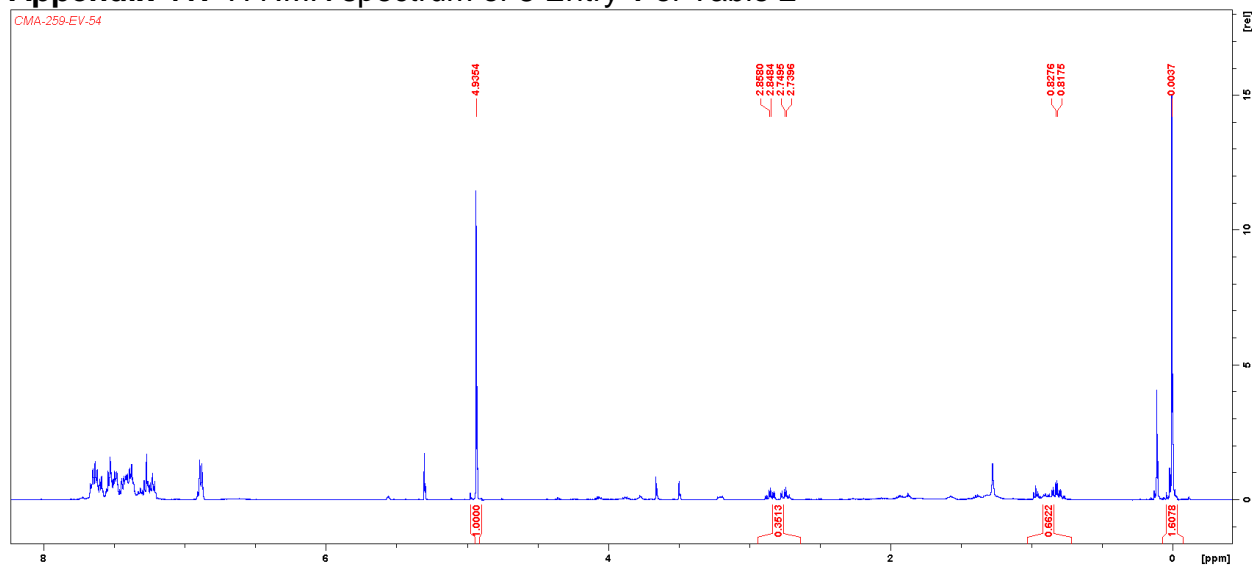




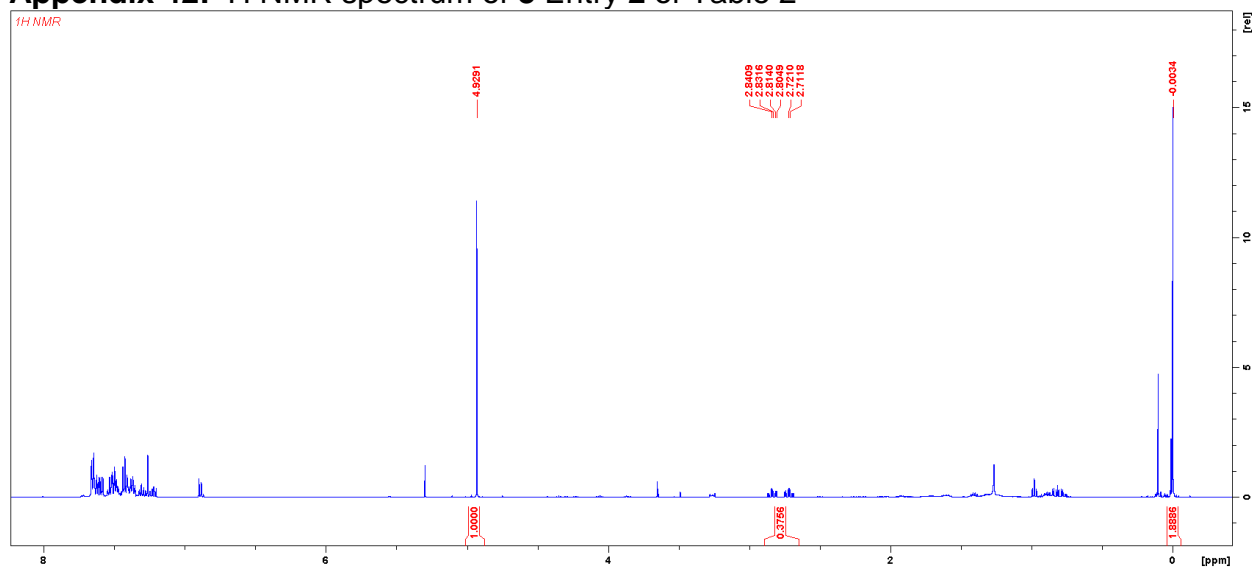
## Appendix 41-46



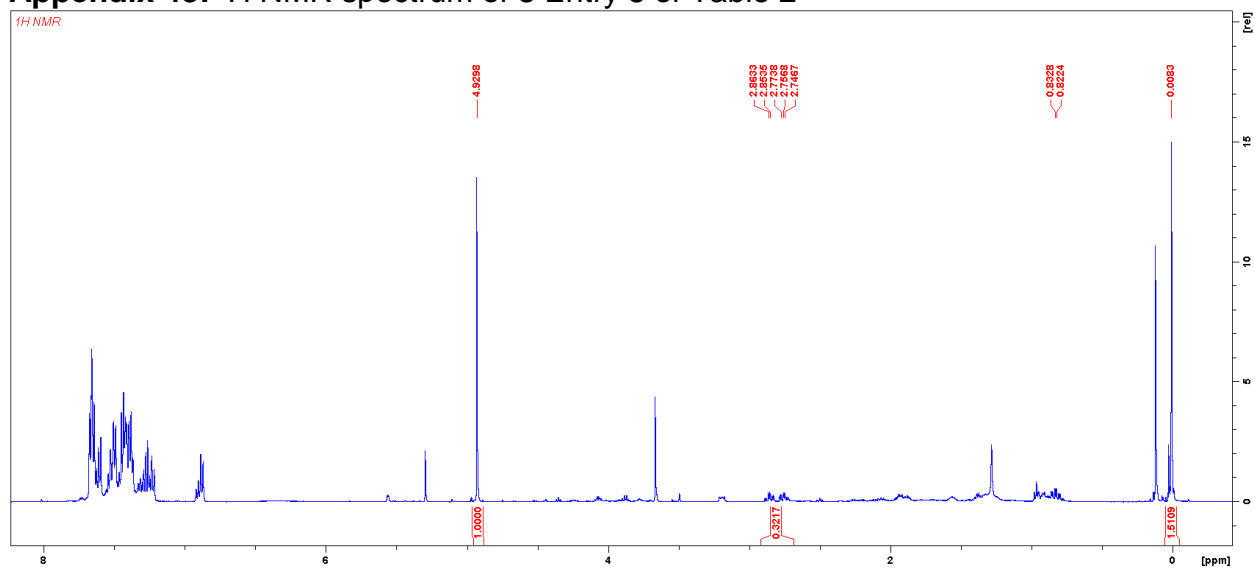
## Appendix 41: $^1\text{H}$ NMR spectrum of **8** Entry 1 of Table 2



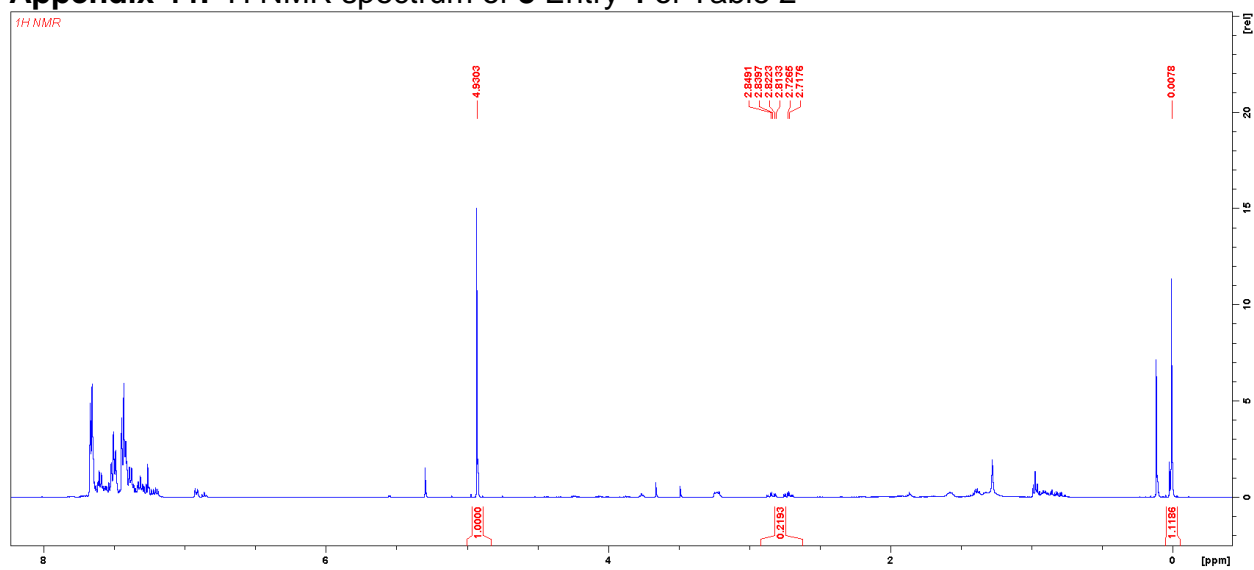
## Appendix 42: $^1\text{H}$ NMR spectrum of **8** Entry 2 of Table 2



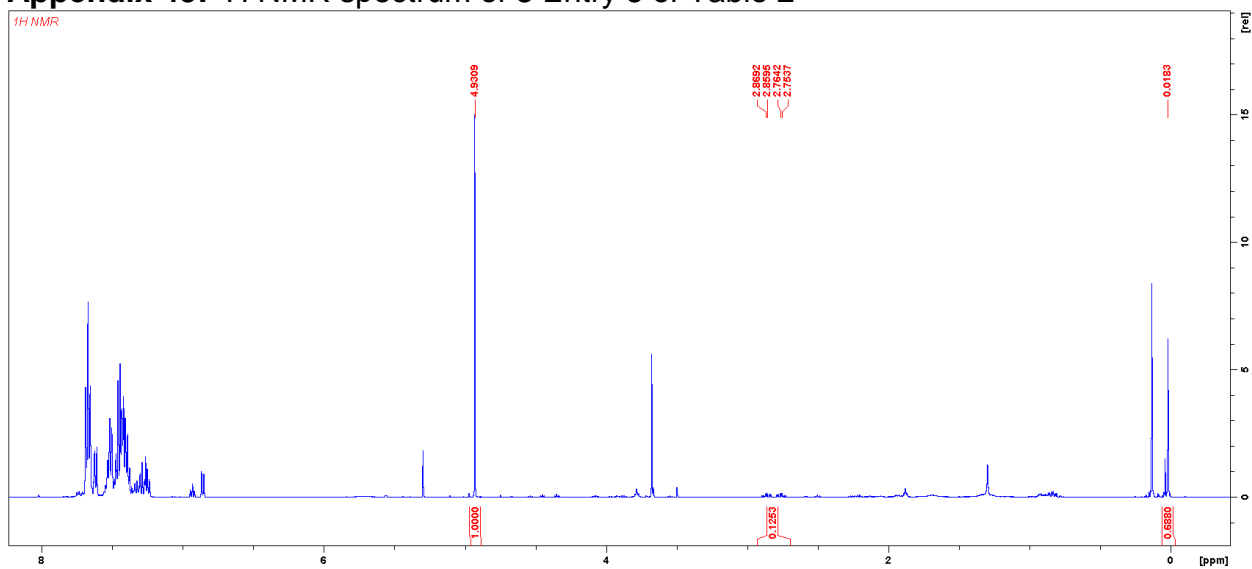
### Appendix 43: <sup>1</sup>H NMR spectrum of **8** Entry 3 of Table 2



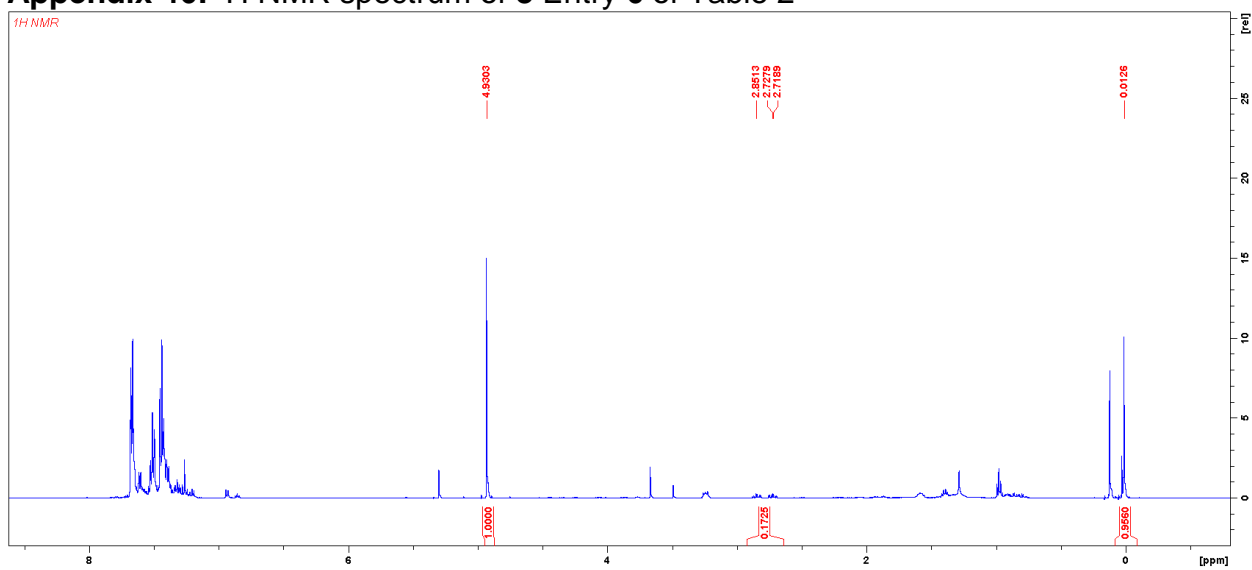
### Appendix 44: <sup>1</sup>H NMR spectrum of **8** Entry 4 of Table 2



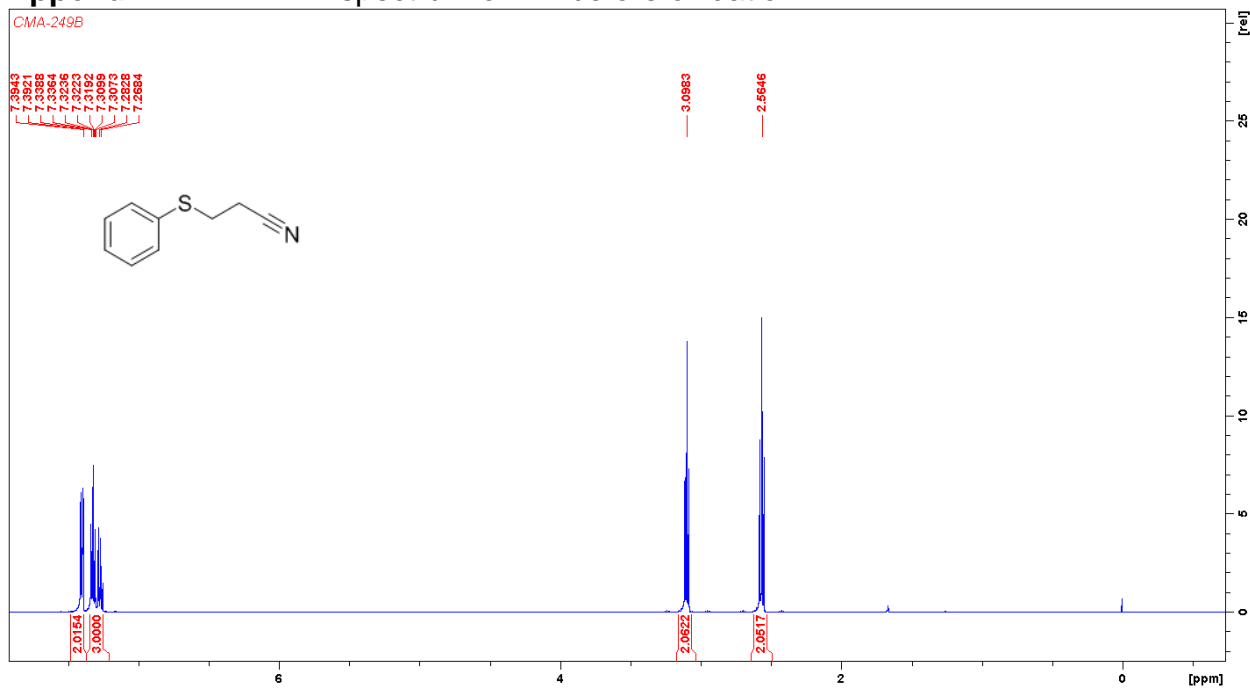
**Appendix 45: <sup>1</sup>H NMR spectrum of 8 Entry 5 of Table 2**



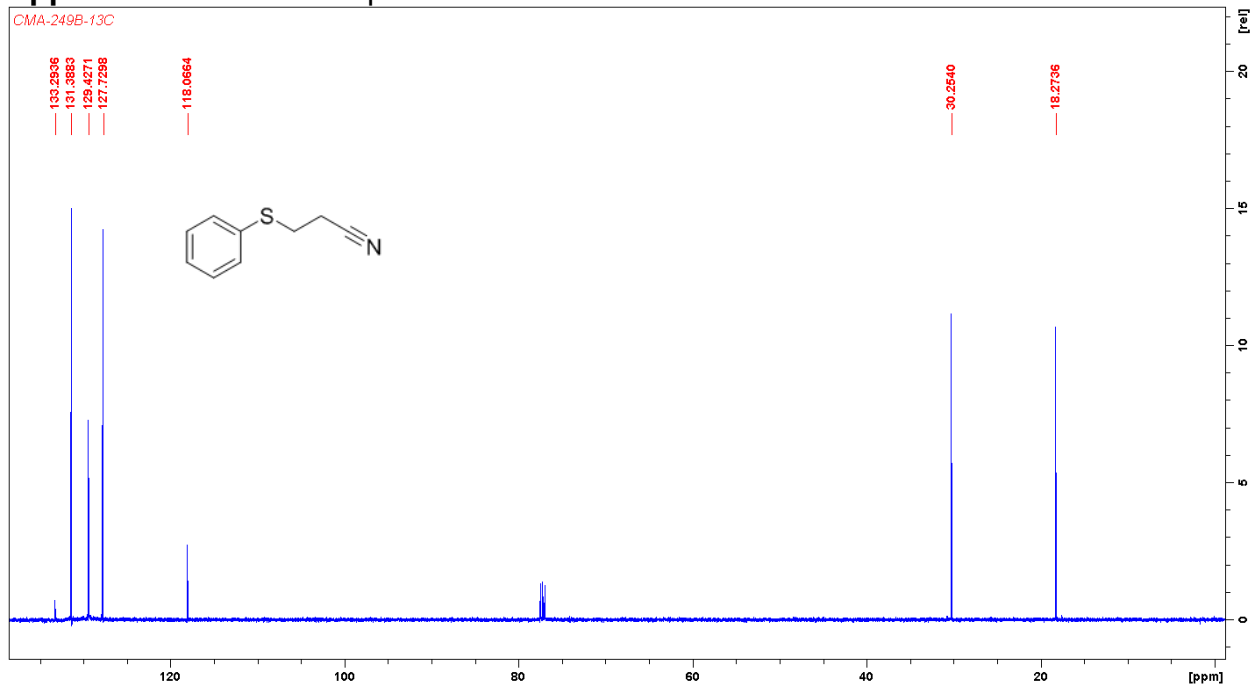
**Appendix 46: <sup>1</sup>H NMR spectrum of 8 Entry 6 of Table 2**



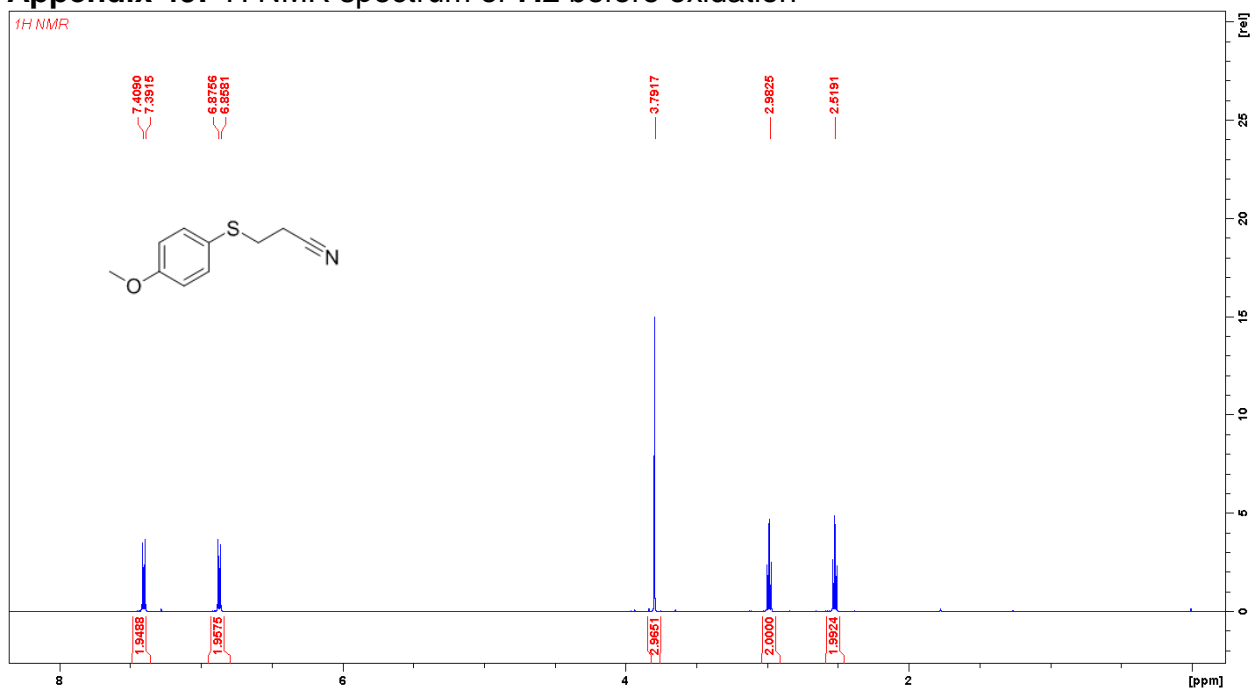
### Appendix 47: <sup>1</sup>H NMR spectrum of 7.1 before oxidation



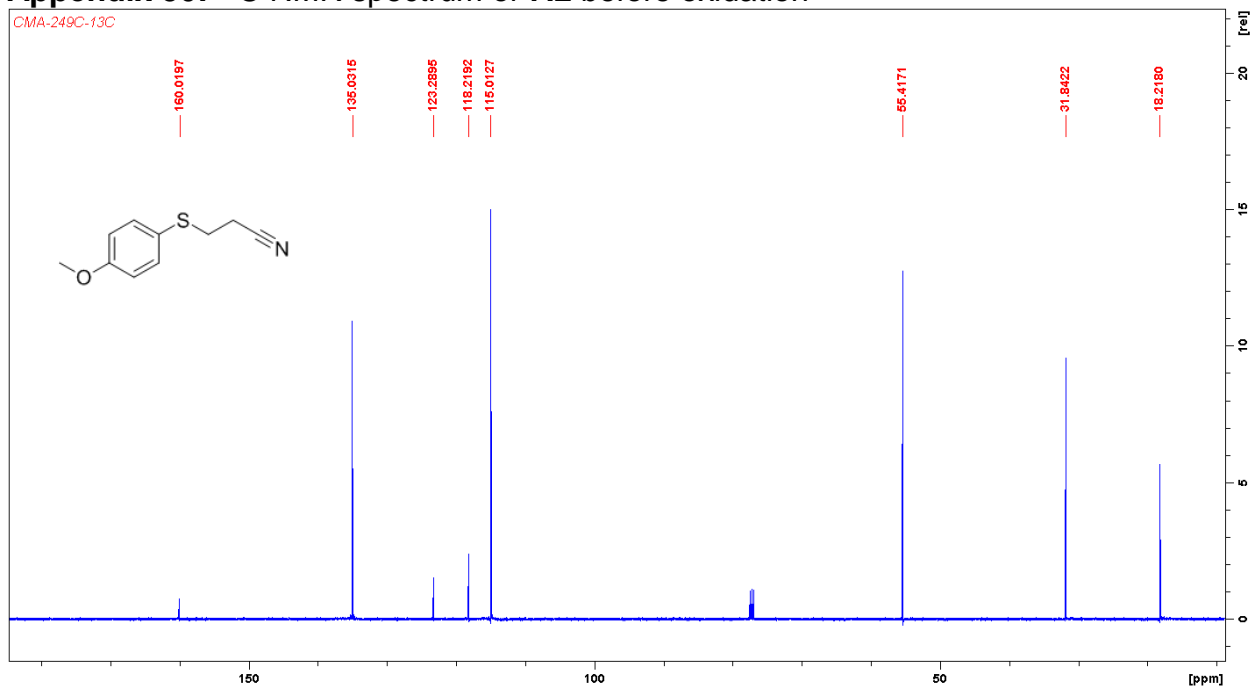
### Appendix 48: <sup>13</sup>C NMR spectrum of 7.1 before oxidation



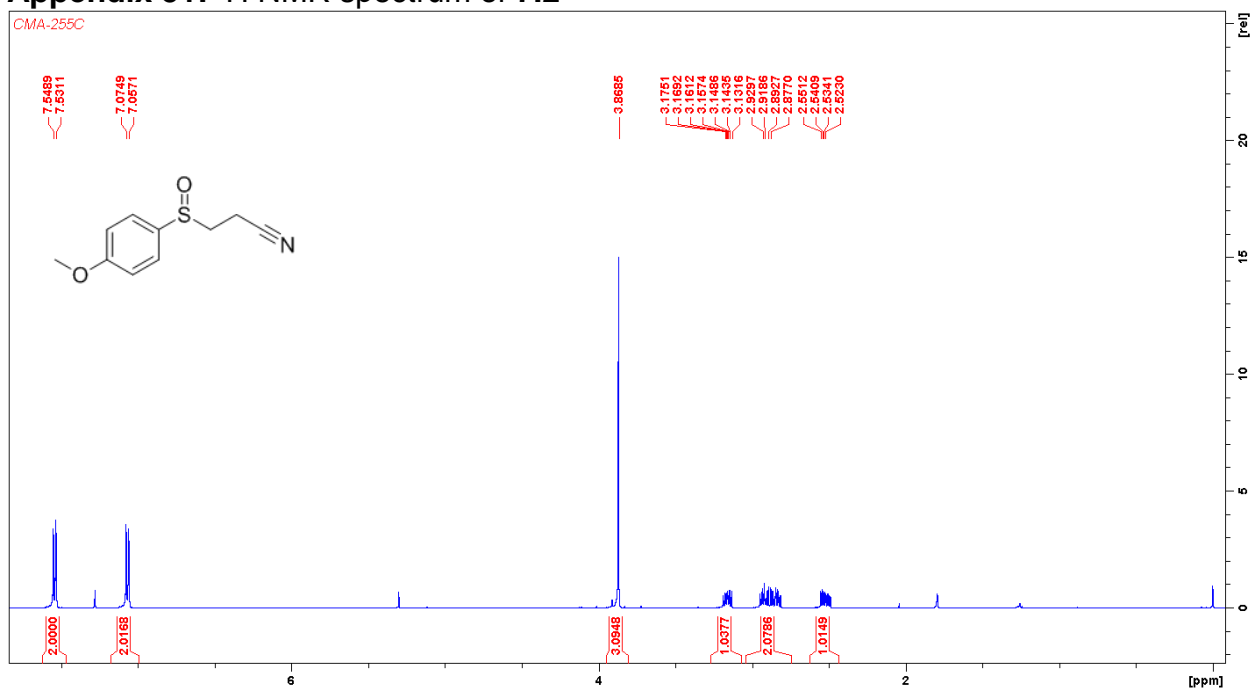
### Appendix 49: <sup>1</sup>H NMR spectrum of 7.2 before oxidation



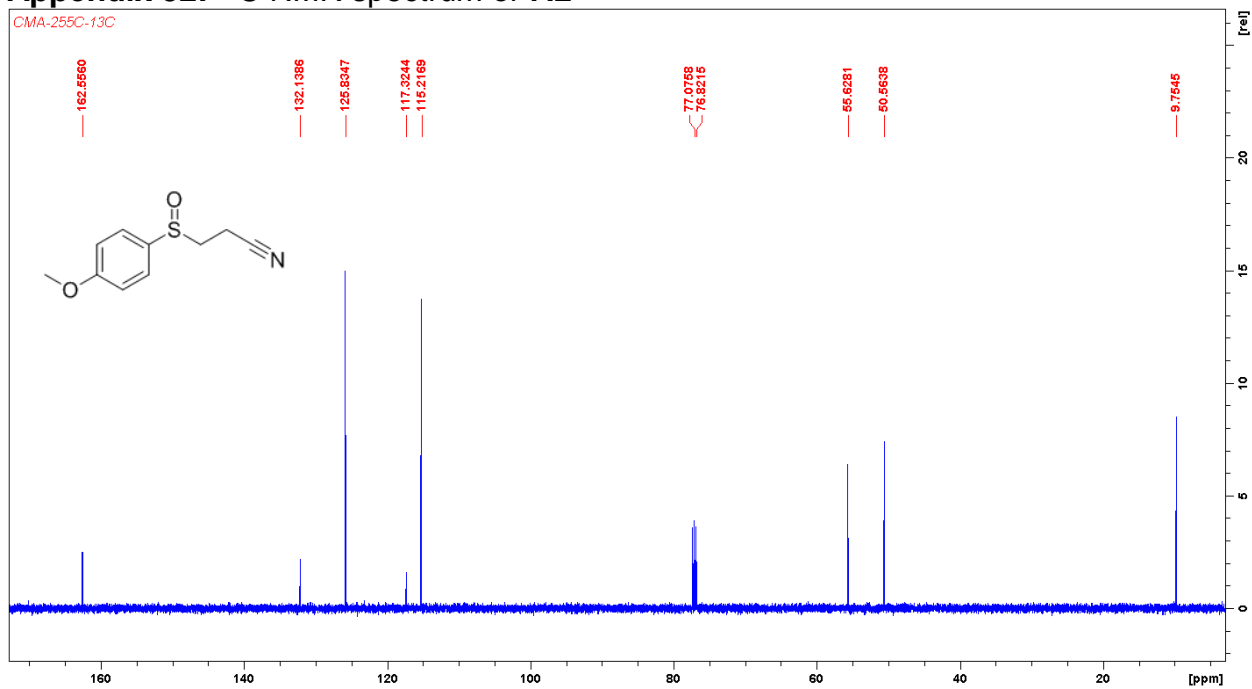
### Appendix 50: <sup>13</sup>C NMR spectrum of 7.2 before oxidation



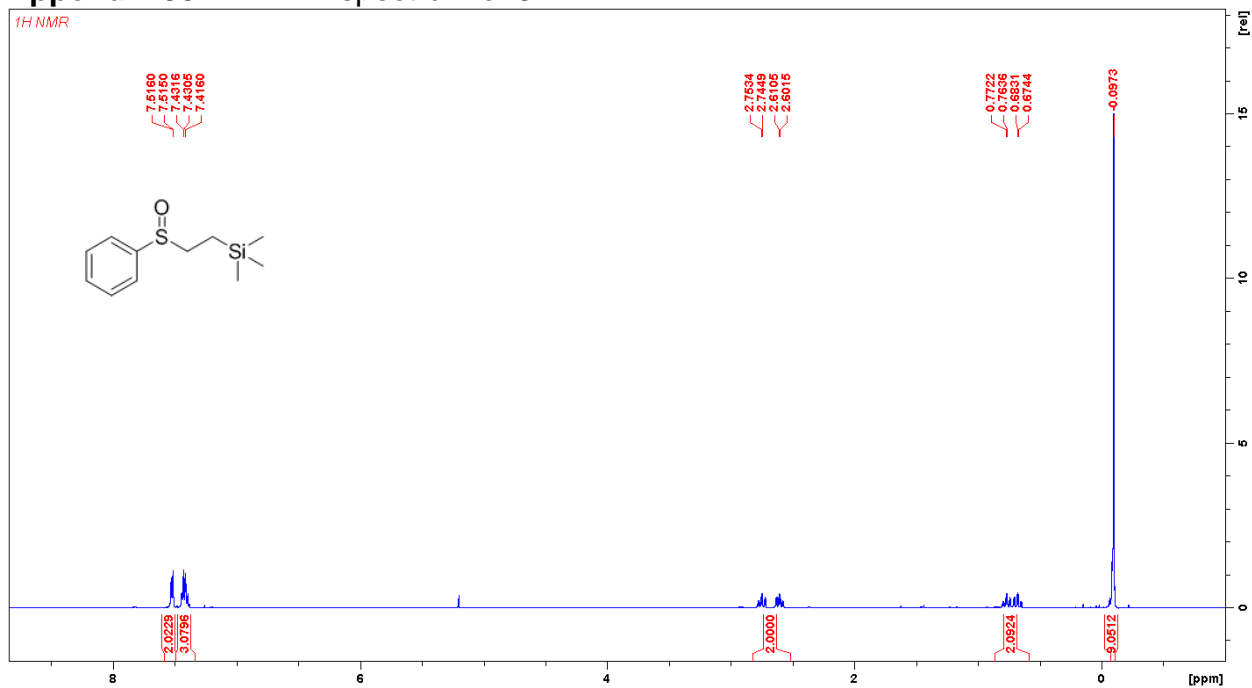
## Appendix 51: <sup>1</sup>H NMR spectrum of 7.2



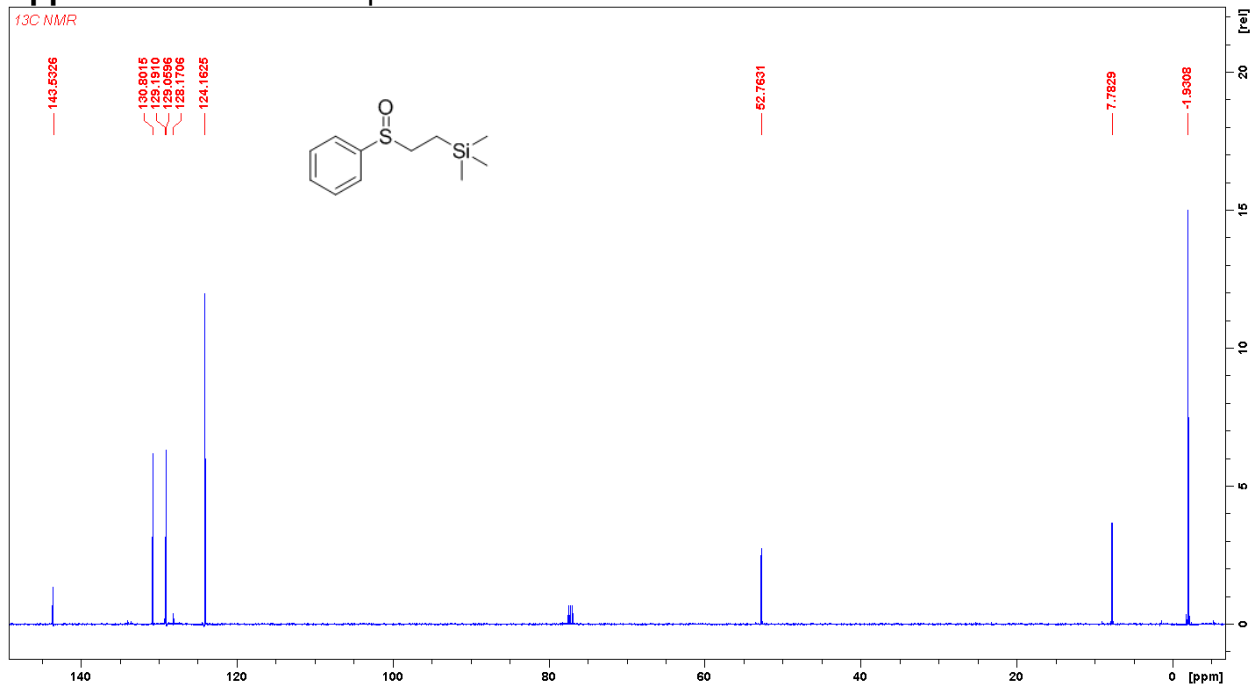
## Appendix 52: <sup>13</sup>C NMR spectrum of 7.2



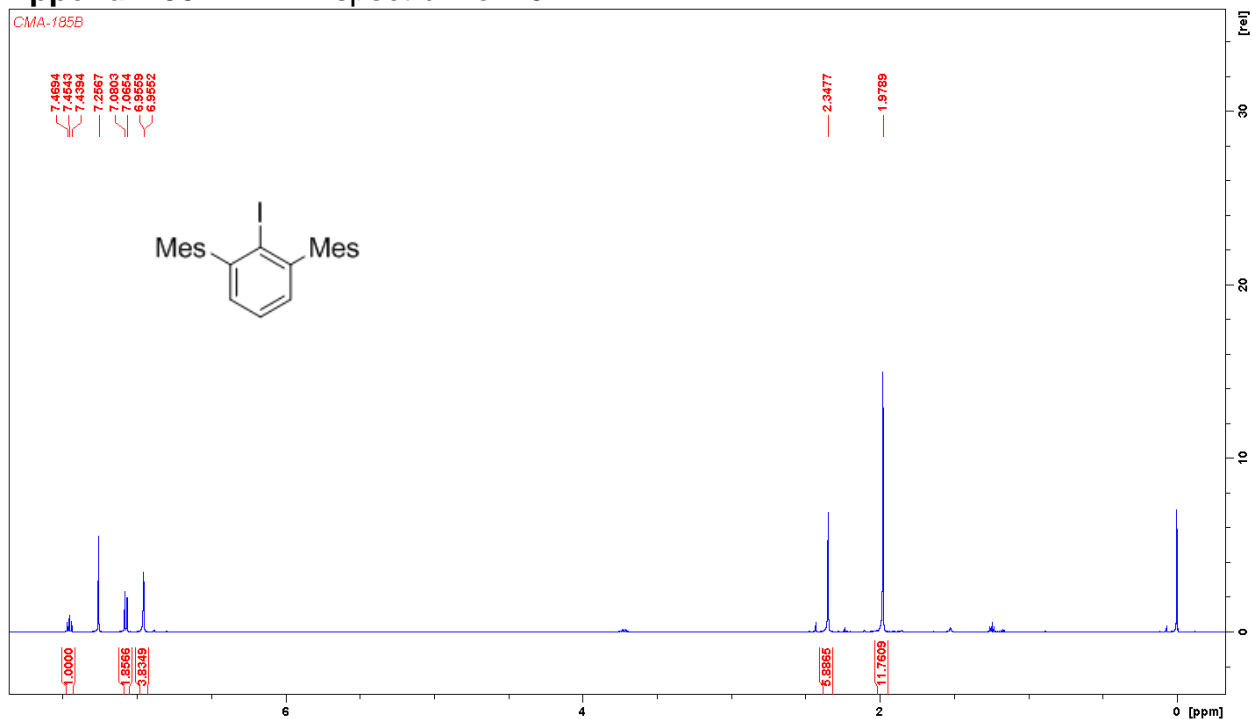
### Appendix 53: <sup>1</sup>H NMR spectrum of 8



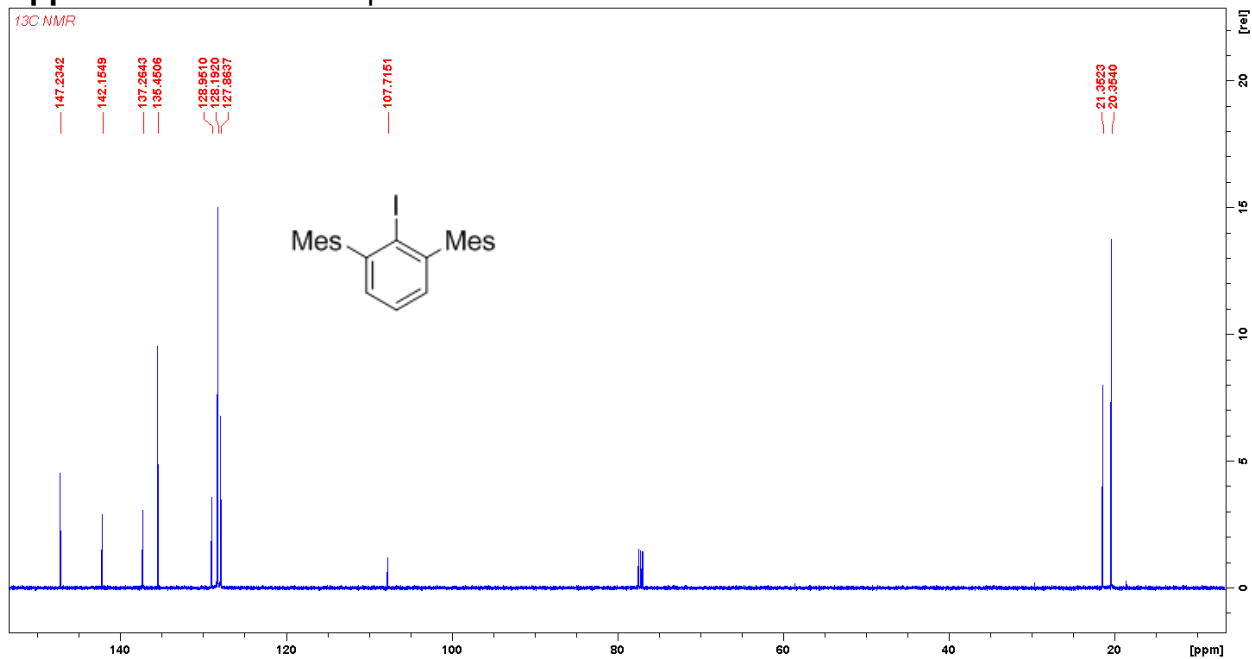
### Appendix 54: <sup>13</sup>C NMR spectrum of 8



### Appendix 55: <sup>1</sup>H NMR spectrum of 10

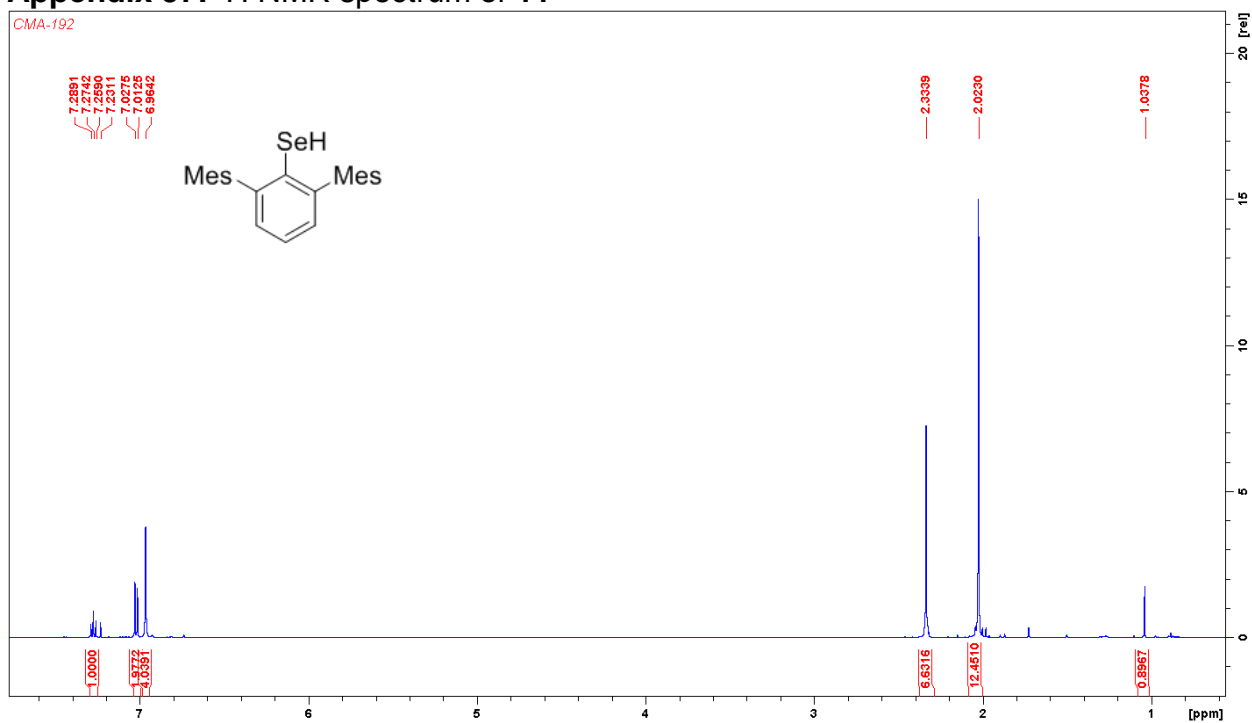


### Appendix 56: <sup>13</sup>C NMR spectrum of 10

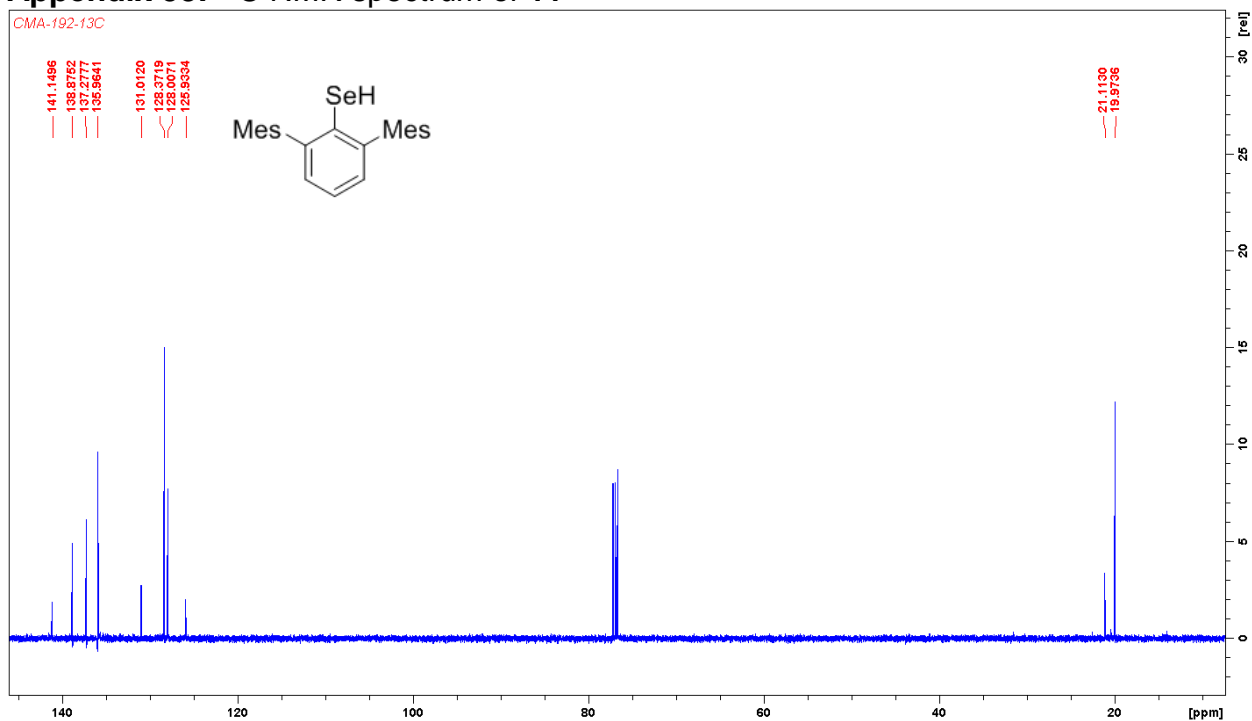




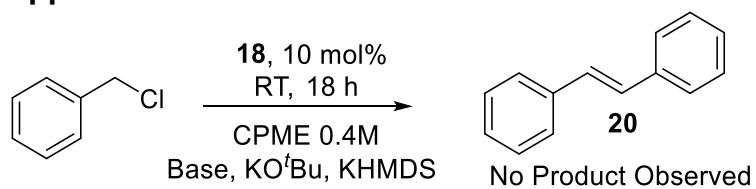
## Appendix 57: <sup>1</sup>H NMR spectrum of 11



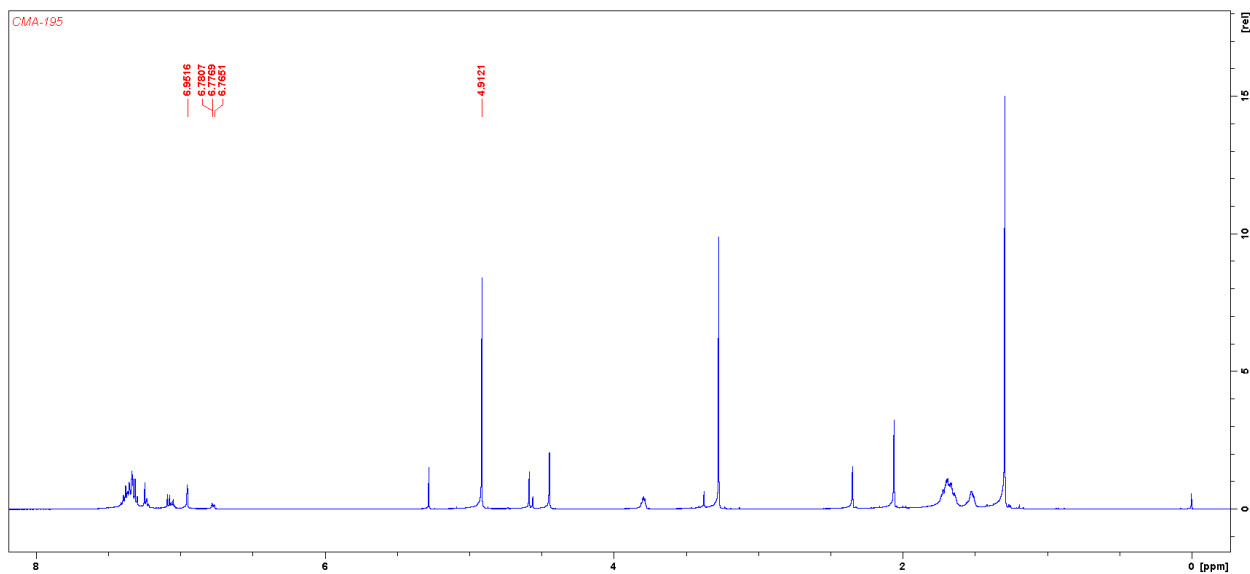
## Appendix 58: <sup>13</sup>C NMR spectrum of 11



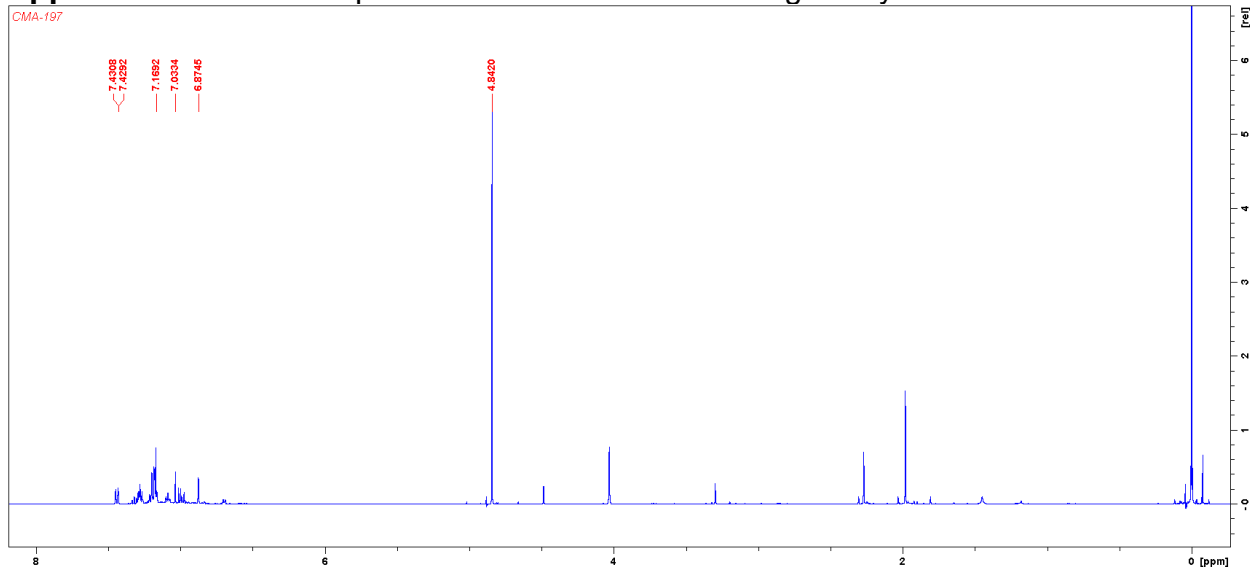
## Appendix 59-60



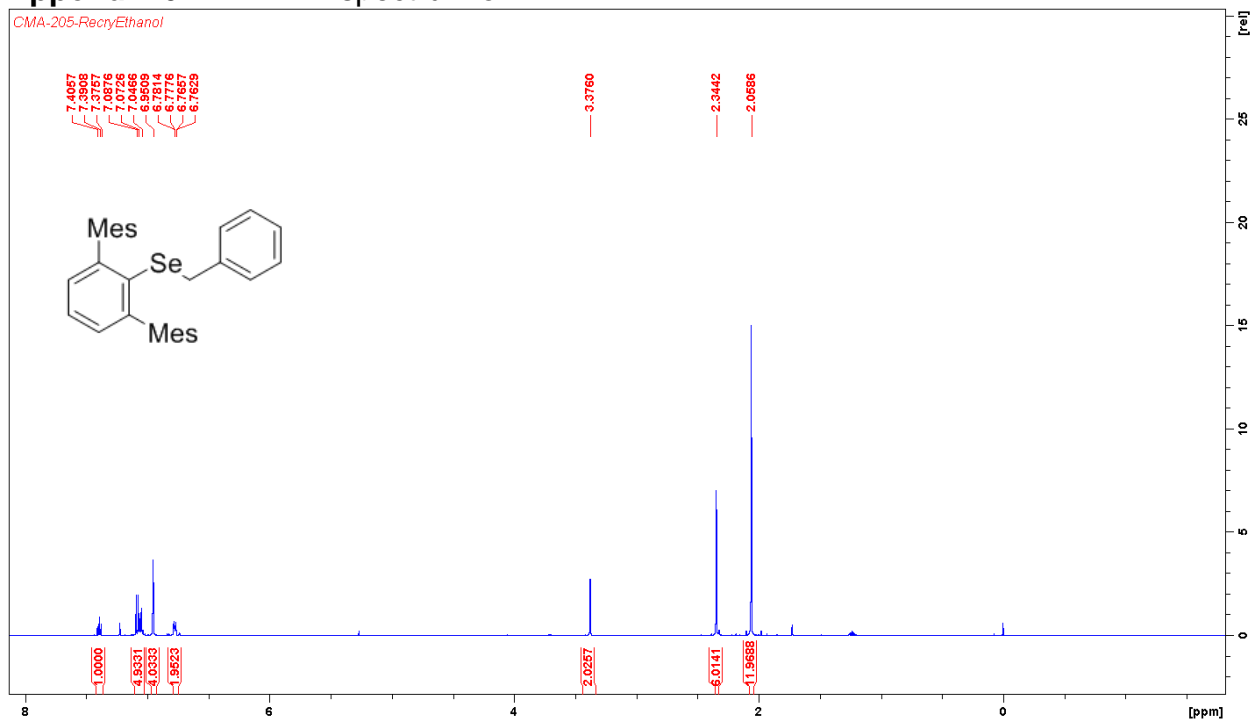
## Appendix 59: $^1\text{H}$ NMR spectrum of absence of **20** using catalyst **18** and $\text{KO}^t\text{Bu}$



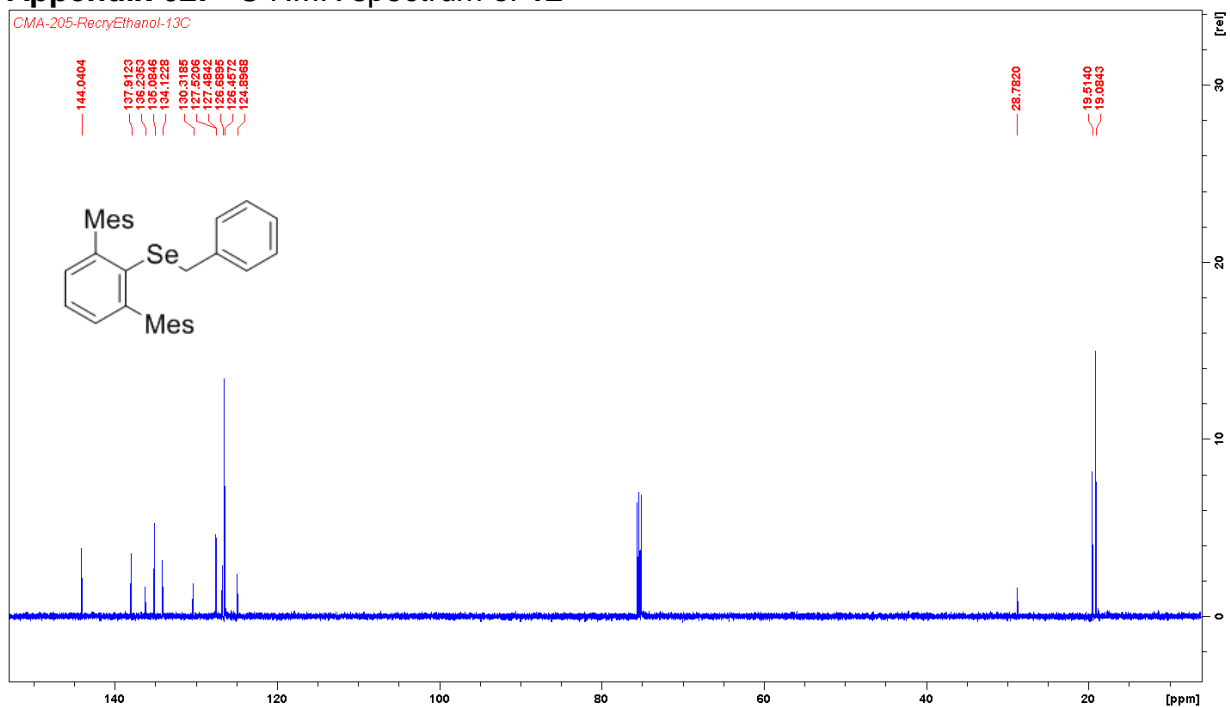
## Appendix 60: $^1\text{H}$ NMR spectrum of absence of **20** using catalyst **18** and KHMDS



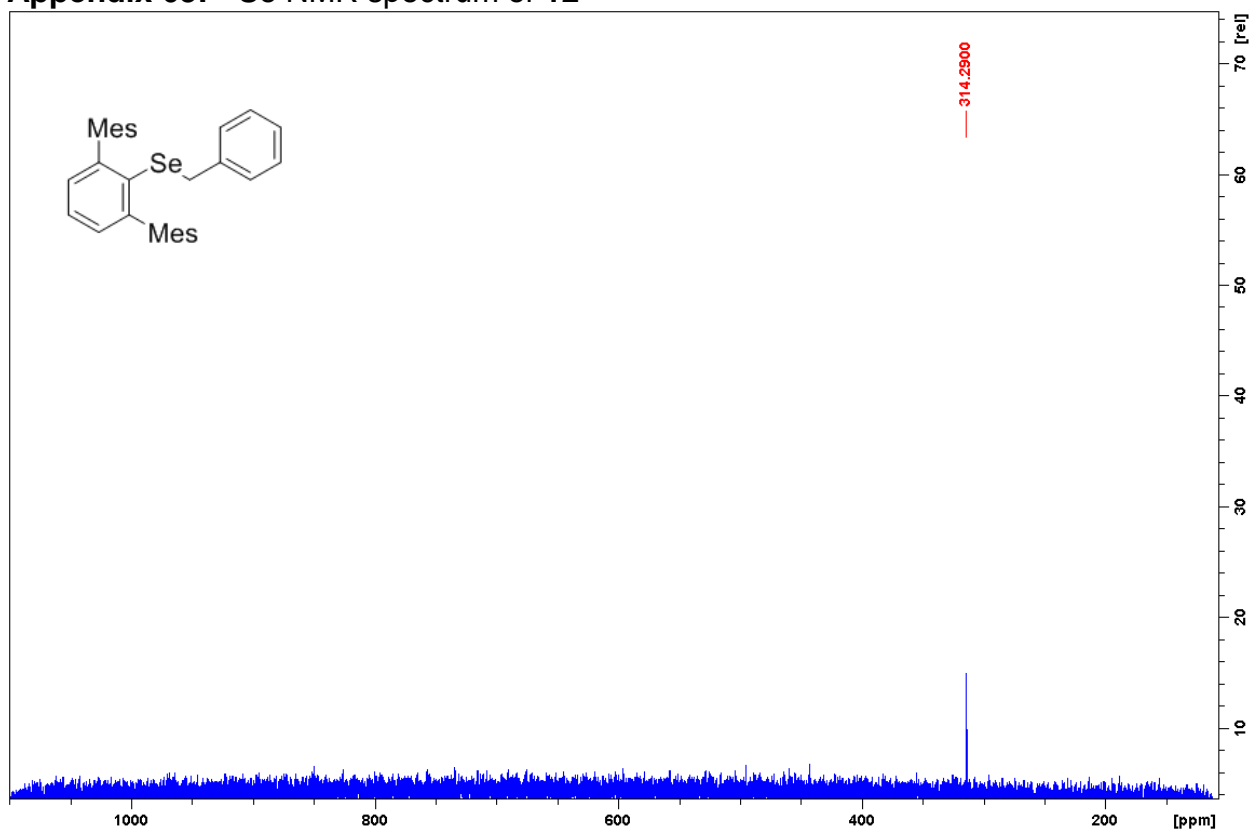
## Appendix 61: <sup>1</sup>H NMR spectrum of 12



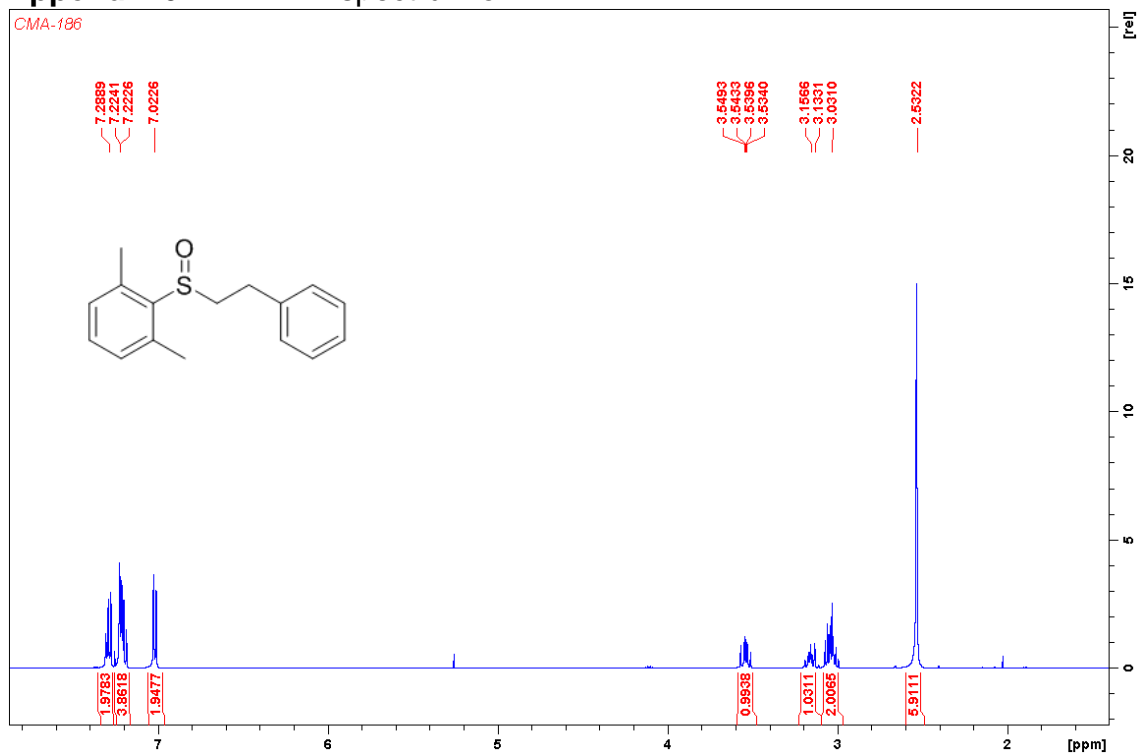
## Appendix 62: <sup>13</sup>C NMR spectrum of 12



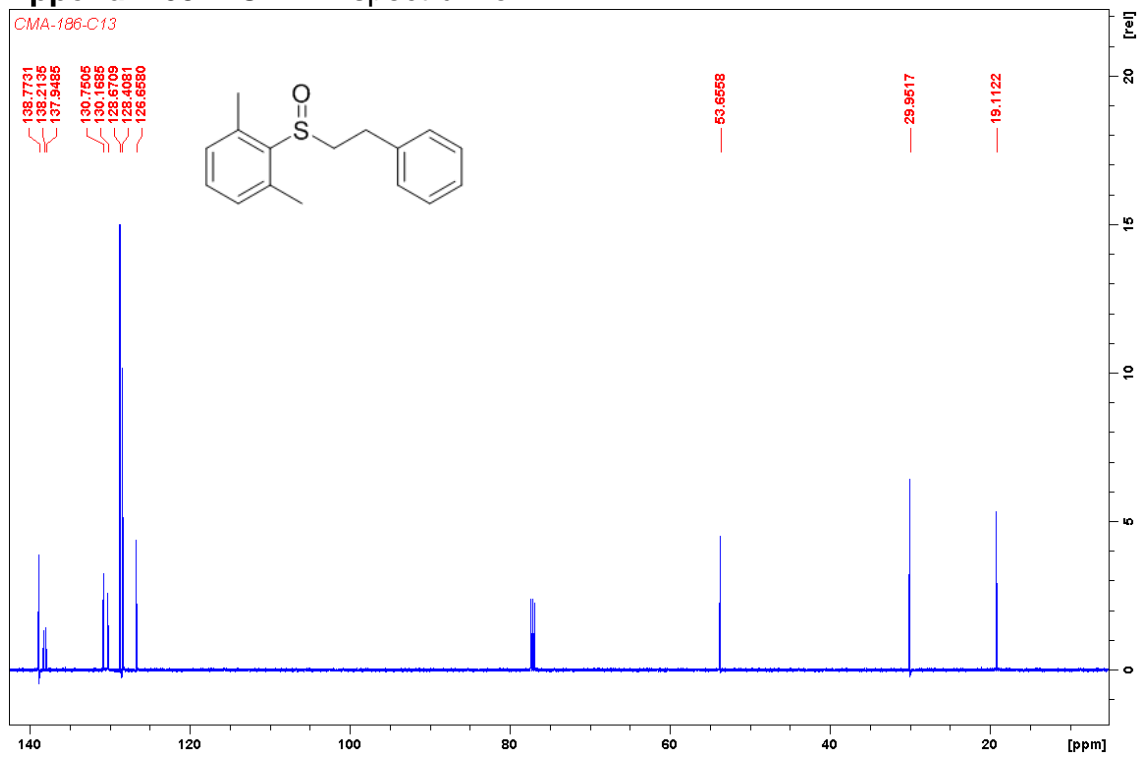
### Appendix 63: $^{77}\text{Se}$ NMR spectrum of 12



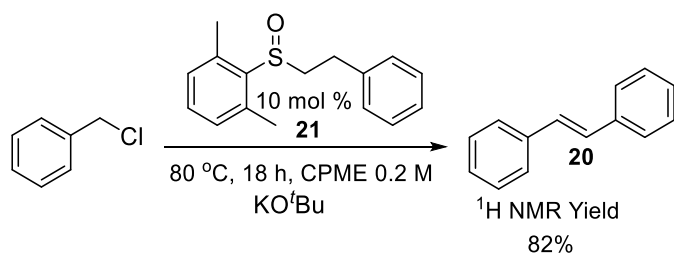
### Appendix 64: $^1\text{H}$ NMR spectrum of 14



# Appendix 65: $^{13}\text{C}$ NMR spectrum of 14



## Appendix 66



### Appendix 66: $^1\text{H NMR}$ spectrum of **21** using catalyst **14**

